



**HAL**  
open science

## **Radium isotopes as submarine groundwater discharge (SGD) tracers: Review and recommendations**

J. Garcia-Orellana, V. Rodellas, J. Tamborski, M. Diego-Feliu, Pieter van Beek, Y. Weinstein, M. Charette, A. Alorda-Kleinglass, H.A. A Michael, Thomas Stieglitz, et al.

### ► To cite this version:

J. Garcia-Orellana, V. Rodellas, J. Tamborski, M. Diego-Feliu, Pieter van Beek, et al.. Radium isotopes as submarine groundwater discharge (SGD) tracers: Review and recommendations. *Earth-Science Reviews*, 2021, 220, pp.103681. 10.1016/j.earscirev.2021.103681 . ird-03264444

**HAL Id: ird-03264444**

**<https://ird.hal.science/ird-03264444>**

Submitted on 18 Jun 2021

**HAL** is a multi-disciplinary open access archive for the deposit and dissemination of scientific research documents, whether they are published or not. The documents may come from teaching and research institutions in France or abroad, or from public or private research centers.

L'archive ouverte pluridisciplinaire **HAL**, est destinée au dépôt et à la diffusion de documents scientifiques de niveau recherche, publiés ou non, émanant des établissements d'enseignement et de recherche français ou étrangers, des laboratoires publics ou privés.

## Journal Pre-proof

Radium isotopes as submarine groundwater discharge (SGD) tracers: Review and recommendations

J. Garcia-Orellana, V. Rodellas, J. Tamborski, M. Diego-Feliu, P. van Beek, Y. Weinstein, M. Charette, A. Alorda-Kleinglass, H.A. Michael, T. Stieglitz, J. Scholten



PII: S0012-8252(21)00182-3

DOI: <https://doi.org/10.1016/j.earscirev.2021.103681>

Reference: EARTH 103681

To appear in: *Earth-Science Reviews*

Received date: 29 December 2020

Revised date: 23 April 2021

Accepted date: 11 May 2021

Please cite this article as: J. Garcia-Orellana, V. Rodellas, J. Tamborski, et al., Radium isotopes as submarine groundwater discharge (SGD) tracers: Review and recommendations, *Earth-Science Reviews* (2021), <https://doi.org/10.1016/j.earscirev.2021.103681>

This is a PDF file of an article that has undergone enhancements after acceptance, such as the addition of a cover page and metadata, and formatting for readability, but it is not yet the definitive version of record. This version will undergo additional copyediting, typesetting and review before it is published in its final form, but we are providing this version to give early visibility of the article. Please note that, during the production process, errors may be discovered which could affect the content, and all legal disclaimers that apply to the journal pertain.

© 2021 Published by Elsevier B.V.

# Radium isotopes as submarine groundwater discharge (SGD) tracers: review and recommendations

J. Garcia-Orellana<sup>1,2,\*</sup>; V. Rodellas<sup>1</sup>; J. Tamborski<sup>3</sup>; M. Diego-Feliu<sup>1</sup>; P. van Beek<sup>4</sup>; Y. Weinstein<sup>5</sup>; M. Charette<sup>6</sup>; A. Alorda-Kleinglass<sup>1</sup>; H.A. Michael<sup>7,8</sup>; T. Stieglitz<sup>9</sup>; J. Scholten<sup>10</sup>

<sup>1</sup>ICTA-UAB, Institut de Ciència i Tecnologia Ambientals, Universitat Autònoma de Barcelona, E-08193 Bellaterra, Spain.

<sup>2</sup>Departament de Física, Universitat Autònoma de Barcelona, E-08193 Bellaterra, Spain.

<sup>3</sup>Department of Ocean and Earth Sciences, Old Dominion University, Norfolk, VA, USA

<sup>4</sup>Laboratoire d'Etudes en Géophysique et Océanographie Spatiales (LEGOS), Université de Toulouse, CNES/CNRS/IRD/Université Toulouse III Paul Sabatier, Toulouse, France

<sup>5</sup>Department of Geography and Environment, Bar-Ilan University, Ramat-Gan, 52900, Israel

<sup>6</sup>Department of Marine Chemistry and Geochemistry, Woods Hole Oceanographic Institution, Woods Hole, MA, USA

<sup>7</sup>Department of Earth Sciences, University of Delaware, Newark, DE, USA

<sup>8</sup>Department of Civil and Environmental Engineering, University of Delaware, Newark, DE, USA

<sup>9</sup>Aix-Marseille Université, CNRS, IRD, INRAE, Coll France, CEREGE, Aix-en-Provence, France.

<sup>10</sup>Institute of Geosciences, Kiel University, Germany

\*Corresponding author:

Jordi Garcia-Orellana Tel (+34) 935868285

e-Mail address: jordi.garcia@uab.cat

27	<b>Abstract</b>
28	<b>[1] Introduction</b>
29	<b>[2] Ra isotopes used as SGD tracers: Historical perspective</b>
30	[2.1] Early days: Ra isotopes as tracers of marine processes (1900 – 1990)
31	[2.2] Development period: Ra as SGD tracers (1990 – 2000).
32	[2.3] The widespread application of Ra isotopes as SGD tracers (2000 – 2020)
33	<b>[3] Submarine Groundwater Discharge: Terminology</b>
34	<b>[4] Mechanisms controlling Ra in aquifers and SGD</b>
35	[4.1] Production & Decay of Ra
36	[4.2] Adsorption and desorption
37	[4.3] Weathering and precipitation
38	[4.4] Groundwater transit time
39	<b>[5] Sources and sinks of Ra isotopes in the water column</b>
40	[5.1] Radium sources
41	[5.2] Radium sinks
42	<b>[6] Ra-derived SGD quantification</b>
43	[6.1] Ra-based approaches to quantify SGD
44	[6.2] Determination of the Ra concentration in the SGD endmember
45	<b>[7] Improving the current use of Ra isotopes as SGD tracers</b>
46	[7.1] Validation of model assumptions and consideration of conceptual uncertainties
47	[7.2] The assumption of steady-state needs to be validated
48	[7.3] Ra isotopes cannot be used indistinctly to trace SGD
49	[7.4] The Ra isotope(s) used need to be carefully selected
50	[7.5] Ra isotopes can contribute identifying the pathways of SGD
51	[7.6] Estimates of SGD-driven solute fluxes need to account for the variable composition of
52	different pathways
53	<b>[8] Additional applications of Ra isotopes in groundwater and marine studies</b>
54	[8.1] Assessment of groundwater transit times in coastal aquifers
55	[8.2] Solute transfer across the sediment–water interface derived from Ra isotopes
56	[8.3] Estimation of timescales in coastal surface waters
57	[8.4] Ra-228 as tracer of offshore solute fluxes
58	<b>[9] Conclusions and the Future stage (&gt;2020)</b>
59	[9.1] Guidelines to conduct a SGD study
60	[9.2] Knowledge gaps and research needs
61	

## 62 Abstract

63

64 Submarine groundwater discharge (SGD) is now recognized as an important process of the  
65 hydrological cycle worldwide and plays a major role as a conveyor of dissolved compounds  
66 to the ocean. Naturally occurring radium isotopes ( $^{223}\text{Ra}$ ,  $^{224}\text{Ra}$ ,  $^{226}\text{Ra}$  and  $^{228}\text{Ra}$ ) are widely  
67 employed geochemical tracers in marine environments. Whilst Ra isotopes were initially  
68 predominantly applied to study open ocean processes and fluxes across the continental  
69 margins, their most common application in the marine environment has undoubtedly  
70 become the identification and quantification of SGD. This review focuses on the application  
71 of Ra isotopes as tracers of SGD and associated inputs of water and solutes to the coastal  
72 ocean. In addition, we review i) the processes controlling Ra enrichment and depletion in  
73 coastal groundwater and seawater; ii) the systematics applied to estimate SGD using Ra  
74 isotopes and iii) we summarize additional applications of Ra isotopes in groundwater and  
75 marine studies. We also provide some considerations that will help refine SGD estimates  
76 and identify the critical knowledge gaps and research needs related to the current use of Ra  
77 isotopes as SGD tracers.

78

79

## 80 [1] Introduction

81

82 Radium (Ra) is the element number 88 in the Periodic Table and it belongs to Group IIA, the  
83 alkaline earth metals. There are four naturally occurring radium isotopes ( $^{224}\text{Ra}$ ,  $^{223}\text{Ra}$ ,  $^{228}\text{Ra}$   
84 and  $^{226}\text{Ra}$ ), which are continuously produced by the decay of their Th-isotope parents of the  
85 uranium and thorium decay series ( $^{228}\text{Th}$ ,  $^{227}\text{Th}$ ,  $^{232}\text{Th}$  and  $^{230}\text{Th}$ , respectively). The most  
86 abundant isotopes are  $^{226}\text{Ra}$  from the  $^{238}\text{U}$  decay chain, an alpha-gamma emitter with a half-  
87 life of 1600 y, and  $^{228}\text{Ra}$  from the  $^{232}\text{Th}$  decay chain, a beta emitter with a half-life of 5.8 y.  
88 There are two short-lived isotopes that also occur naturally,  $^{223}\text{Ra}$  and  $^{224}\text{Ra}$ , which are  
89 alpha-gamma emitters from the  $^{235}\text{U}$  and  $^{232}\text{Th}$  decay chains with half-lives of 11.4 d and 3.6  
90 d, respectively. Uranium and thorium are widely distributed in nature, mainly in soils,  
91 sediments and rocks, and thus the four Ra isotopes are continuously produced in the  
92 environment at a rate that depends on the U and Th content and the half-life of each Ra  
93 isotope.

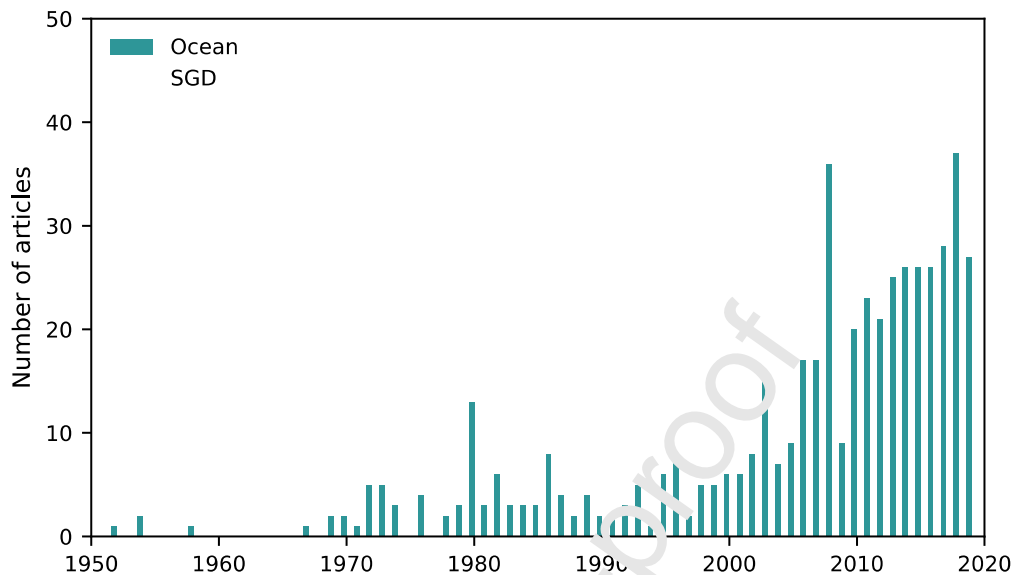
94

95 Radium isotopes are widely recognized as important geochemical tracers in marine  
96 environments, mainly because i) they behave conservatively in seawater (i.e., lack of  
97 significant chemical and biological additions or removal); ii) they decay at a known rate and  
98 iii) they are primarily produced from water-rock and sediment-water interactions.  
99 Consequently, Ra isotopes have been traditionally used to trace land-ocean interaction  
100 processes (e.g., Charette et al., 2016; Elsinger and Moore, 1983; Knauss et al., 1978), which  
101 is also referred to as boundary exchange processes (e.g., Jeandel, 2016), as well as to  
102 estimate mixing rates, apparent ages or residence times, in particular in coastal and ocean  
103 waters (e.g., Annett et al., 2013; Burt et al., 2013a; Ku and Luo, 2008; Moore, 2000a, 2000b;  
104 Moore et al., 2006; Tomasky-Holmes et al., 2013), but also in aquifers (e.g., Diego-Feliu et  
105 al., 2021; Kraemer, 2005; Liao et al., 2020; Molina-Porras et al., 2020) and hydrothermal  
106 systems (e.g., Kadko and Moore, 1980; Neuholz et al., 2020).

107

108 Whilst initially applied to study open ocean processes and to estimate different exchange  
109 processes across the continental margins, the most common application of Ra isotopes in  
110 the marine environment has undoubtedly been the quantification of water and solute fluxes  
111 from land to the coastal sea, driven by Submarine Groundwater Discharge (SGD) (Figure 1)  
112 (Ma and Zhang, 2020). Radium isotopes have been used to quantify SGD in a wide range of  
113 marine environments, including sandy beaches (e.g., Bokuniewicz et al., 2015; Evans and  
114 Wilson, 2017; Rodellas et al., 2014), bays (e.g., Beck et al., 2008; Hwang et al., 2005; Lecher  
115 et al., 2016; Zhang et al., 2017), estuaries (e.g., Luek and Beck, 2014; Wang and Du, 2016;  
116 Young et al., 2008), coastal lagoons (e.g., Gattacceca et al., 2011; Rapaglia et al., 2010;  
117 Tamborski et al., 2019), salt marshes (e.g., Charette et al., 2003), large continental shelves  
118 (e.g., Liu et al., 2014; Moore, 1996; Wang et al., 2014), ocean basins (e.g., Moore et al.,  
119 2008; Rodellas et al., 2015a) and the global ocean (e.g., Kwon et al., 2014). SGD is now  
120 recognized as an important process worldwide and plays a major role as a conveyor of  
121 dissolved compounds to the ocean (e.g., nutrients, metals, pollutants) (Cho et al., 2018;  
122 Moore, 2010; Rodellas et al., 2015a). Thus, SGD has significant implications for coastal  
123 biogeochemical cycles (e.g., Adolf et al., 2019; Andrisoa et al., 2019; Garcés et al., 2011;  
124 Garcia-Orellana et al., 2016; Ruiz-González et al., 2021; Santos et al., 2021; Sugimoto et al.,  
125 2017). This review is focused on the application of Ra isotopes as tracers of SGD-derived  
126 inputs of water and solutes to the coastal ocean but also aims to provide some

127 considerations that will help refine SGD estimates and identify critical knowledge gaps and  
 128 research needs related to the current use of Ra isotopes as SGD tracers.  
 129



130  
 131 **Figure 1.** Record of published research articles that used the keywords 1) ‘radium’ and ‘submarine  
 132 ground-water discharge’ (n= 511) and 2) ‘radium’ and ‘ocean’ (n= 477), as indexed by Web of Science.  
 133 Articles related to NORM, radiation protection or radionuclide concentrations have been removed from the  
 134 record of ‘radium’ and ‘ocean’.  
 135

## 136 [2] Radium isotopes used as SGD tracers: Historical perspective

137

### 138 [2.1] Early days: Radium isotopes as tracers of marine processes (1900 – 1990)

139

140 Radium was discovered from pitchblende ore in 1889 by Marie Sklodowska-Curie and Pierre  
 141 Curie, representing one of the first elements discovered by means of its radioactive  
 142 properties (Porcelli et al., 2014). This historic discovery initiated a remarkable use of Ra for  
 143 medical, industrial and scientific purposes, including its use as an ocean tracer. Early oceanic  
 144 investigations revealed elevated  $^{226}\text{Ra}$  activities in deep-sea sediments (Joly, 1908), but the  
 145 first measurement of  $^{226}\text{Ra}$  activities in seawater was performed in 1911 to characterize the  
 146 penetrating radiation observed in the ionization chambers of ships at sea (Simpson et al.,  
 147 1911). However, it was not until the publication of the first profile of Ra activities in  
 148 seawater and sediments off the coast of California by Evans et al. (1938), which suggested  
 149 the influence of sediments on the increase of seawater  $^{226}\text{Ra}$  activities with depth, that the  
 150 use of Ra isotopes to study oceanographic processes was considered. The first true  
 151 application of Ra as an oceanic tracer was by Koczy (1958), who showed that the primary  
 152 oceanic source of  $^{226}\text{Ra}$  was  $^{230}\text{Th}$  decay in marine sediments, and who initiated the use of  
 153 one-dimensional vertical diffusion models to describe the upward flux and characteristic  
 154 concentration profiles of  $^{226}\text{Ra}$ . Shortly thereafter, Koczy (1963) estimated that  
 155 approximately 1 – 5 % of the actual  $^{226}\text{Ra}$  present in seawater was supplied by rivers. This  
 156 was followed by a study of water column mixing and ventilation rates in the different

157 oceans (Broecker et al., 1967). A global-scale picture of the distribution of long-lived Ra  
158 isotopes ( $^{226}\text{Ra}$  and  $^{228}\text{Ra}$ ) was first provided by the Geochemical Ocean Sections Study  
159 (GEOSECS – 1972 – 1978; e.g., Chan et al., 1977; Trier et al., 1972).

160  
161 In the mid 1960s, Blanchard and Oakes (1965) reported elevated activities of  $^{226}\text{Ra}$  in coastal  
162 waters relative to open ocean waters. The detection of significant activities of  $^{228}\text{Ra}$  in both  
163 surface and bottom waters led to the understanding that the distribution of radium  
164 depended on sediments but also on other sources that introduced Ra into the oceans  
165 (Kaufman et al., 1973; Moore, 1969). Few years later, Li et al. (1977) observed a higher  
166 concentration of  $^{226}\text{Ra}$  in the Hudson River estuary compared with those observed either in  
167 the river itself or in the adjacent surface ocean water, proposing that  $^{226}\text{Ra}$  was released by  
168 estuarine and continental shelf sediments, which represents an important source of  $^{226}\text{Ra}$  to  
169 the ocean. This was further corroborated by measurements in the Pee Dee River-Winyah  
170 Bay estuary, in South Carolina, USA, by Elsinger and Moore (1977) who concluded that Ra  
171 desorption from sediments could quantitatively explain the increase of  $^{226}\text{Ra}$  in brackish  
172 water. Several studies followed these initial investigations, highlighting the importance of  
173 coastal sediments in the release of long-lived Ra-isotopes to coastal waters (e.g., Li and  
174 Chan, 1979; Moore, 1987).

175  
176 Measurement of  $^{226}\text{Ra}$  and  $^{228}\text{Ra}$  in seawater samples was relatively complex prior to the  
177 wide-scale availability of high-purity germanium (HPGe) gamma detectors and the  
178 extraction of Ra from seawater using manganese-impregnated acrylic fibers. While  $^{226}\text{Ra}$   
179 was measured in a few liters of seawater (1 – 10 L) by the emanation of  $^{222}\text{Rn}$  (Mathieu et  
180 al., 1988), the measurement of  $^{228}\text{Ra}$  required greater volumes (often  $\gg 100$  L). The  
181 quantification of  $^{228}\text{Ra}$  proceeded either via the extraction of  $^{228}\text{Ac}$  and the measurement of  
182 its beta activity or via the partial ingrowth of  $^{228}\text{Th}$  over a period of at least 4 – 12 months  
183 and the measurement via the alpha recoil of  $^{228}\text{Th}$  or via its daughter  $^{224}\text{Ra}$  by a proportional  
184 counter (Moore, 1981; Moore, 1969). The introduction of manganese-impregnated acrylic  
185 fibers for sampling Ra isotopes in the ocean was also a key advance in the use of Ra as a  
186 tracer in marine environments (Moore, 1976; Moore and Reid, 1973). Before the  
187 development of this approach, large volumes of seawater and long and laborious  
188 procedures were required to concentrate Ra isotopes via  $\text{BaSO}_4$  precipitation (Kaufman et  
189 al., 1973; Moore, 1969, 1972; Trier et al., 1972). Since then, Ra isotopes in marine waters  
190 are concentrated in situ with minimum time and effort by manganese-impregnated acrylic  
191 fibers. More recently, mass spectrometry has been used for  $^{226}\text{Ra}$  determination in  
192 seawater, such as thermal ionization mass spectrometry (TIMS) (e.g., Ollivier et al., 2008),  
193 multicollector inductively coupled plasma mass spectrometry (MC-ICP-MS) (e.g., Hsieh and  
194 Henderson, 2011) or single-collector sector field (ICP-MS) (e.g., Vieira et al., 2021).

195  
196 The application of the short-lived  $^{223}\text{Ra}$  and  $^{224}\text{Ra}$  as tracers of marine processes lagged the  
197 long-lived Ra isotopes by several years due to analytical limitations and because their  
198 potential use in oceanic studies was limited due to their shorter half-lives (11.4 d and 3.6 d  
199 for  $^{223}\text{Ra}$  and  $^{224}\text{Ra}$ , respectively). Short-lived Ra isotopes were first applied to estuarine  
200 mixing studies, which have time-scales of 1 – 10 days. Elsinger and Moore (1983) published  
201 one of the first studies on the distribution of  $^{224}\text{Ra}$ ,  $^{226}\text{Ra}$  and  $^{228}\text{Ra}$ , which was focused on  
202 the mixing zone of the Pee Dee River-Winyah Bay and Delaware Bay estuaries (USA). They  
203 showed that the main source of Ra-isotopes were desorption and diffusion from suspended

204 and bottom sediments, which together contributed to the non-conservative increase of the  
205 three isotopes in the river-sea mixing zone. Shortly thereafter, Bollinger and Moore (1984)  
206 suggested that  $^{224}\text{Ra}$  and  $^{228}\text{Ra}$  fluxes in a salt marsh from the US eastern coast could be  
207 supported by bioirrigation and bioturbation (i.e. sediment reworking and pumping driven by  
208 benthic fauna, respectively). Levy and Moore (1985) concluded that the potential use of  
209  $^{224}\text{Ra}$  as a tracer required a much better understanding of its input functions in coastal  
210 zones. The authors classified Ra sources into two main groups: (1) primary sources that  
211 include desorption from estuaries and salt marsh particles and; (2) secondary sources such  
212 as dissolved  $^{228}\text{Th}$  present in the water column, longshore currents that may transport  $^{224}\text{Ra}$   
213 from other areas and in situ production from  $^{228}\text{Th}$  decay adsorbed on suspended particles  
214 or bottom sediments.

215

## 216 [2.2] Development period: Radium isotopes as SGD tracers (1990 - 2000).

217

218 Whilst the concept of SGD had been introduced in several early hydrological-based studies  
219 (e.g., Bokuniewicz, 1992, 1980; Capone and Bautista, 1985; Cooper, 1959; Freeze and  
220 Cherry, 1979; Glover, 1959; Johannes, 1980; Kohout, 1966; Toth, 1963), the role of  
221 groundwater as a major conveyor of Ra isotopes to the coastal ocean was not established  
222 until the benchmark papers of Burnett et al. (1990), Veeh et al. (1995) and Rama and Moore  
223 (1996). Burnett et al. (1990) suggested that the high  $^{226}\text{Ra}$  activities in water from the  
224 Suwannee estuary (USA) and offshore were most likely supplied by submarine springs or  
225 seeps. Veeh et al. (1995) demonstrated that the “traditional” Ra sources to coastal waters  
226 (e.g., rivers, sediments) were insufficient to support the  $^{226}\text{Ra}$  activities in waters from the  
227 Spencer Gulf (South Australia), suggesting an external source for the excess  $^{226}\text{Ra}$ , such as  
228 the “submarine discharge of groundwater from granitic basement rocks”. The importance of  
229 groundwater as a source of Ra to the coastal sea led Rama and Moore (1996) to apply for  
230 the first time the four naturally occurring Ra isotopes (which they defined as the radium  
231 quartet) as tracers for quantifying groundwater flows and water exchange (North Inlet salt  
232 marsh, South Carolina, USA). One key finding of this study was that extensive mixing  
233 between fresh groundwater and saline marsh porewater occurred in the subsurface marsh  
234 sediment before discharging to the coastal ocean, resulting in a groundwater discharge that  
235 was not entirely fresh but included a component of seawater circulating through the coastal  
236 aquifer. This concept was previously demonstrated in a hydrology-based study in Great  
237 South Bay (NY, USA) conducted by Bokuniewicz (1992), and it decisively contributed  
238 towards defining the term SGD.

239

240 Awareness of the volumetric and chemical importance of SGD was significantly increased by  
241 Moore (1996), who linked  $^{226}\text{Ra}$  enrichments in coastal shelf waters of the South Atlantic  
242 Bight to large amounts of direct groundwater discharge. Moore suggested that the volume  
243 of SGD over this several hundred-kilometer coastline was comparable to the observed  
244 discharge from rivers, although the SGD probably included brackish and saline groundwater.  
245 In a commentary on this article, Younger (1996) questioned the inclusion of salty  
246 groundwater as a component of SGD, and its comparison to freshwater discharge to the  
247 coastal zone via rivers. The rebuttal by Church (1996) argued that SGD, regardless of its  
248 salinity, is chemically distinct from seawater and therefore can exert a significant control on  
249 coastal ocean biogeochemical cycles.

250

251 In the same year, Moore and Arnold (1996) published the design of the Radium Delayed  
252 Coincidence Counter (RaDeCC), an alpha detector system that allowed a simple and reliable  
253 determination of the short-lived Ra isotopes ( $^{223}\text{Ra}$  and  $^{224}\text{Ra}$ ) based on an original design of  
254 Giffin et al. (1963). Since its introduction, the RaDeCC system has become the reference  
255 technique for quantifying short-lived radium isotopes in water samples, as it allows a robust  
256 and rapid  $^{223}\text{Ra}$  and  $^{224}\text{Ra}$  determination with a simple setup at a relatively low cost. The full  
257 potential of short-lived Ra isotopes was described shortly after, when Moore published two  
258 studies providing conceptual models to derive ages of coastal waters and estimate coastal  
259 mixing rates using  $^{223}\text{Ra}$  and  $^{224}\text{Ra}$  (Moore, 2000b, 2000a).

260

261 In the period of 1990 - 2000, these pioneering researchers opened a new era in Ra isotope  
262 application to SGD quantification, including the development of most of the conceptual  
263 models, approaches and techniques that are currently in use.

264

### 265 [2.3] The widespread application of Ra isotopes as SGD tracers (2000 – 2020)

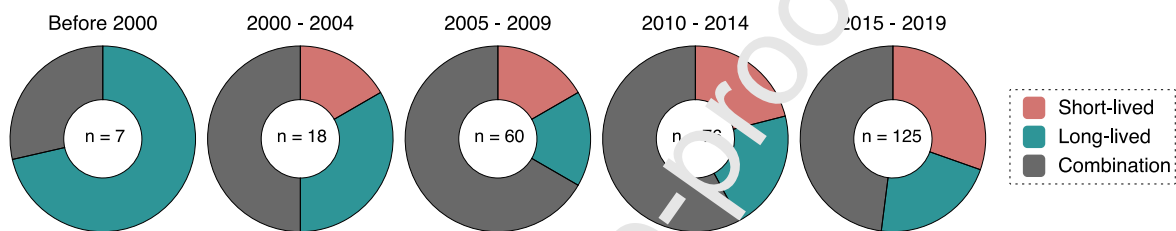
266

267 The pioneering work on Ra isotopes of the 1990s, the increased understanding of the  
268 importance of SGD in coastal biogeochemical cycles, the technical improvements of Ra  
269 determination via HPGe and the commercialization of the first RaDeCC systems led to a  
270 rapid increase in the number of studies using Ra isotopes as tracers of SGD (Figure 1).  
271 Hundreds of scientific articles have been published since then. During the 2000s, while  
272 some studies only used long-lived Ra isotopes as SGD tracers (e.g., Charette and Buesseler,  
273 2004; Kim et al., 2005; Krest et al., 2007), most studies combined measurements of short-  
274 lived Ra isotopes to estimate water residence times (or mixing rates) and long-lived Ra  
275 isotopes to quantify SGD fluxes (e.g., Charette et al., 2003, 2001; Kelly and Moran, 2002;  
276 Moore, 2003). However, a few studies quantified SGD fluxes by using only short-lived Ra  
277 isotopes (Figure 2; Boehm et al., 2004; Krest and Harvey, 2003; Paytan et al., 2004). One of  
278 the first studies where SGD fluxes were derived exclusively from short-lived Ra isotopes  
279 ( $^{223}\text{Ra}$  and  $^{224}\text{Ra}$ ) was conducted at Huntington Beach (CA, USA) by Boehm et al. (2004).  
280 Their flux estimates based on  $^{223}\text{Ra}$  and  $^{224}\text{Ra}$  were supported by a later analysis of  $^{226}\text{Ra}$  at  
281 this location and by the results of a hydrological numerical model (Boehm et al., 2006). At  
282 the same period, Howard et al. (2005) and Paytan et al. (2006) used only short-lived Ra  
283 isotopes to estimate SGD fluxes of water and associated nutrients. Over the last decade  
284 there has been a growing volume of studies using only the short-lived Ra isotopes as tracers  
285 of SGD (e.g., Baudron et al., 2015; Ferrarin et al., 2008; Garcia-Orellana et al., 2010; Krall et  
286 al., 2017; Shellenbarger et al., 2006; Tamborski et al., 2015; Trezzi et al., 2016). This relative  
287 abundance of publications, in which only short-lived Ra isotopes are used, is in contrast with  
288 those conducted in previous decades, in which long-lived Ra isotopes were the most applied  
289 tracers (Figure 2).

290

291 The methodological advances in the measurement of short-lived Ra isotopes have also  
292 contributed to their widespread application as tracers of other coastal processes, such as  
293 water and solute transfer across the sediment-water interface (also referred to as  
294 porewater exchange (Cai et al., 2014), groundwater age as well as flow rates in coastal  
295 aquifers (Kiro et al., 2013, 2012; Diego-Feliu et al., 2021), secondary permeability in animal  
296 burrows (Stieglitz et al., 2013), transfer of sediment-derived material inputs (Burt et al.,  
297 2013b; Sanial et al., 2015; Vieira et al., 2020, 2019), and horizontal and vertical coastal

298 water mixing rates (Annett et al., 2013; Charette et al., 2007; Colbert and Hammond, 2007).  
 299 Numerous new uses of the RaDeCC system have occurred in recent years, including the  
 300 development of approaches to measure  $^{223}\text{Ra}$  and  $^{224}\text{Ra}$  in sediments (Cai et al., 2014, 2012)  
 301 or  $^{228}\text{Ra}$  and  $^{226}\text{Ra}$  activities in water (Diego-Feliu et al., 2020; Geibert et al., 2013; Peterson  
 302 et al., 2009; Waska et al., 2008), as well as quantification advancements and guidelines  
 303 (Diego-Feliu et al., 2020; Moore, 2008; Selzer et al., 2021). There is still a widespread  
 304 application of long-lived Ra isotopes, particularly to quantify SGD occurring over long flow  
 305 paths (Moore, 1996; Rodellas et al., 2017; Tamborski et al., 2017a), SGD into entire ocean  
 306 basins or the global ocean (Cho et al., 2018; Kwon et al., 2014; Moore et al., 2008; Rodellas  
 307 et al., 2015a) and as a shelf flux gauge (Charette et al., 2016). Some investigations have also  
 308 considered how to combine short- and long-lived Ra isotopes to discriminate between  
 309 different SGD flow paths and sources (e.g., Charette et al., 2008; Moore, 2003; Rodellas et  
 310 al., 2017; Tamborski et al., 2017a).  
 311



312 **Figure 2.** Number of research articles published in 5-year periods in which Ra isotopes have been used as  
 313 tracers of SGD. The articles were classified according to the Ra isotopes used: only short-lived ( $^{223}\text{Ra}$   
 314 and/or  $^{224}\text{Ra}$ ), only long-lived ( $^{226}\text{Ra}$  and/or  $^{228}\text{Ra}$ ) or a combination of both. The search was performed  
 315 using the words "SGD or Submarine Groundwater Discharge" AND "Ra or Radium" as keywords in "Web  
 316 of Science" (n= 477). Reviews, method articles and studies not applying Ra isotopes as tracer of SGD-  
 317 related processes were excluded from this classification. A total of 286 articles were considered in this  
 318 classification analysis.  
 319  
 320

### 321 [3] Submarine Groundwater Discharge: Terminology

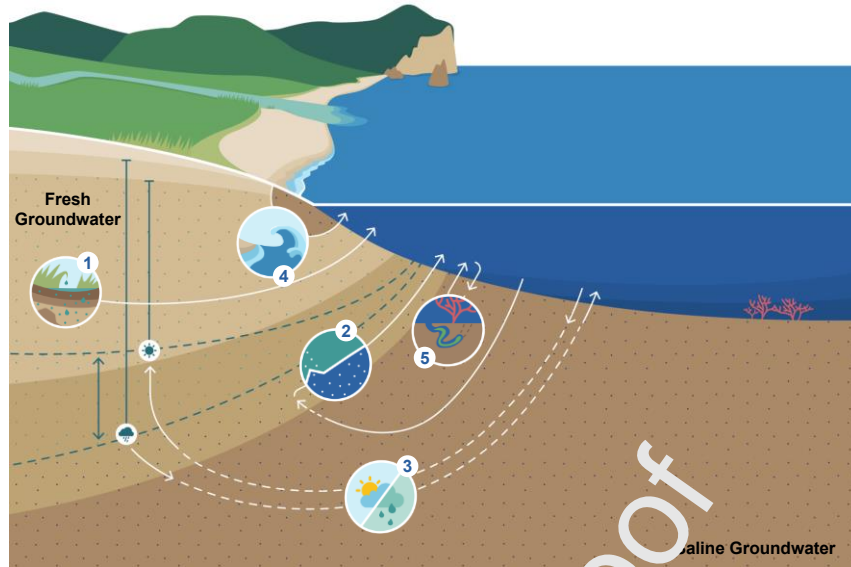
322  
 323 Initially, the concept of groundwater discharge into the oceans had been investigated  
 324 largely by hydrologists who considered the discharge of meteoric groundwater as a  
 325 component of the hydrological budget (Manheim, 1967). Thereafter, with the involvement  
 326 of oceanographers interested in the influence of SGD on the chemistry of the ocean, the  
 327 definition evolved, with SGD now encompassing both meteoric groundwater and circulated  
 328 seawater (Bokuniewicz, 1992; Church, 1996; Moore, 1996; Rama and Moore, 1996). The  
 329 interest in SGD has increasingly grown within the scientific community as it is now  
 330 recognized as an important pathway for the transport of chemical compounds between land  
 331 and ocean, which can strongly affect marine biogeochemical cycles at local, regional and  
 332 global scales (e.g., Cho et al., 2018; Luijendijk et al., 2020; Rahman et al., 2019; Rodellas et  
 333 al., 2015a).  
 334

335 The definition of SGD has been discussed in several review papers in the marine geosciences  
 336 field (e.g., Burnett et al., 2002, 2001, 2003; Church, 1996; Knee and Paytan, 2011; Moore,  
 337 2010; Santos et al., 2012; Taniguchi et al., 2019, 2002). Here, we will adopt the most  
 338 inclusive definition, where SGD represents "the flow of water through continental and

339 *insular margins from the seabed to the coastal ocean, regardless of fluid composition or*  
340 *driving force”* (Burnett et al., 2003; Taniguchi et al., 2019). We are thus including those  
341 centimeter-scale processes that can transport water and associated solutes across the  
342 sediment-water interface, which are commonly referred to as porewater exchange (PEX) or  
343 benthic fluxes, and are sometimes excluded from the SGD definition because of its short  
344 length scale (<1 m) (e.g., Moore, 2010; Santos et al., 2012). We are also implicitly  
345 considering that groundwater (defined as “any water in the ground”) is synonymous with  
346 porewater (Burnett et al., 2003) and that the term “coastal aquifer” includes permeable  
347 marine sediments. The term “subterranean estuary” (STE), which is widely used in the SGD  
348 literature, is also used in this review to refer to the part of the coastal aquifer that  
349 dynamically interacts with the ocean (Duque et al., 2020; Moore, 1999), determined in the  
350 hydrological literature as the fresh-saline water interface (FSI) or the mixing zone.

351  
352 Within this broad definition of SGD we incorporate disparate water flow processes, some  
353 involving the discharge of fresh groundwater and others encompassing the circulation of  
354 seawater through the subterranean estuary, or a mixture of both. These processes can be  
355 grouped into five different SGD pathways according to the characteristics of the processes  
356 (George et al., 2020; Michael et al., 2011; Robinson et al., 2018; Santos et al., 2012) (Figure  
357 3): 1) **Terrestrial groundwater discharge** (usually fresh groundwater), driven by the  
358 hydraulic gradient between land and the sea; 2) **Density-driven seawater circulation**,  
359 caused by either density gradients along the freshwater-saltwater interface, or  
360 thermohaline gradients in permeable sediments; 3) **Seasonal exchange of seawater**, driven  
361 by the movement of the freshwater-saltwater interface due to temporal variations in  
362 aquifer recharge or sea level fluctuations; 4) **Shoreface circulation of seawater**, including  
363 intertidal circulation driven by tidal inundation (at beach faces, salt marshes or mangroves)  
364 and wave set-up; and 5) **cm-scale porewater exchange (PEX)**, driven by disparate  
365 mechanisms such as current-bedform interactions, bioirrigation, tidal and wave pumping,  
366 shear flow, ripple migration, etc. Notice that whereas all of these processes force water flow  
367 through the sediment-water interface, the discharge of terrestrial groundwater (Pathway 1)  
368 and, to a lesser extent, density-driven seawater circulation (Pathway 2), which also contains  
369 a fraction of freshwater, are the only mechanisms that represents a net source of water to  
370 the coastal ocean. Pathways 3 – 5 can be broadly classified as “saline SGD”; the summation  
371 of all five pathways is generally considered “total SGD”.

372



373

**Figure 3.** Conceptual diagram of an unconfined coastal aquifer including the major Submarine Groundwater Discharge pathways, subdivided according to the driving mechanism: 1) Terrestrial groundwater discharge (usually fresh groundwater); 2) Density-driven seawater circulation; 3) Seasonal exchange of seawater; 4) Shoreface seawater circulation; and 5) cm-scale porewater exchange (PEX). Pathways 1, 2 and 3 could be extended farther offshore in systems with confined units.

374

#### 375 [4] Mechanisms controlling Ra in aquifers and SGD

376

377 One of the main characteristics that makes Ra isotopes useful tracers of SGD is that coastal  
 378 groundwater is often greatly enriched with Ra isotopes relative to coastal seawater (Burnett  
 379 et al., 2001). The enrichment of groundwater with Ra isotopes is originated from the  
 380 interaction of groundwater with rocks, soils or minerals that comprise the geological matrix  
 381 of the coastal aquifer. Some studies have summarized the various sources and sinks of Ra  
 382 isotopes in coastal groundwater (Kiro et al., 2012; Krishnaswami et al., 1982; Luo et al.,  
 383 2018; Porcelli et al., 2014; Tricca et al., 2001). The most common natural processes that  
 384 regulate the activity of Ra isotopes in groundwater are: 1) radioactive production from Th  
 385 isotopes and decay; 2) adsorption and desorption from the aquifer solids and 3) weathering  
 386 and precipitation. The transit time of groundwater in the coastal aquifer can further  
 387 regulate process 1 (Figure 4).

388

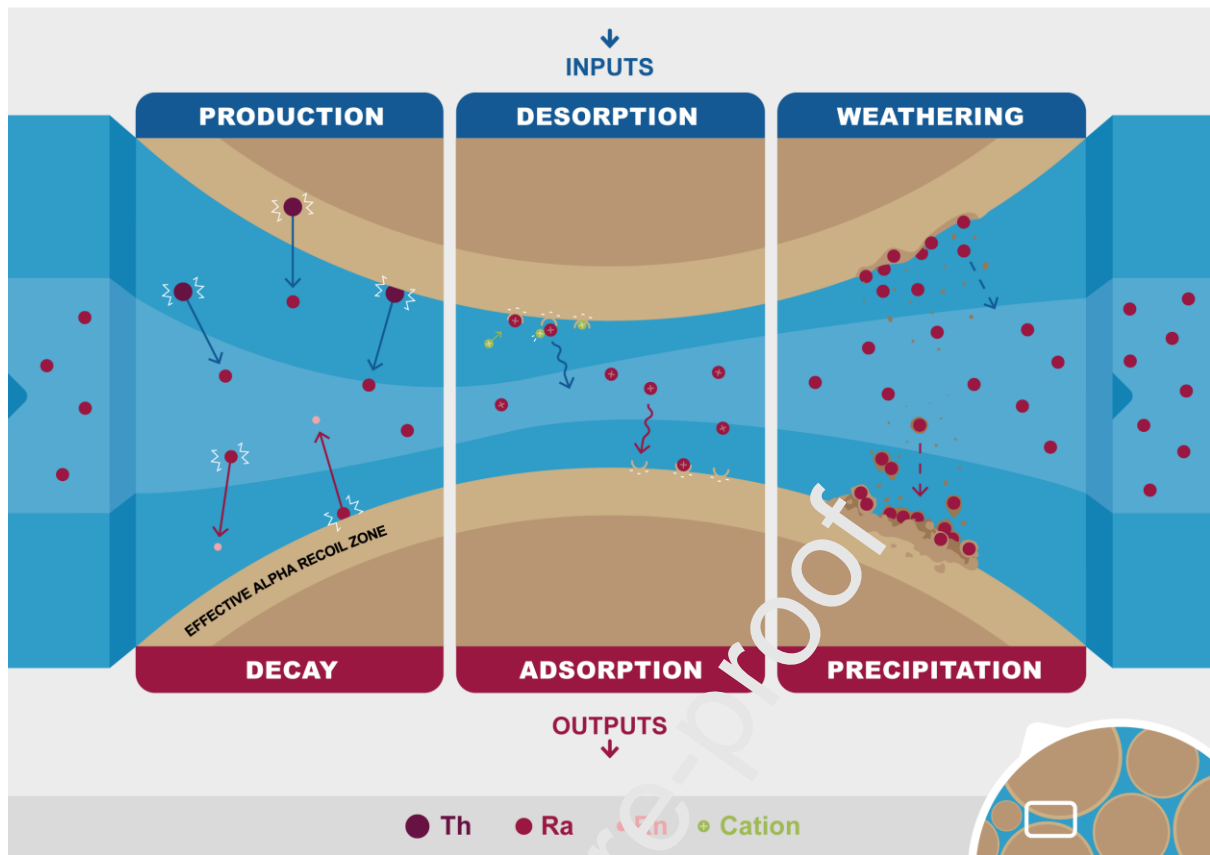


**Figure 4.** Conceptual model of the main processes determining the abundance of Ra isotopes in groundwater from a coastal aquifer. Blue and brown colour represents the liquid and solid phases, respectively. The light brown color represents the effective alpha recoil zone for Ra isotopes, which depends on the aquifer solids and the energy of the Ra alpha particle (the recoil distance usually ranges, on average, between 300 and 400 Å (Sun and Semkow, 1998)).

389

#### 390 [4.1] Radioactive production and decay

391

392 Ra activity in groundwater is controlled, in part, by the production and decay rates of each  
 393 radionuclide in both the groundwater and the geological matrix (Figure 4). Radium isotope  
 394 production depends on the continuous decay of Th isotopes ( $^{230}\text{Th}$ ,  $^{232}\text{Th}$ ,  $^{228}\text{Th}$ , and  $^{227}\text{Th}$ )  
 395 from the U and Th decay chains, which are predominantly contained in aquifer solids.  
 396 Therefore, the U and Th content of the geological matrix regulates the production rate.  
 397 Concentrations of U and Th can vary significantly depending on the host material (igneous  
 398 rocks:  $1.2 - 75 \text{ Bq}\cdot\text{kg}^{-1}$  of U and  $0.8 - 134 \text{ Bq}\cdot\text{kg}^{-1}$  of Th; metamorphic rocks:  $25 - 60 \text{ Bq}\cdot\text{kg}^{-1}$   
 399 of U and  $20 - 110 \text{ Bq}\cdot\text{kg}^{-1}$  of Th; and sedimentary rocks:  $<1.2 - 40 \text{ Bq}\cdot\text{kg}^{-1}$  of U and  $<4$  and  $40$   
 400  $\text{Bq}\cdot\text{kg}^{-1}$  of Th) (Ivanovich and Harmon, 1992). For instance, carbonate minerals are enriched  
 401 in U relative to Th, while clays are enriched in Th. As a consequence, groundwater flowing  
 402 through formations with different lithologies have different activity ratios of Ra isotopes  
 403 (e.g.,  $^{228}\text{Ra}/^{226}\text{Ra}$  AR, where AR means activity ratio), which can be used to identify and  
 404 distinguish groundwater inflowing from different hydrogeologic units (Charette and  
 405 Buesseler, 2004; Moore, 2006a; Swarzenski et al., 2007a) (see Section 6). On the other  
 406 hand, radioactive decay depends only on the activity of Ra isotopes in groundwater and  
 407 their specific decay constants.

408

409 Not all of the Ra produced in the aquifer is directly transferred to groundwater. The fraction  
410 of available Ra (i.e., the exchangeable Ra pool) includes the Th dissolved in groundwater  
411 (usually a negligible fraction) and mainly the Ra produced in the effective alpha recoil zone  
412 (i.e., by the Th bound in the outer mineral lattice and by the surface-bound, i.e., adsorbed  
413 Th) (Figure 4). The decay of Th in the effective alpha recoil zone mobilizes part of the  
414 generated Ra from this zone to the adjacent pore fluid due to the alpha-decay recoil energy  
415 (Sun and Semkow, 1998; Swarzenski, 2007; Figure 4). The extent of the effective alpha recoil  
416 zone is specific to each type of solid (i.e., mineralogy) and is a function of the size and of the  
417 surface characteristics of the aquifer solid grains (Beck and Cochran, 2013; Sun and  
418 Semkow, 1997; Swarzenski, 2007; Diego-Feliu et al., 2021). The greater the specific surface  
419 area of solids in the aquifer, the greater the fraction of Th in the effective recoil zone and  
420 thus, the pool of Ra available for solid-solution exchange (Copenhaver et al., 1993; Porcelli  
421 and Swarzenski, 2003). The influence of alpha recoil can produce deviations in the  
422 groundwater Ra isotopic ratios in relation to that expected from host rock ratios, since each  
423 Ra isotope is generated after a different number of decay events in each of the decay  
424 chains. For instance, when Ra isotopes in groundwaters are in equilibrium with aquifer  
425 solids, the alpha recoil process alone may produce equilibrium  $^{226}\text{Ra}/^{228}\text{Ra}$  ratios up to 1.75  
426 that of the host rock  $^{238}\text{U}/^{232}\text{Th}$  ratio and  $^{224}\text{Ra}/^{228}\text{Ra}$  equilibrium ratios ranging from 1 to 2.2  
427 (e.g. Krishnaswami et al. 1982; Davidson and Dickson, 1986; Swarzenski, 2007; Diego-Feliu  
428 et al., 2021).

429  
430 Several methods are described in the literature determining how Ra recoil can be estimated.  
431 These methods can be classified into five groups: (1) experimental determination of  
432 emanation rates of daughter radionuclides from aquifer solids into groundwater (Hussain,  
433 1995; Rama and Moore, 1984); (2) experimental determination of the parent radionuclide  
434 within the alpha-recoil zone (Cai et al., 2014, 2012; Tamborski et al., 2019); (3) theoretical  
435 calculations focused on determining the alpha-recoil supply based on properties of the host  
436 material (e.g., density, surface area; Yigoshi, 1971; Semkow, 1990; Sun and Semkow, 1998);  
437 (4) mathematical fitting to advective transport models (Krest and Harvey, 2003), and (5) in-  
438 situ determination via supply rate of  $^{222}\text{Rn}$  (Copenhaver et al., 1992; Krishnaswami et al.,  
439 1982; Porcelli and Swarzenski, 2003).

440

#### 441 [\[4.2\] Adsorption and desorption](#)

442

443 In fresh groundwater, Ra is usually and preferentially bound to aquifer solids, although a  
444 small fraction is found in solution as  $\text{Ra}^{2+}$ . The adsorption of Ra on solid surfaces depends on  
445 the cation exchange capacity (CEC) of the aquifer solids, but also on the chemical  
446 composition of groundwater. The higher the CEC, the higher the content of Ra that may be  
447 potentially adsorbed on the grain surface of aquifer solids (e.g., Beck and Cochran, 2013;  
448 Beneš et al., 1985; Kiro et al., 2012; Nathwani and Phillips, 1979; Vengosh et al., 2009). The  
449 ionic strength of the solution, governed mainly by the groundwater salinity, has been  
450 recognized as the most relevant factor controlling the exchange of Ra between solid and  
451 groundwater (Beck and Cochran, 2013; Gonnee et al., 2013; Kiro et al., 2012; Webster et  
452 al., 1995). High ionic strength (i.e., high salinity) hampers the adsorption of  $\text{Ra}^{2+}$  due to  
453 competition with other cations dissolved in groundwater (e.g.,  $\text{Na}^+$ ,  $\text{K}^+$ ,  $\text{Ca}^{2+}$ ) and promotes  
454 the desorption of surface-bound Ra due to cationic exchange. As a consequence, Ra is  
455 typically more enriched in brackish to saline groundwater than in fresh groundwater.

456 Exceptions may include carbonate aquifers where mineral dissolution is more important  
457 than desorption in driving groundwater Ra activities. Thus, Ra activities in coastal  
458 groundwater may vary substantially, depending on the subsurface salinity distribution,  
459 which is dynamic due to the interaction between the inland groundwater table elevation  
460 and marine driving forces (e.g., tides, waves and storms, mean sea-level). Other physico-  
461 chemical properties of groundwater, such as temperature and pH may also control the  
462 solid-solution partitioning (adsorption/desorption) of Ra in coastal aquifers. Beck and  
463 Cochran (2013) reviewed the role of temperature and pH, concluding that while there is a  
464 Ra adsorption with increasing pH, there is no clear effect of temperature on the adsorption  
465 of Ra onto aquifer solids.

466  
467 In order to estimate the relative distribution of Ra between solid and solution, a distribution  
468 coefficient,  $K_D$  [ $\text{m}^3 \cdot \text{kg}^{-1}$ ], is commonly used. This coefficient is defined as the ratio of the  
469 concentration of Ra on the solid surface per mass of solid [ $\text{Bq} \cdot \text{g}^{-1}$ ] to the amount of Ra  
470 remaining in mass of the solution at equilibrium [ $\text{Bq} \cdot \text{m}^{-3}$ ], and considers the Ra chemical  
471 equilibrium processes of adsorption-desorption ( $K_D = \text{Ra}_{\text{adsorbed}}/\text{Ra}_{\text{desorbed}}$ ), but not the  
472 processes of weathering. The distribution coefficient is one of the most relevant parameters  
473 for understanding the Ra distribution in coastal aquifers and for applying transport models  
474 of Ra in groundwater. Radium distribution coefficient values span several orders of  
475 magnitude, depending on the composition of groundwater and aquifer solids (Kumar et al.,  
476 2020). Many authors analyzed the influence of different solid and water compositions  
477 within different experimental settings. The distribution coefficient is commonly determined  
478 by batch experiments (e.g., Beck and Cochran, 2013; Colbert and Hammond, 2008; Gonnee  
479 et al., 2008; Rama and Moore, 1996; Tachet et al., 2001; Tamborski et al., 2019; Willett and  
480 Bond, 1995). The distribution coefficient of Ra, which ranges widely from  $10^{-2}$  to  $10^2 \text{ m}^3 \text{ kg}^{-1}$   
481 in coastal aquifers (Beck and Cochran, 2013; Kumar et al., 2020), has also been determined  
482 by other methods such as adsorption-desorption modelling (e.g., Copenhaver et al., 1993;  
483 Webster et al., 1995); chromatographic columns tests (e.g., Meier et al., 2015; Relyea,  
484 1982); and chemical equilibrium calculations (Puigdomenech and Bergstrom, 1995).

485

#### 486 [4.3] Weathering and precipitation

487

488 Radium isotopes are also supplied to groundwater by weathering processes, including  
489 dissolution and breakdown of rocks or minerals containing Ra that may occur during the  
490 flow of groundwater through the coastal aquifer. The intensity of weathering processes  
491 mainly depends on the physicochemical properties of groundwater, such as temperature,  
492 pH, redox potential or ionic strength, and on the characteristics of the geological matrix  
493 (e.g., mineralogy, specific surface area of aquifer solids) (Chabaux et al., 2003). Since the  
494 interaction between fresh and saline groundwater in the subterranean estuary is also often  
495 accompanied by a redox gradient (Charette and Sholkovitz, 2006; McAllister et al., 2015),  
496 the dissolution of hydrous oxides under reducing conditions may increase the activity of Ra  
497 isotopes in groundwater (Beneš et al., 1984; Gonnee et al., 2008). Conversely, mineral  
498 precipitation processes can remove Ra from groundwater. Due to the very low molar  
499 activities of Ra in groundwaters, the removal of Ra from groundwater usually occurs by co-  
500 precipitation with other phases.  $\text{Ra}^{2+}$  may co-precipitate with Mn and Fe hydrous oxides  
501 under oxidizing and high pH (>7) conditions (Gonnee et al., 2008; Porcelli et al., 2014), as

502 well as with sulfates [e.g., (Ba, Ra, Sr)SO<sub>4</sub>] or carbonate [(Ca, Ra)CO<sub>3</sub>] (Kiro et al., 2013, 2012;  
503 Porcelli et al., 2014). However, due to the relatively long time scales of weathering and  
504 precipitation processes, these vectors are often considered to exert negligible controls on  
505 the activities of <sup>224</sup>Ra, <sup>223</sup>Ra and <sup>228</sup>Ra in coastal groundwaters, although they might be  
506 relevant for <sup>226</sup>Ra (Porcelli and Swarzenski, 2003).  
507

#### 508 [4.4] Groundwater transit time

509

510 The last fundamental factor that regulates the activities of Ra isotopes in aquifers is the time  
511 of groundwater to travel along a certain flow path, commonly known as groundwater transit  
512 time, which also represents the time that the groundwater is in contact with the solids in  
513 the aquifer (Diego-Feliu et al., 2021; Rajaomahafisoa et al., 2019; Vengosh et al., 2009). In  
514 SGD studies the groundwater transit time is instrumental to understand the degree of Ra  
515 isotope enrichment in groundwater since it entered the aquifer through one of its  
516 boundaries (e.g., aquifer recharge of freshwater or sea water infiltration through permeable  
517 sediments). Groundwater transit time largely depends on the hydraulic conductivity of the  
518 system and the physical mechanisms that are forcing the groundwater advective flow. The  
519 hydraulic conductivity describes the transmissive properties of a porous medium (for a  
520 given fluid) and thus clearly influences the groundwater flow velocity (Freeze and Cherry,  
521 1979). For instance, hydraulic conductivity in unconsolidated silty-clay aquifers is typically  
522 on the order of 1 - 100 cm·d<sup>-1</sup>, while in unconsolidated sandy aquifers it is significantly  
523 higher (10<sup>2</sup> - 10<sup>4</sup>; Zhang and Schaap, 2019). An extreme example is represented by karstic or  
524 volcanic coastal aquifers, where localized hydraulic conductivity can reach values of ~10<sup>7</sup>  
525 cm·d<sup>-1</sup> (Li et al., 2020). On the other hand, physical mechanisms driving groundwater flow  
526 also control the groundwater velocity (as well as the spatial scale of the process), and  
527 therefore the groundwater transit times. In coastal aquifers, these driving forces include the  
528 terrestrial hydraulic gradient and their seasonal oscillations, shoreface circulation and tidal  
529 pumping, wave setup and wave pumping, bioirrigation, flow- and topography-induced  
530 advection, among others (Santos et al., 2012). These forces can be linked to the five SGD  
531 pathways outlined in Section 3. Obviously, groundwater transit times are not only  
532 determined by the driving mechanism itself, but also by the intensity and frequency of the  
533 physical forces (e.g., wave and tidal frequency and amplitude, magnitude and seasonality of  
534 the hydraulic gradient, recurrence and intensity of strong episodic wave events, etc.)  
535 (Rodellas et al., 2020; Sawyer et al., 2013).  
536

537

538 The common way to evaluate the effect of transit time on the degree of enrichment of Ra  
539 isotopes in groundwater is usually performed using 1-D advective-dispersive solute  
540 transport models. These models commonly assume: i) steady state aquifer conditions (i.e.,  
541 activities do not vary with time;  $dA/dt = 0$ ); ii) that the effects of dispersive and diffusive  
542 transport in relation to advective transport are negligible, and iii) that the exchange  
543 between the solid surfaces and the solution principally occurs via ion exchange, neglecting  
544 the processes of weathering or precipitation (Kiro et al., 2012; Michael et al., 2011;  
545 Tamborski et al., 2017a; Diego-Feliu et al., 2021). The underlying assumptions of these

545 simple models may not be valid for all groundwater systems, although they allow  
546 understanding of Ra distribution within aquifers. Based on these models, the activities of Ra  
547 isotopes in groundwater increase along a flow path towards an equilibrium with Th activities  
548 in the aquifer solids (i.e., Th activities in the alpha recoil zone). This equilibrium, defined as  
549 bulk radioactive equilibrium by Diego-Feliu et al. (2021), is reached when the activities of Ra  
550 do not vary along the groundwater flowpath ( $dA/dt = 0$ ). The characteristic groundwater  
551 transit time needed to reach equilibrium between the isotopes of Ra and Th depends on the  
552 distribution coefficient of Ra ( $K_D$ ), which relates the amount of Ra desorbed and adsorbed  
553 on grain surfaces ( $K_D = Ra_{adsorbed}/Ra_{desorbed}$ ), as well as on the decay constant of each Ra  
554 isotope (production and decay) (Beck et al., 2013; Michael et al., 2011). The Ra loss due to  
555 advective transport when Ra is predominantly desorbed (low  $K_D$ ; e.g.,  $\sim 10^{-2} \text{ m}^3 \text{ kg}^{-1}$ ) is higher  
556 than when Ra is mostly adsorbed onto grain surfaces (high  $K_D$ ; e.g.,  $\sim 10^2 \text{ m}^3 \text{ kg}^{-1}$ ).  
557 Consequently, the characteristic groundwater time to reach the equilibrium with Th  
558 isotopes decreases as the distribution coefficient of Ra increases (Figure 5). If Ra was  
559 completely desorbed (e.g.,  $K_D \sim 0 \text{ m}^3 \text{ kg}^{-1}$ ), the time required to produce 50% of the  
560 equilibrium activity of a given Ra isotope would be equal to its half-life. However, in natural  
561 environments ( $K_D \sim 10^{-3}$  to  $10^3 \text{ m}^3 \text{ kg}^{-1}$ ; Beck and Cochran, 2013), this activity would be  
562 reached within a significantly shorter time, ranging from minutes to hours for the short-  
563 lived Ra isotopes, from hours to days for  $^{228}\text{Ra}$  and from days to years for  $^{226}\text{Ra}$  (Figure 5).  
564 Therefore, the enrichment rate of Ra isotopes strongly depends on the characteristics of the  
565 coastal aquifer (e.g., the higher the salinity, the longer the time to reach equilibrium  
566 concentrations is). The relative difference between the characteristic transit time of each  
567 isotope is equivalent to the ratio of their decay constants. For instance, the transit time  
568 needed for  $^{228}\text{Ra}$  to reach equilibrium with  $^{232}\text{Th}$  is  $\sim 570$  times higher ( $\lambda_{Ra-228}/\lambda_{Ra-224}$ )  
569 than that for  $^{224}\text{Ra}$  to reach the equilibrium with  $^{228}\text{Th}$ . Characteristic transit times can be  
570 converted to equilibrium distances by assuming a constant velocity of groundwater through  
571 the aquifer. Considering a velocity on the order of  $1 \text{ cm d}^{-1}$ , all of the Ra isotopes would  
572 reach equilibrium within a few centimeters along the flow path in fresh groundwaters, while  
573 lengths would be on the order of tens of cm for  $^{223}\text{Ra}$  and  $^{224}\text{Ra}$ ,  $\sim 1 \text{ m}$  for  $^{228}\text{Ra}$  and  $\sim 500 \text{ m}$   
574 for  $^{226}\text{Ra}$  in saline groundwater. Notice that these lengths are specific for the assumed  
575 velocity and the distribution coefficients used. For instance, Tamborski et al. (2019) showed  
576 that short-lived Ra isotopes reached secular equilibrium after a flowpath of several meters  
577 in a sandy barrier beach from a hypersaline coastal lagoon, when groundwater velocities  
578 were on the order  $10 - 100 \text{ cm} \cdot \text{d}^{-1}$ .

579

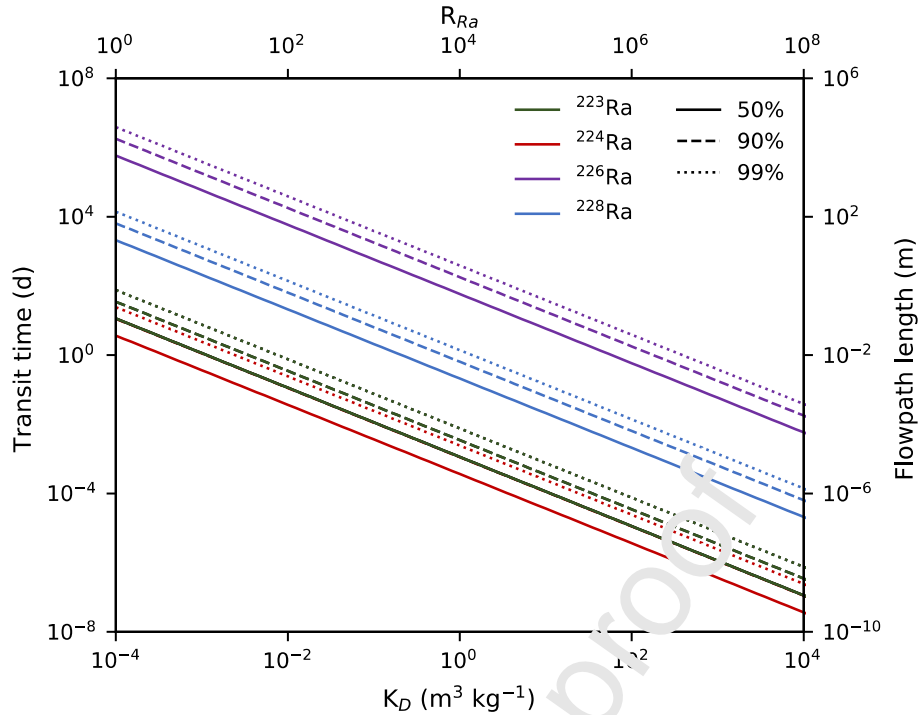


**Figure 5.** Transit time of groundwater with aquifer ponds required to produce 50%, 90% and 99% of equilibrium activity for each Ra isotope as a function of the distribution coefficient ( $K_D$ ) and the retardation factor ( $R_{Ra}$ ) of Ra (see definition in 8.1). Results are derived from a one-dimensional model formulated in Diego-Feliu et al. (2011) and Michael et al. (2011). Distance is also shown considering a groundwater velocity of  $1 \text{ cm d}^{-1}$ . Notice that the scale of the Ra distribution coefficient and the retardation coefficient are logarithmic. Notice that the 50% line of  $^{223}\text{Ra}$  overlays the 90% line of  $^{224}\text{Ra}$ .

580

581 Given that physical mechanisms control the groundwater transit times in the subterranean  
 582 estuary, the five pathways of SGD described in section 3 are likely to be differently enriched  
 583 in Ra isotopes, as they have different driving forces and spatio-temporal scales. The  
 584 enrichment rate of Ra isotopes in each SGD pathway can be evaluated by comparing the  
 585 ingrowth rates of different Ra isotopes with the most common spatio-temporal scales and  
 586 groundwater salinities of the different pathways (Figure 6). Assuming a relatively  
 587 homogeneous geological matrix, groundwater salinities are likely to control the  $K_D$  of the  
 588 different SGD pathways. As an orientative threshold, here we consider that a given Ra  
 589 isotope becomes significantly enriched along a specific SGD pathway when 50% of its  
 590 equilibrium activity has been reached (Figure 6). This 50% enrichment is an arbitrary  
 591 (though reasonable) threshold because the ability of tracing Ra inputs from a given pathway  
 592 depends on several site-specific factors, such as equilibrium activities, U/Th concentration in  
 593 the coastal geological matrix, magnitude of SGD flow and interferences from other Ra  
 594 sources (e.g., sediments, rivers). However, this qualitative comparison allows the  
 595 identification of those SGD pathways that might be significantly enriched in the different Ra  
 596 isotopes (Figure 6). As illustrated in this assessment, short-lived Ra isotopes may become  
 597 enriched in all of the SGD pathways. On the other hand, the transit time within the coastal  
 598 aquifer of short-scale processes (e.g., cm-scale porewater exchange and shoreface seawater

599 circulation) is not sufficient to produce measurable long-lived Ra isotopes activities (King,  
 600 2012; Michael et al., 2011; Moore, 2010; Rodellas et al., 2017).  
 601

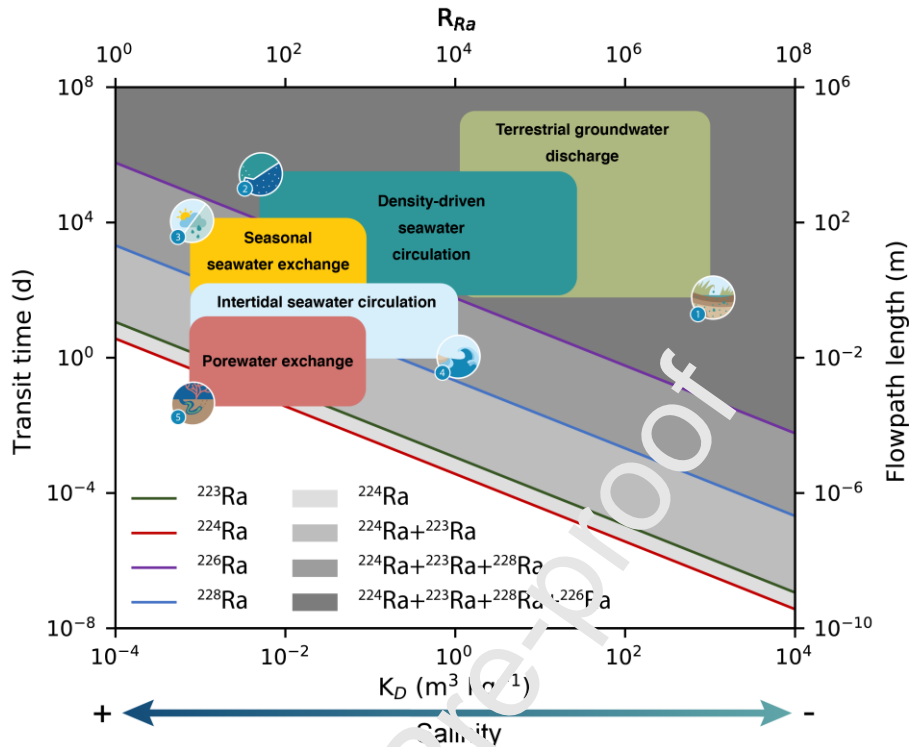


**Figure 6.** The spatio-temporal scales of different SGD pathways considering a groundwater advection rate of 1 cm d<sup>-1</sup>. Qualitative boundaries for the different pathways are based on common spatial scales and  $K_D$  of the different pathways (note that  $R = 1 + K_D \rho_b / \Phi$ ). The transit time required to produce more than 50% of the different Ra isotopes is also indicated (solid lines represent 50% of production; see Figure 5)

602

## 603 [5] Sources and sinks of Ra isotopes in the water column

604

605 The application of Ra isotopes as tracers of SGD in the marine environment (at local,  
 606 regional and global scales) requires a comprehensive understanding of their sources and  
 607 sinks in the water column. As summarized in several studies (e.g., Charette et al., 2008;  
 608 Moore, 2010, 1999; Rama and Moore, 1996; Swarzenski et al., 2007), the most common  
 609 sources of Ra isotopes to the ocean can be classified into six groups: 1) Atmospheric input  
 610 from wet or dry deposition ( $F_{atm}$ ); 2) Discharge of surface water, such as rivers or streams  
 611 ( $F_{river}$ ); 3) Diffusive fluxes from underlying permeable sediments ( $F_{sed}$ ); 4) Input from  
 612 offshore waters ( $F_{in-ocean}$ ); 5) Production of Ra in the water column from the decay of Th  
 613 parents ( $F_{prod}$ ) and 6) inputs from SGD ( $F_{SGD}$ ). Major sinks of Ra in coastal systems are 1)  
 614 Internal coastal cycling, which includes the biological or chemical removal of Ra isotopes  
 615 through co-precipitation with minerals such as Ba sulfates or Fe (hydr)oxides and Ra uptake  
 616 ( $F_{cycling}$ ); 2) Radioactive decay of Ra ( $F_{decay}$ ) and 3) Export of Ra offshore ( $F_{out-ocean}$ ). A  
 617 conceptual generalized box model summarizing all the pathways of removal or enrichment  
 618 of Ra isotopes in the coastal environment is presented in Figure 7.  
 619

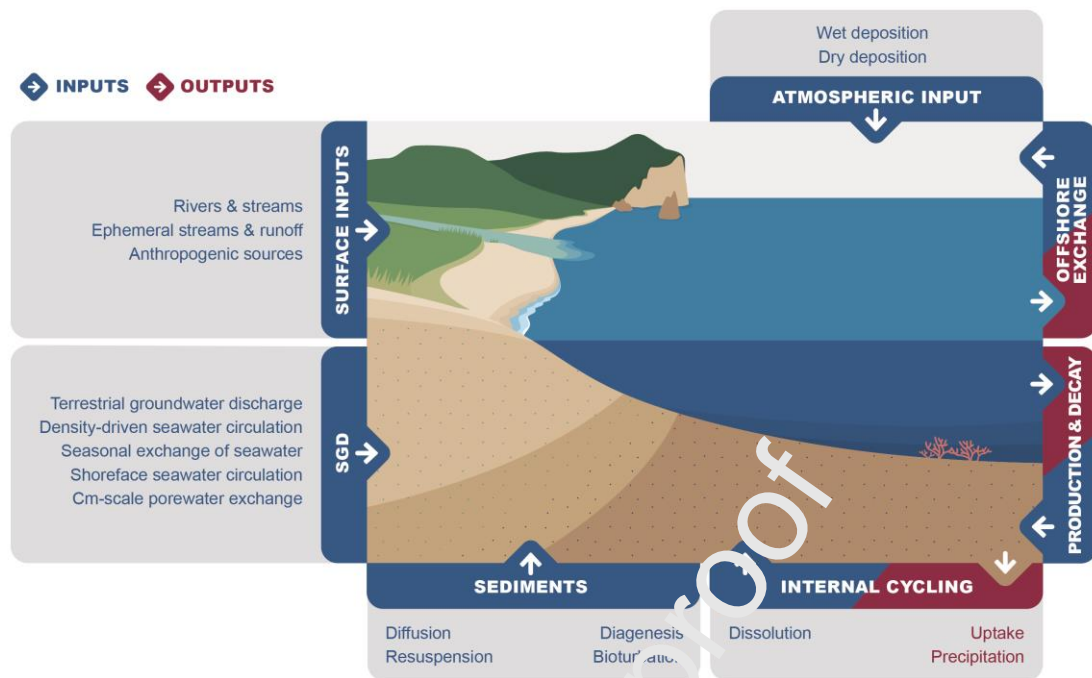


**Figure 7.** Conceptual model illustrating the sources (blue) and sinks (red) of Ra isotopes in the coastal ocean.

620

621

### 622 [5.1] Radium sources

623

624 The relative magnitude of the different Ra sources will vary according to the characteristics  
 625 of the study site (e.g., presence of rivers or streams, characteristics of sediments, water  
 626 column depth), as well as the half-life of the specific Ra isotope used in the mass balance  
 627 (Figure 8). The different source terms for Ra isotopes into the coastal ocean and their  
 628 relative importance are described below (excluding the Ra inputs from offshore waters  
 629 ( $F_{in-ocean}$ ), which will be considered in the net Ra exchange with offshore waters (see  
 630 chapter 5.2)).

631

632 The input of Ra through **atmospheric deposition** onto oceans ( $F_{atm}$ ) includes dissolved Ra in  
 633 precipitation and, mainly, desorption from atmospheric dust or ash entering the water  
 634 column. The highest relative contribution of Ra from atmospheric sources will be expected  
 635 to occur in large basins (i.e., the higher the ratio of ocean surface area to coastline length,  
 636 the higher the potential importance of atmospheric inputs is) and/or in areas affected by  
 637 large atmospheric inputs (e.g., areas affected by the deposition of large amounts of dust or  
 638 ash). However, even in large areas affected by Saharan dust inputs (e.g., the Atlantic Ocean  
 639 or the Mediterranean Sea), the percentage of the atmospheric contribution is less than 1%  
 640 of the total Ra inputs (Moore et al., 2008; Rodellas et al., 2015a) (Figure 8). Atmospheric  
 641 input is expected to be smaller in areas such as bays or coves, and therefore it is commonly  
 642 neglected in Ra mass balances (Charette et al., 2008).

643

644 **Surface water inputs ( $F_{\text{river}}$ )** includes both the fraction of Ra dissolved in surface waters and  
645 the desorption of Ra from river-borne particles as these particles encounter salty water.  
646 Surface water input includes both rivers and streams discharge and inputs from freshwater  
647 and salt marshes, stormwater runoff and anthropogenic sources, such as discharge from  
648 wastewater treatment facilities. There are several studies that have quantified the  
649 contribution of Ra from **rivers and streams** to coastal and open ocean areas (Krest et al.,  
650 1999; Moore, 1997; Moore and Shaw, 2008; Ollivier et al., 2008; Rapaglia et al., 2010). Most  
651 of the studies conclude that the fraction of dissolved Ra in river waters is a minor  
652 contribution compared with the Ra desorbed from surface water-borne particles (Krest et  
653 al., 1999; Moore et al., 1995; Moore and Shaw, 2008). The importance of surface water as a  
654 Ra source obviously depends on the presence (and significance) of rivers and streams in the  
655 investigated area. The relative contribution of surface water might be significant in estuaries  
656 or other areas influenced by river discharge (e.g., Beck et al., 2008; Key et al., 1985; Luek  
657 and Beck, 2014; Moore et al., 1995; Moore and Shaw, 2008) (Figure 8). **Marshes** are also  
658 commonly considered as a major source of Ra due to both erosion of the marsh and  
659 subsequent desorption of Ra from particles and porewater exchange (Beck et al., 2008;  
660 Bollinger and Moore, 1993, 1984; Charette, 2007; Tamborski et al., 2017c). **Runoff or**  
661 **ephemeral streams** following a major rain event (Moore et al., 1998) is an additional input.  
662 Anthropogenic activities like **channels, oil and gas installations, outfalls and waste water**  
663 **treatment plants** may also supply Ra to coastal waters, although in most cases they prove  
664 to be a minor Ra source (e.g., Beck et al., 2007; Eriksen et al., 2009; Rodellas et al., 2017;  
665 Tamborski et al., 2020).

666  
667 **Sediments** are a ubiquitous source of Ra isotopes ( $F_{\text{sed}}$ ), but their relative importance as a Ra  
668 source is highly dependent on the characteristics of the sediment (e.g., sediment grain size,  
669 sediment mineral composition, porosity), the specific Ra isotope considered, the mechanism  
670 that releases Ra from the sediments and the spatial scale of the study area (Figure 8).  
671 Mechanisms that may release Ra from sediments, excluding groundwater flow, are  
672 molecular diffusion, erosion, bioturbation, or sediment resuspension. High Ra in the pore-  
673 water results in a **molecular diffusion** of Ra from the sediments to the water column (e.g.,  
674 Beck et al., 2008; Garcia-Orellana et al., 2014; Garcia-Solsona et al., 2008). Other processes  
675 such as **sediment resuspension, diagenesis and bioturbation** may also enhance the  
676 exchange of Ra between sediment and the water column (e.g., Burt et al., 2014; Garcia-  
677 Orellana et al., 2014; Moore, 2007; Rodellas et al., 2015b; Tamborski et al., 2017c). For  
678 instance, bioturbation has been suggested to increase the  $^{228}\text{Ra}$  flux by a factor of two over  
679 the flux due to molecular diffusion only (Hancock et al., 2000). In sediments of the Yangtze  
680 estuary, bioirrigation was found to be more important for the  $^{224}\text{Ra}$  flux from the sediments  
681 than molecular diffusion and sediment bioturbation (Cai et al., 2014). The significance of Ra  
682 input from sediments largely depends on the production time of each Ra isotope relative to  
683 the Ra-releasing mechanism. Inputs from sediments can typically be ignored for long-lived  
684 Ra isotopes in small-scale studies due to their long production times (e.g., Alorda-Kleinglass  
685 et al., 2019; Beck et al., 2008, 2007; Garcia-Solsona et al., 2008). However, in basin-wide or  
686 global-scale studies, the large seafloor area results in long-lived Ra sediment input that  
687 might be comparable to SGD input (Moore et al., 2008; Rodellas et al., 2015a) (Figure 8).  
688 The fast production of short-lived Ra isotopes in sediments, which is set by their decay  
689 constants, results in a near-continuous availability of  $^{223}\text{Ra}$  and  $^{224}\text{Ra}$  in sediments, which  
690 can result in comparatively larger fluxes of short-lived Ra isotopes to the water column

691 relative to the long-lived ones. Particularly in areas with coarse-grained sediments with low  
 692 Ra availability for sediment-water exchange, fluxes of longer-lived Ra isotopes from seafloor  
 693 sediments usually account for a minor fraction of the total Ra inputs (Beck et al., 2008,  
 694 2007; Garcia-Solsona et al., 2008). However, sediments can turn into a major source of Ra  
 695 isotopes to the water column in shallow water bodies, in systems covered by fine-grained  
 696 sediments (substrate with a high specific surface area), sediments with a high content of U  
 697 and Th-series radionuclides, and/or in areas affected by processes that favor the Ra  
 698 exchange between sediments and overlying waters, such as bioturbation (Cai et al., 2014),  
 699 sediment resuspension (Burt et al., 2014; Rodellas et al., 2015b) or seasonal hypoxia  
 700 (Garcia-Orellana et al., 2014).

701  
 702 The **production of Ra isotopes** from their dissolved Th parents ( $F_{prod}$ ) is commonly avoided  
 703 in SGD studies by reporting Ra activities as “excess” activities in relation to their respective  
 704 progenitors. This is usually a minor Ra source because Th is a particle reactive element and  
 705 is rapidly scavenged by particles sinking through the water column. The amount of  $^{232}Th$ ,  
 706 which is introduced into the water column by dissolution from particles supplied by rivers,  
 707 runoff, atmospheric deposition or resuspension, is very low and therefore water column  
 708 dissolved  $^{232}Th$  activities are usually orders of magnitude lower than its daughter  $^{228}Ra$ .  
 709 Dissolved activities of  $^{227}Th$  (and  $^{227}Ac$ ),  $^{228}Th$  and  $^{230}Th$  in the water column are also low and  
 710 thus the production of  $^{223}Ra$ ,  $^{224}Ra$  and  $^{226}Ra$  from their decay generally represents a minor  
 711 source term.

712  
 713 **Submarine Groundwater Discharge ( $F_{SGD}$ )** is often a primary source of Ra isotopes to the  
 714 ocean (Figure 8) and it is the target flux in SGD investigations. This term includes Ra inputs  
 715 from any water flow across the sediment-water interface, which can be supplied through  
 716 the five different SGD pathways outlined in Section 3 (Figure 3). Different SGD pathways  
 717 occur at different locations (e.g., nearshore, beachface, offshore) and have different  
 718 groundwater compositions (e.g. fresh, brackish or saline groundwater) and characteristic  
 719 groundwater transit times within the subterranean estuary (e.g., hours-days for cm-scale  
 720 porewater exchange and months-decades for terrestrial groundwater discharge). All of  
 721 them are, however, potential sources of Ra isotopes to the ocean and thus need to be taken  
 722 into account when Ra isotopes are used as SGD tracer.

723

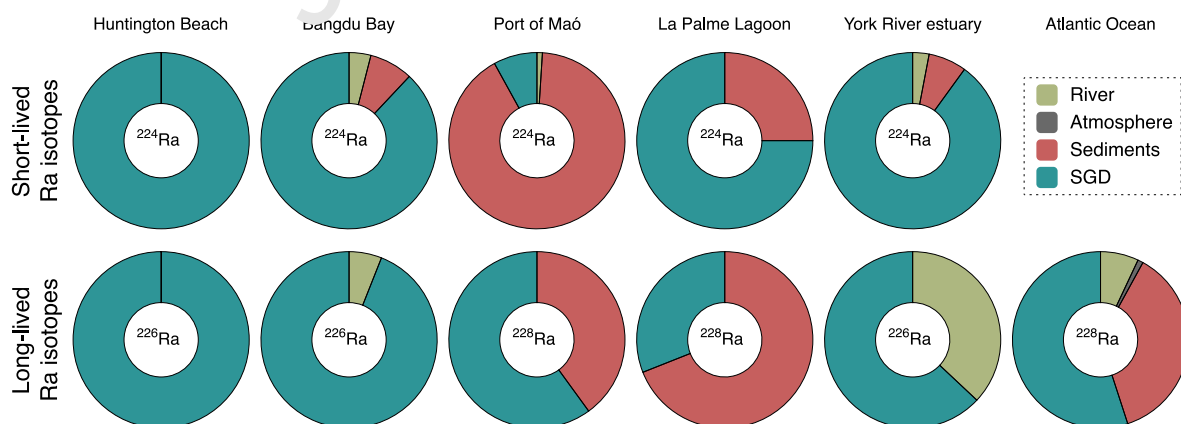


**Figure 8.** Relative contribution of different sources (river, atmosphere, sediments and SGD) to the total  $^{224}Ra$  (upper row) and long-lived Ra isotopes (lower row) for six study sites with distinct characteristics: Huntington Beach, USA (sandy intertidal beach face; Boehm et al., 2004 and 2006);

Bangdu Bay, Korea (semi-enclosed bay on a volcanic island; Hwang et al., 2005); Port of Maó, Spain (semi-enclosed harbor with large resuspension of sediments; Rodellas et al., 2015); La Palme Lagoon, France (micro-tidal coastal lagoon with karst springs; Tamborski et al., 2018); York River estuary, USA (micro-tidal estuary; Luek and Beck, 2014); Atlantic Ocean (upper 1000 m of water column; Moore et al., 2008). The sites are organized according to increasing water residence times of the study area (left to right). The Ra isotope used is indicated in the middle of the pie chart.

724

## 725 [5.2] Radium sinks

726

727 The two main Ra sinks for most of the coastal systems are the decay of Ra isotopes in the  
 728 water column ( $F_{\text{decay}}$ ) and net Ra exchanged with offshore waters ( $F_{\text{out-ocean}} - F_{\text{in-ocean}}$ ). As  
 729 with the Ra sources, the relevance of the Ra sink terms is largely dependent on the  
 730 characteristics of the water body (mainly water residence time) and on the Ra isotope used  
 731 (Figure 9). Other sinks are grouped together as **internal cycling** ( $F_{\text{cycling}}$ ). These processes  
 732 include Ra co-precipitation with salts (e.g. barium sulphate) or Fe-Mn (hydr)oxides that  
 733 occur in estuaries, coastal lagoons or polluted areas (e.g., Riorda-Kleinglass et al., 2019;  
 734 Kronfeld et al., 1991; Neff and Sauer, 1995; Snavely, 1989), the scavenging of Ra with sinking  
 735 particles (Moore et al., 2008; Moore and Dymond, 1991; van Beek et al., 2007), uptake by  
 736 biota, including the incorporation into calcium carbonate, barium sulphate or calcium  
 737 phosphate lattice of shells and fish bones (Iyengar and Rao, 1990; Szabo, 1967), and the  
 738 adsorption of Ra to the outer surface of algae's or to their internal non-living tissue  
 739 components (Neff, 2002). These various internal cycling processes are generally a negligible  
 740 Ra sink compared to radioactive decay and exchange with offshore waters. However, when  
 741 using long-lived Ra isotopes and conducting basin-scale and global ocean budgets (i.e., low  
 742 decay and low exchange),  $F_{\text{cycling}}$  should be taken into account (Moore et al., 2008;  
 743 Rodellas et al., 2015a) (Figure 9).

744

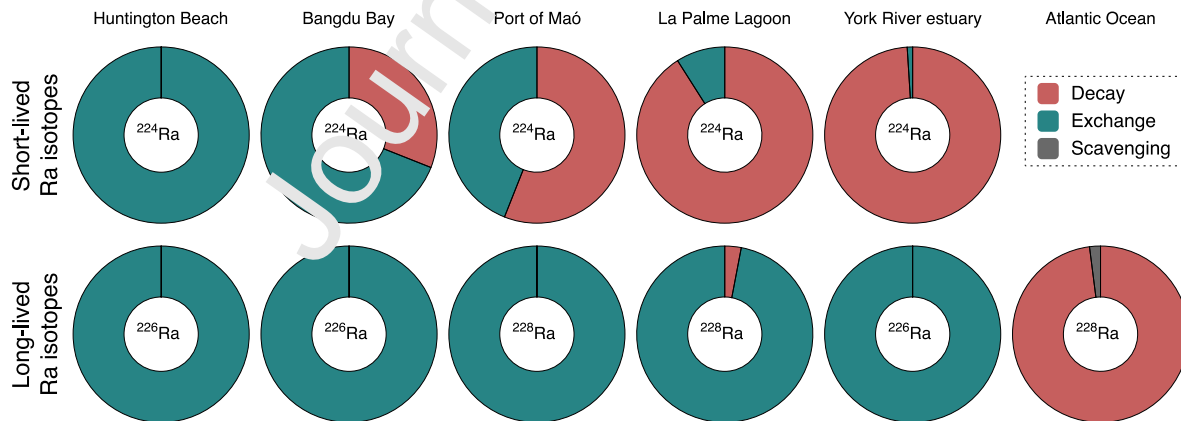


**Figure 9.** Relative contribution of different sinks (decay, exchange and scavenging) to the total  $^{224}\text{Ra}$  (upper row) and long-lived Ra isotopes (lower row) outputs for six study sites with distinct characteristics (see Figure 8 for site references and details).

745

746 The **decay of Ra isotopes** ( $F_{\text{decay}}$ ) is characteristic output term of mass balances using  
 747 radioactive isotopes as tracers. The loss of Ra due to decay is usually a term that is relatively  
 748 easy to constrain because it only depends on the Ra inventory of the study site and the  
 749 decay constant of the isotope used. Thus, when decay is a primary sink of Ra in the system  
 750 studied, the removal of Ra can be accurately determined provided that the Ra water-column

751 inventory has been adequately determined (Rapaglia et al., 2012). The importance of the  
 752 decay term will depend on the half-life of the isotope used and the water residence time of  
 753 the system studied, as illustrated in Figures 9 and 10. The loss of Ra due to radioactive decay  
 754 is negligible for long-lived Ra isotopes in coastal areas with relatively short residence times  
 755 ( $< 100$  days) (Figure 9). In regional and global-scale studies, the decay of  $^{228}\text{Ra}$  needs to be  
 756 considered and usually represents the main sink of this isotope (e.g., Charette et al., 2015;  
 757 Kwon et al., 2014; Liu et al., 2018; Moore et al., 2008; Rodellas et al., 2015a) (Figure 9). On  
 758 the contrary,  $^{226}\text{Ra}$  can be considered as a stable element in SGD studies because decay is  
 759 negligible on the time-scale of processes occurring in coastal or regional systems. For the  
 760 short-lived Ra isotopes, the removal of Ra due to decay must be accounted for in mass  
 761 balances for most coastal regions (Figure 9). However, in rapidly flushed systems it may be  
 762 almost negligible for  $^{223}\text{Ra}$  and to a lesser extent for  $^{224}\text{Ra}$  (i.e., residence times on the order  
 763 of few hours) (e.g., Alorda-Kleinglass et al., 2019; Boehm et al., 2004; Trezzi et al., 2016)  
 764 (Figures 9 and 10).  
 765

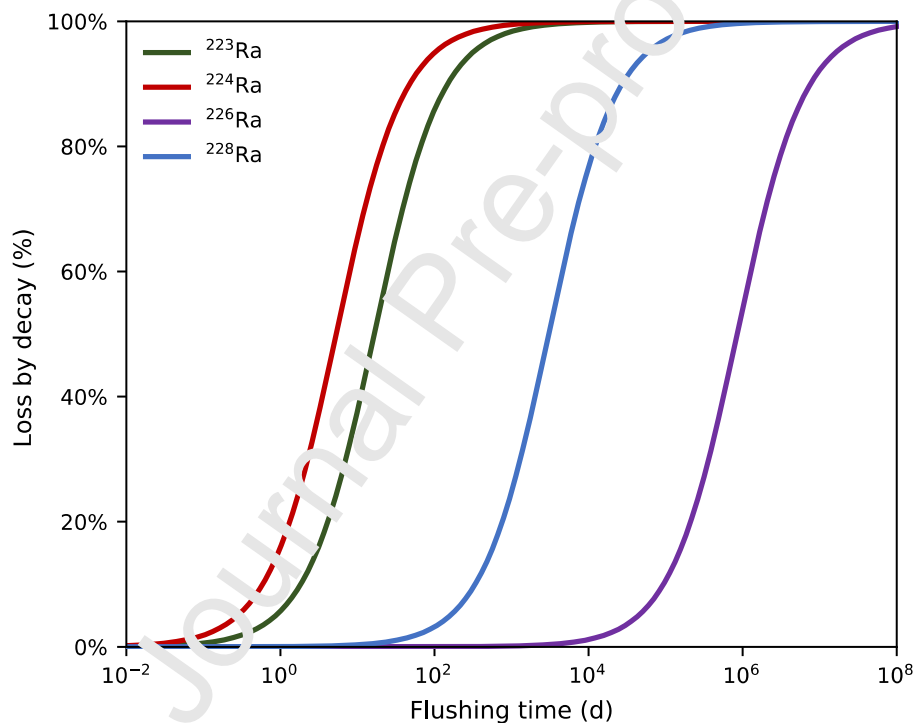


**Figure 10.** Relative contribution of the decay term in Ra mass balances as a function of flushing time (d) in a study area . Notice that the scale of the flushing time is logarithmic.

766  
 767 The relative contribution of the exchange of Ra isotopes due to the mixing between coastal  
 768 and open waters (**offshore exchange** - the difference between  $F_{\text{out-ocean}}$  and  $F_{\text{in-ocean}}$ ) depends  
 769 on the study site. Nearshore waters usually have higher Ra concentrations than offshore  
 770 waters, and thus there is usually a net export of Ra offshore. The loss of Ra due to the  
 771 mixing between coastal and open waters is directly linked to the flushing time of Ra in the  
 772 coastal system. In open coastal systems or sites with relatively short flushing times (e.g.,  
 773 systems with short water residence times and/or high dispersive mixing with offshore  
 774 waters), the export of Ra isotopes offshore is frequently the primary removal term and thus,  
 775 it is commonly one of the most critical parameters to be determined in Ra mass balances,  
 776 particularly for the long-lived Ra isotopes (Figure 10) (Tamborski et al., 2020). In semi-

777 enclosed or enclosed coastal environments (e.g., bays, coastal lagoons, coves), flushing  
 778 times are usually long, and Ra losses due to mixing with offshore waters is less important for  
 779 the short-lived Ra isotopes. However, for the long-lived Ra isotopes this process is the main  
 780 sink even in these semi-enclosed water bodies (Figure 9), requiring an appropriate  
 781 characterization of the mixing term to obtain an accurate quantification of SGD. Different Ra  
 782 isotopes are commonly combined to constrain offshore exchange (e.g., Moore, 2000; Moore  
 783 et al., 2006) (see section 8.3), although this output term can also be estimated using other  
 784 approaches such as hydrodynamic and numerical models (e.g., Chen et al., 2003; Lin and Liu,  
 785 2019; Warner et al., 2010), tidal prism (e.g., Dyer, 1973; Petermann et al., 2018; Sheldon  
 786 and Alber, 2008) or direct current/flow measurements (e.g., Rodellas et al., 2012;  
 787 Shellenbarger et al., 2006).  
 788

## 789 [6] Quantification of SGD using Ra isotopes

790

### 791 [6.1] Ra-based approaches to quantify SGD

792

793 Ra isotopes are suitable SGD tracers mainly because i) activities in groundwater are typically  
 794 1 - 2 orders of magnitude higher than in coastal seawater; ii) Ra isotopes in coastal areas are  
 795 usually primarily sourced from SGD; iii) they behave conservatively in seawater and iv) they  
 796 have different half-lives (ranging from 3.7 days to 1600 years), therefore allowing the  
 797 tracing of coastal processes on a variety of time-scales. The common approach to quantify  
 798 SGD is to quantify first the Ra flux supplied by SGD ( $F_{SGD}$ ; Bq d<sup>-1</sup>), regardless of the SGD  
 799 pathway considered, and subsequently convert it into a volumetric water flow (SGD; m<sup>3</sup> d<sup>-1</sup>)  
 800 by characterizing the Ra activity in the discharging groundwater (i.e., the SGD endmember,  
 801  $C_{Ra-SGD}$ ; Bq m<sup>-3</sup>) (Equation 1).  
 802

803

$$803 \quad SGD = \frac{F_{SGD}}{C_{Ra-SGD}} \quad (1)$$

804

805 There are three basic strategies to quantify total SGD fluxes ( $F_{SGD}$ ) using Ra isotopes: i) mass  
 806 balances; ii) endmember mixing models and iii) offshore flux determination from horizontal  
 807 eddy diffusive mixing. The most comprehensive and widely applied approach is the **Ra mass**  
 808 **balance**, where the flux of Ra supplied by SGD is usually quantified by a “flux by difference  
 809 approach”, which considers all the potential Ra sources and sinks identified in Figure 7:  
 810

811

$$811 \quad \frac{\partial AV}{\partial t} = (F_{atm} + F_{river} + F_{sed} + F_{prod} + F_{in-ocean} + F_{Ra-SGD}) - (F_{cycling} + F_{decay} +$$

$$812 \quad F_{out-ocean}) \quad (2)$$

813

814 where  $A$  is the average Ra activity in the study area,  $V$  is the volume affected by SGD and  $t$  is  
 815 time (i.e.,  $\frac{\partial AV}{\partial t}$  is the change of Ra activity in the study area over time). This approach is often  
 816 simplified in coastal areas by neglecting the commonly minor Ra sources and sinks  
 817 (atmospheric inputs, production and internal cycling) and assuming that the system is in  
 818 steady state (i.e.,  $\frac{\partial AV}{\partial t} = 0$ ), and thus all quantifiable Ra input fluxes are subtracted from the  
 819 total output with the residual being attributed to SGD:  
 820

$$F_{Ra-SGD} = \frac{(A - A_{ocn})V}{t_w} + AV\lambda - F_{river} - F_{sed} \quad (3)$$

821

822

823 where  $A_{ocn}$  is the Ra activity of the open ocean water that exchanges with the study area,  $t_w$   
 824 is the flushing time of Ra in the system due to mixing and  $\lambda$  is the radioactive decay constant  
 825 of the specific Ra isotope used. Notice that the first and second terms on the right side of  
 826 the equation describe offshore exchange (i.e.,  $F_{out-ocean} - F_{in-ocean}$ ) and radioactive decay,  
 827 respectively. Flushing time is an integrative time parameter used to describe the solute (Ra  
 828 isotopes) transport processes in a surface water body (due to both advection and  
 829 dispersion) and it relates the mass of a tracer and its renewal rate due to mixing (Monsen et  
 830 al., 2002). Notice also that we refer to flushing time of Ra due to mixing only, as if it were a  
 831 conservative and stable solute. Some authors use the concept of water residence time (i.e.,  
 832 the time a water parcel remains in a waterbody before exiting through one of the  
 833 boundaries) to refer to  $t_w$ , but this term is not appropriate for systems influenced by  
 834 dispersive mixing (such as many of coastal sites) or evaporation where tracers and water are  
 835 transported due to different mechanisms. This approach is commonly applied in  
 836 environments where the distribution of Ra isotopes in the study site is influenced by  
 837 multiple Ra sources and sinks (Figure 7). The accuracy of the estimated Ra flux supplied by  
 838 SGD will thus largely depend on the accuracy with which the most relevant sources and  
 839 sinks of Ra are determined (Rodellas et al, 2021). Indeed, given that SGD is quantified by a  
 840 difference of fluxes, large uncertainties are often associated with the SGD estimates in  
 841 systems where SGD fluxes only represent a minor fraction of total inputs. Most studies  
 842 quantify total SGD with a mass balance by using a single Ra isotope and use other short-  
 843 lived isotopes to estimate the flushing time ( $t_w$ ) (see chapter 8.3) that is required in SGD  
 844 estimations (Equation 3) (e.g., Gu et al., 2012; Kim et al., 2008; Krall et al., 2017). Ra  
 845 isotopes can also be combined through concurrent mass balances to simultaneously  
 846 quantify SGD derived from different aquifers or pathways (Rodellas et al., 2017).

847

848 The second approach estimates SGD fluxes using *mixing models* between different  
 849 endmembers (e.g., Charette and Buesseler, 2004; Charette, 2007; Moore, 2003; Young et  
 850 al., 2008). This approach is essentially a simplification of the mass balance approach where  
 851 all Ra inputs are attributed to water flows (e.g., groundwater, rivers) and where the mixing  
 852 offshore is assumed to represent the main Ra sink (Moore, 2003). This approach is thus  
 853 recommended for environments where mixing between SGD and the ocean controls the  
 854 distribution of Ra in the study site and where other Ra sources (e.g., sediment inputs) and  
 855 sinks (e.g., decay) can be neglected. If various Ra isotopes are used, this method can also be  
 856 used to distinguish the relative contribution of SGD and other water sources (e.g., rivers;  
 857 Dulaiova et al., 2006) or to separate different SGD components (e.g., SGD fluxes from  
 858 confined and unconfined aquifers (Charette and Buesseler, 2004; Moore, 2003), terrestrial  
 859 SGD and marsh porewater (Charette, 2007). For example, one can consider a system with  
 860 two Ra sources (e.g. SGD1 and SGD2), aside from offshore exchange. SGD inputs can be  
 861 estimated by defining the major contributors to the Ra isotope budgets of two isotopes (for  
 862 example,  $^{226}\text{Ra}$  and  $^{228}\text{Ra}$ ) and solve a series of simultaneous equations (Moore, 2003).

863

864

$$f_{ocn} + f_{SGD1} + f_{SGD2} = 1 \quad (4)$$

865

$$^{228}\text{Ra}_{ocn} \cdot f_{ocn} + ^{228}\text{Ra}_{SGD1} \cdot f_{SGD1} + ^{228}\text{Ra}_{SGD2} \cdot f_{SGD2} = ^{228}\text{Ra} \quad (5)$$

$$^{226}\text{Ra}_{\text{ocn}} \cdot f_{\text{ocn}} + ^{226}\text{Ra}_{\text{SGD1}} \cdot f_{\text{SGD1}} + ^{226}\text{Ra}_{\text{SGD2}} \cdot f_{\text{SGD2}} = ^{226}\text{Ra} \quad (6)$$

where  $^{228}\text{Ra}$  and  $^{226}\text{Ra}$  represent the measured Ra activity for a given time period,  $f$  is the water mass fraction contributed by coastal ocean mixing ( $f_{\text{ocn}}$ ), the SGD source 1 ( $f_{\text{SGD1}}$ ) and the SGD source 2 ( $f_{\text{SGD2}}$ ), and the Ra isotope endmembers are identified by the same series of subscripts. With this approach, the  $f_{\text{SGD}}$  can be determined for each location where there is a Ra isotope measurement ( $^{228}\text{Ra}$ ). Short-lived Ra isotopes can also be used in the equations by incorporating their decay term. This approach is particularly useful to resolve changes in mixing between different Ra sources over tidal time-scales, e.g., within marsh creeks (Charette, 2007). The fractional SGD contributions derived from this mixing model can be converted into volumetric fluxes by considering the time scales of water mass transport in the system under study, as follows:

$$\text{SGD} = \frac{V \cdot f_{\text{SGD}}}{t_w} \quad (7)$$

If the water outflow of the system can be directly measured (e.g., using an Acoustic Doppler Current Profiler – ADCP), then the endmember fraction can be directly multiplied by the measured flow (e.g., Rodellas et al., 2012; Tamborski et al., 2021).

The third approach is based on using offshore transects of short-lived Ra isotopes to estimate coastal mixing rates via the offshore mixing coefficient of solute dispersivity,  $K_h$  [ $\text{m}^2 \cdot \text{s}^{-1}$ ], which can be used in conjunction with the offshore gradient of long-lived Ra isotopes to estimate the **offshore export** of  $^{228}\text{Ra}$  or  $^{226}\text{Ra}$  (Moore, 2015, 2000b). Several assumptions are required to apply this model: i) there is no additional input of Ra beyond the nearshore source, ii) the system is in steady state on the timescale of the isotope used (see section 7.3), iii) advection is negligible in any direction; iv) the open ocean Ra isotope activities are negligible and v) a flat seabed or the presence of a stratified water column of a constant thickness (Knee et al., 2011; Moore, 2015, 2000b). Considering these assumptions, the measured log-linear decrease in the activity of  $^{223}\text{Ra}$  or  $^{224}\text{Ra}$  offshore can be used to determine  $K_h$  from the following simplified advection-diffusion equation (Equation 8).

$$A_x = A_0 e^{-x\sqrt{\lambda/K_h}} \quad (8)$$

where  $A_0$  and  $A_x$  are the Ra activities at the coast and at a distance  $x$  from the coast, respectively. A detailed discussion on the model and its assumptions is included in Moore (2015, 2000b). The mixing coefficient  $K_h$  derived from the logarithmic-linear scale plot of the short-lived Ra isotopes activities is then combined with the offshore gradient of long-lived radium isotopes (linear-linear decrease) to estimate the export offshore of  $^{228}\text{Ra}$  or  $^{226}\text{Ra}$ . This long-lived Ra flux offshore needs to be balanced by Ra inputs from all the potential sources, and thus estimating SGD from this approach requires subtracting the contribution of all the sources aside SGD from the estimated flux offshore (similar to the mass balance approach) (Moore, 2015, 2000b). This approach is recommended for open coastal systems where the export of long-lived Ra isotopes offshore due to diffusive mixing is frequently the primary removal term for  $^{226}\text{Ra}$  and  $^{228}\text{Ra}$  (e.g., Bejannin et al., 2020; Boehm et al., 2006; Dulaiova et al., 2006; Rodellas et al., 2014). One of the advantages of using this approach is that it allows combining short-lived Ra estimates of  $K_h$  with solute gradients offshore to

911 obtain the rate of solute transport offshore (e.g., Charette et al., 2007). For these reasons,  
912 this approach has been widely applied in oceanographic studies focused on the transport of  
913 solutes supplied by a combination of boundary exchange processes and is generally not  
914 applied to discriminate different Ra sources (e.g., SGD, rivers, sediments) (e.g., Charette et  
915 al., 2016; Jeandel, 2016; Vieira et al., 2020, 2019).

916

## 917 [6.2] Determination of the Ra concentration in the SGD endmember

918

919 The above-mentioned approaches of SGD quantification rely on an appropriate  
920 characterization of the Ra activity in the discharging groundwater (i.e., the SGD  
921 endmember) (Equation 1). This characterization and selection of the Ra activity in the  
922 discharging groundwater often represents the main source of uncertainty for the final SGD  
923 estimates, since Ra activities in the coastal aquifer can vary significantly (1 – 3 orders of  
924 magnitude) over space and time depending on the geochemical and hydrogeological  
925 characteristics at each study site (e.g., Cerdà-Domènech et al., 2017; Cho and Kim, 2016;  
926 Cook et al., 2018; Duque et al., 2019; Gonnee et al., 2013, 2008; Michael et al., 2011).  
927 Several studies highlighted the inherent difficulties and uncertainties related to the  
928 selection of representative SGD endmembers (Cerdà-Domènech et al., 2017; Cho and Kim,  
929 2016; Cook et al., 2018; Gonnee et al., 2013; Michael et al., 2011). There is no general  
930 framework to characterize SGD endmembers valid for all study sites. The SGD endmember is  
931 commonly determined from near-shore piezometers or inland wells (e.g., Charette et al.,  
932 2013; Garcia-Solsona et al., 2010a; Tovar-Sánchez et al., 2014), porewaters collected at the  
933 seafloor, usually within the first meter below the sediment-water interface (Rodellas et al.,  
934 2017; Tamborski et al., 2018), direct measurements of SGD actually discharging to the  
935 system through seepage meters or springs (Ester Garcia-Solsona et al., 2010; Montiel et al.,  
936 2018; Weinstein et al., 2007) or laboratory experiments to estimate the Ra activity in  
937 equilibrium with sediments (Beck et al., 2008; Garcia-Solsona et al., 2008). Once  
938 groundwater samples are collected at different locations and/or times, in most published  
939 studies Ra values are averaged to obtain a ‘representative average’ SGD endmember (e.g.,  
940 Beck et al., 2007; Kwon et al., 2014; Lee et al., 2012; Rapaglia et al., 2010).

941

942 An important consideration when determining the SGD endmember is that the selected Ra  
943 concentration needs to be representative of the discharging groundwater. In coastal  
944 systems with a dominant pathway, the Ra endmember concentration should thus be  
945 representative of this pathway. Whilst this recommendation is self-evident, many studies  
946 have overlooked or they assumed that the sampled endmember is representative for the  
947 SGD pathways. Given the general and inherent difficulties of sampling SGD, a common  
948 strategy to obtain SGD endmembers is measuring Ra concentrations in existing wells or  
949 piezometers, which are generally installed in the freshwater (or brackish) zone of the coastal  
950 aquifer. However, these wells may not span the range of Ra activities along the salinity  
951 gradients in a subterranean estuary and thus they are not necessarily representative of the  
952 SGD endmember in sites dominated by saline SGD (Pathways 2 to 5) (Michael et al., 2011).  
953 Cho and Kim (2016) highlighted and discussed this issue at a global scale and showed that  
954 the endmembers frequently used to estimate total SGD are often low salinity groundwater  
955 samples (i.e., with relatively low Ra concentrations), even if SGD fluxes are composed mainly  
956 of circulated seawater (Pathways 2 to 5). These authors re-evaluated previous SGD  
957 estimates for the Atlantic Ocean and for the global ocean by using only endmembers with

958 salinities  $\sim > 10$  and showed these fluxes were likely overestimated two- to three-fold only  
959 because non-representative low-salinity groundwaters were included in the determination  
960 of the SGD endmember (Cho and Kim, 2016). On the other hand, if SGD mainly consists of  
961 seawater circulation with short transit times within the subterranean estuary (e.g.,  
962 shoreface seawater circulation or cm-scale porewater exchange), the long-lived isotope  
963 activities (e.g.,  $^{228}\text{Ra}$ ) of circulated seawater (Pathways 2 to 5) may be much lower than  
964 terrestrial water activities (even in fresh water of Pathway 1). This bias towards on-shore  
965 borehole/well data (long transit times) may actually result in an underestimation of SGD, in  
966 particular in basin-scale studies.

967

968 In more complex settings where several SGD pathways coexist, the SGD endmember should  
969 account for the different Ra enrichments in the SGD pathways that occur in the study area  
970 and should reflect the relative contributions of these different pathways. Obtaining the  
971 representative Ra endmember concentration thus requires, in addition to determining the  
972 Ra activity in each pathway, constraining the relative contribution of each SGD pathway.  
973 This is difficult and requires previous knowledge of the fluxes from different pathways,  
974 which is usually not available (Cook et al., 2018; Michael et al., 2011). In addition, when  
975 seawater and groundwater mix, there are salinity gradients and redox interfaces, which  
976 promote geochemical reactions (Gonneea et al., 2008; Moore, 1999; Rocha et al., 2021),  
977 that can further complicate differentiation between the different groundwater discharge  
978 processes. To simplify this approach, previous studies have argued that some of these  
979 pathways are negligible either because the driving forces are not significant (e.g., no tidal-  
980 driven recirculation in microtidal environments, Alorda-Kleinglass et al., 2019; Krall et al.,  
981 2017; Rodellas et al., 2017; Trezzi et al., 2016) or because low permeabilities of ocean  
982 sediments restrict inputs from some SGD pathways (e.g., Beck et al., 2007; Michael et al.,  
983 2011, 2005). Some authors also identified groundwater pathways, which were weakly  
984 enriched in the specific Ra isotope used, and then argued that the system was not  
985 significantly influenced by Ra input from this pathway (e.g., Beck et al., 2007; Garcia-  
986 Solsona et al., 2008; Moore et al., 2019). It should be additionally noted that different SGD  
987 pathways often mix before discharge and do not occur as isolated processes. When two  
988 pathways mix before discharge, this mixed SGD can be treated as a single pathway,  
989 provided that the Ra concentration in this mixed flow is appropriately characterized (Cook  
990 et al., 2018).

991

## 992 [7] Improving the current use of Ra isotopes as SGD tracers

993

994 Ra isotopes have been widely applied to quantify SGD all kind of locations worldwide and in  
995 a large range of physical environments (e.g., lagoons, wetlands, estuaries, bays or ocean  
996 basins). The estimates of SGD derived from Ra isotopes are based on conceptual  
997 assumptions that are often not properly justified or validated, and may involve large  
998 uncertainties that are usually not quantifiable and could lead to inaccuracies or unrealistic  
999 of the SGD estimates. In this section, we discuss some key considerations with the aim of  
1000 improving future applications of Ra isotopes as SGD tracers.

1001

### 1002 [7.1] Validation of model assumptions and consideration of conceptual uncertainties

1003

1004 The magnitude of SGD can be quantified using a variety approaches, including field methods  
1005 (e.g., seepage meters, natural tracers and piezometric level measurements) or  
1006 computational approaches (e.g., water budget models and numerical solutions of the  
1007 groundwater flow equation) (Taniguchi et al., 2019). Each of these approaches is prone to  
1008 certain biases and is limited in both the spatial coverage and the SGD pathways it is  
1009 capturing (Burnett et al., 2006; Zhou et al., 2018). Using different approaches can yield  
1010 order-of-magnitude differences in SGD at individual locations and, thus, the selection of the  
1011 method itself constitutes the first source of uncertainty in any SGD study (Rodellas et al.,  
1012 2021; Zhou et al., 2018).

1013  
1014 Tracer approaches are based on conceptual models that represent an abstraction of a  
1015 complex and dynamic natural system. Thus, the a second additional source of uncertainty is  
1016 linked to the conceptualization of the natural system, the so-called conceptual or structural  
1017 uncertainty (Regan et al., 2002). In the case of Ra isotopes there are three models (or  
1018 concepts) commonly applied to quantify SGD (see 6.1): “Mass balance model” and “mixing  
1019 model”, which are both based on Ra budgets using lumped parameter models, and a  
1020 “offshore export model”, which is based on a simplified analytical solution to describe Ra  
1021 transport. Each one of these models is extremely sensitive to its specific simplifications,  
1022 assumptions and boundary conditions used to approximate the real system. For instance, Ra  
1023 “mass balances” are strongly influenced by the sources and sinks of Ra included in the  
1024 model (e.g., some studies assume that all Ra input can be directly attributed to SGD) and,  
1025 mainly, by the parameterization of the different input and output terms and their intrinsic  
1026 assumptions. Indeed, the use of different methods or parameterizations to quantify the  
1027 same term in the mass balance (e.g., different approaches to estimate offshore exchange  
1028 rates, sediment diffusion or to produce an averaged Ra concentration in the study area)  
1029 may lead to order-of-magnitude discrepancies in Ra-derived SGD estimates (Rodellas et al.,  
1030 2021). The mass balance approach also assumes that the integrative parameters can  
1031 appropriately represent the system (e.g., the model assumes that offshore exchange occurs  
1032 with an average Ra concentration.). Similarly, the “offshore export” model is essentially a  
1033 simplification of the 1-D advection-dispersion equation and is very sensitive to the boundary  
1034 conditions and basic assumptions of this approach. These assumptions may not be correct  
1035 in environments with along-shore and across-shore currents (advection cannot be  
1036 neglected), with radiu. inputs occurring beyond the nearshore source, with not uniform  
1037 vertical profiles of Ra isotopes or non-negligible Ra concentrations offshore, or in systems  
1038 with a sloped seabed (see e.g., Hancock et al., 2006; Lamontagne and Webster, 2019a,  
1039 2019b). Additionally, all the Ra models are often based on the assumption that mixing  
1040 processes affect all the isotopes alike, either through the estimation of flushing times or  
1041 water ages ( $t_w$ ) using pairs of isotopes (see section 8.3) or by using an offshore diffusivity  
1042 coefficient ( $K_h$ ) derived from one isotope to evaluate the transport of another one  
1043 (Lamontagne and Webster, 2019b). Since Ra transport offshore is often controlled by  
1044 dispersion, which integrates processes operating at different temporal and spatial scales,  
1045 mixing parameters (e.g.,  $t_w$  or  $K_h$ ) are scale dependent and should be independently  
1046 evaluated for each tracer (Lamontagne and Webster, 2019b; Moore, 2015; Okubo, 1976).  
1047 Finally, and most importantly, almost all studies assume that the system is in steady state  
1048 and that all model parameters are constant on the timescale the tracer resides in the  
1049 system, assumptions that are very often not met – in particular for long-lived isotopes – and  
1050 that should be carefully evaluated (see 7.2).

1051

1052 The reliability of Ra approaches to quantify SGD may thus be limited and scientists should  
 1053 be aware of these limitations and try to validate their assumptions and constrain the  
 1054 uncertainties of the estimated flows. Overcoming these limitations is not straightforward  
 1055 and there is not a general framework for accounting for these conceptual uncertainties or  
 1056 validating assumptions. Some authors have suggested evaluating the most sensitive  
 1057 parameters using multiple approaches and obtaining final SGD fluxes as an ensemble of  
 1058 results (e.g., Rodellas et al., 2021b), combining multiple independent methods to constrain  
 1059 the magnitude of SGD (e.g., Zhou et al., 2018) or developing more complex transport  
 1060 models (e.g., Lamontagne and Webster, 2019b). For example, combining ‘terrestrial’  
 1061 hydrogeological, oceanographic or geophysical approaches with tracers tools may help to  
 1062 improve SGD estimates. Producing more robust estimates of SGD is clearly a major open  
 1063 research topic in SGD and Ra investigations (see 9.2).

1064

## 1065 [7.2] The assumption of steady-state needs to be validated

1066

1067 A key general assumption in all the Ra-based approaches to quantify SGD is that all Ra fluxes  
 1068 (e.g., SGD-driven Ra flux, Ra diffusion from sediments, radioactive decay, Ra export  
 1069 offshore) are constant with respect to the timescale of the Ra isotope used and that the  
 1070 system is in steady state (i.e., Ra inputs equal Ra outputs). Therefore, any appropriate SGD  
 1071 study should validate these assumptions considering the time the tracer resides in the  
 1072 system, i.e. the tracer residence time (Rodellas et al., 2021). The average residence time of  
 1073 Ra isotopes in the surface water system depends on the rate of removal of the isotope and  
 1074 thus on their different sinks. Given that the residence time of Ra isotopes ( $t_{Ra}$ ) in most of the  
 1075 systems is mainly controlled by radioactive decay and export offshore (see Figure 9), it can  
 1076 be estimated following Equation 9 (Rodellas et al., 2021):

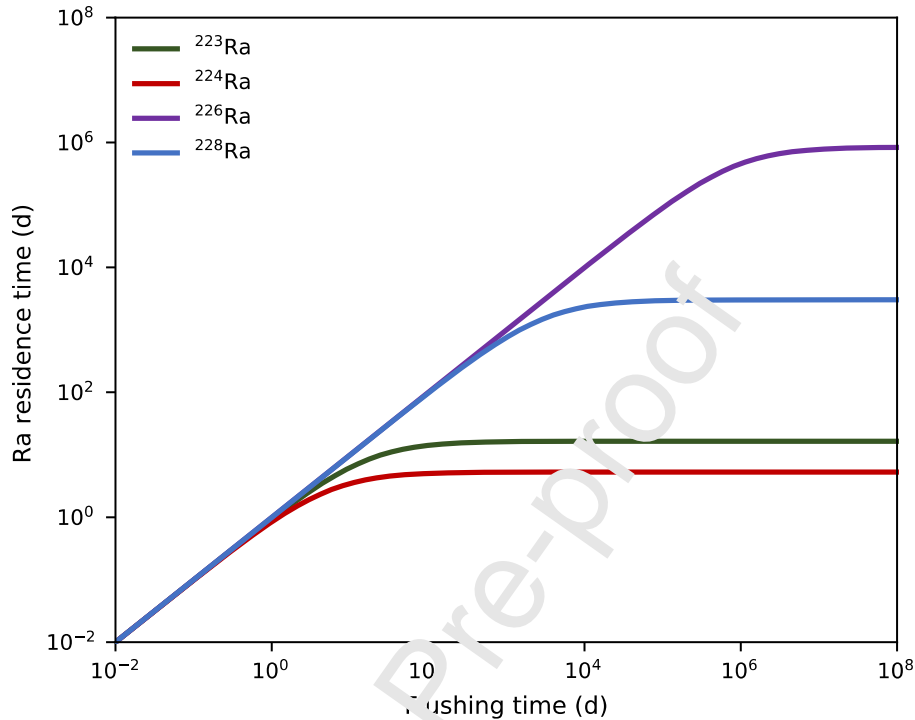
1077

$$1078 \quad t_{Ra} \approx \frac{1}{\lambda + \frac{1}{t_w}} \quad (9)$$

1079

1080 where  $\lambda$  is the radioactive decay constant of the specific Ra isotope used and  $t_w$  is the  
 1081 flushing time in the system due to mixing. This flushing time is equivalent to mean water  
 1082 residence time in systems where the influence of evaporation and dispersion are negligible.  
 1083 Characteristic Ra residence time for study sites with different mixing timescales (i.e.,  
 1084 different flushing times) are shown in Figure 11. In systems where the timescales of  
 1085 transport processes exceeds that of radioactive decay ( $1/t_w \gg \lambda$ ), the Ra residence time in  
 1086 the system is comparable to the temporal scale of coastal mixing. Thus, the assumptions of  
 1087 constant fluxes and steady state need to be validated on timescales of transport processes  
 1088 (Moore, 2015; Rodellas et al., 2021). For systems with negligible mixing processes relative to  
 1089 the isotope half-life ( $1/t_w \ll \lambda$ ), the Ra temporal scale is controlled by the radioactive decay  
 1090 of each isotope. In this latter case, the assumption of steady state and constant fluxes need  
 1091 to be validated on a timescale comparable to the mean life of the specific isotope used.  
 1092 Validating this assumption might thus be particularly challenging for long-lived Ra isotopes  
 1093 in systems with long flushing times. In those dynamic systems that present a relevant  
 1094 temporal variability on the timescale of the tracer used (e.g., systems with variable surface  
 1095 water inputs, temporal changes of SGD or variable mixing offshore), the evolution of Ra  
 1096 concentration in sources, sinks and inventories in the water column need to be understood.

1097 Neglecting the transience of these parameters could lead to significant errors on the final  
 1098 SGD estimates. In such non-steady state systems, a dynamic modelling approach might  
 1099 provide a better representation of the studied system (Gilfedder et al., 2015).  
 1100  
 1101



1102  
 1103 **Figure 11:** Average residence times for different Ra isotopes as function of flushing time due  
 1104 to mixing (based on Rodellas et al., 2021).  
 1105

### 1106 [7.3] Ra isotopes cannot be used indistinctly to trace SGD

1107  
 1108 Ra isotopes have been commonly used to estimate total SGD, often without consideration  
 1109 as to whether the Ra isotope used is actually capturing the entire discharge pathway(s)  
 1110 underlying these flows. This raises the question of whether or not the four Ra isotopes  
 1111 provide the same SGD estimates and if they therefore can be used indistinctly.  
 1112

1113 In an idealized case where there is a unique SGD pathway or source, for instance, a karstic  
 1114 or volcanic area with a main coastal spring that dominates over any diffuse, non-point  
 1115 source discharge. In this case, all Ra isotopes should yield the same SGD flux, provided that  
 1116 i) all the Ra sources (aside from SGD) and sinks are appropriately constrained, ii)  
 1117 groundwater is sufficiently enriched with the Ra isotope used as a tracer, and iii) the SGD  
 1118 endmember is properly characterized. However, most natural systems do not satisfy these  
 1119 idealized conditions because of the ubiquitous presence of multiple driving forces (e.g.,  
 1120 hydraulic gradient, wave and tidal pumping, bioirrigation) that result in concurrent inputs of  
 1121 Ra from different SGD pathways (Figure 3). As illustrated in Figure 6, the different SGD  
 1122 pathways are likely to have different groundwater composition and characteristic  
 1123 groundwater transit times, resulting in isotope-specific Ra enrichments, which may differ by  
 1124 orders of magnitude among different SGD pathways (Diego Feliu et al., 2021; Michael et al.,

1125 2011). Different Ra isotopes are thus incorporating different pathways in a characteristic  
1126 proportion, and thus they are likely to produce different SGD estimates. For instance, whilst  
1127 SGD estimates based on  $^{223}\text{Ra}$  and  $^{224}\text{Ra}$  are likely to incorporate inputs from all the  
1128 pathways, long-lived Ra isotopes may not incorporate SGD induced by short-scale processes  
1129 (cm-scale circulation or shoreface saline circulation) (King, 2012; Michael et al., 2011;  
1130 Moore, 2010; Rodellas et al., 2017) (Figure 6). Therefore, when SGD is discharging via  
1131 multiple pathways, all four Ra isotopes cannot be used indistinctly to obtain total SGD.

1132  
1133 Most Ra-based SGD studies aim at obtaining a single estimate of the total magnitude of  
1134 SGD. In these cases, SGD is often treated as a single source, regardless of the difference in  
1135 Ra activities of the multiple pathways, and only a single endmember is determined to  
1136 represent the 'average' Ra activity in groundwater discharging into the study site (i.e.,  $C_{\text{Ra-SGD}}$   
1137 in Equation 1). However, this Ra endmember should not be obtained from simple  
1138 averages of all the SGD samples collected, because of possible biases towards the most  
1139 sampled pathway. Michael et al. (2011) illustrated this issue by comparing SGD estimates  
1140 obtained by sampling different pathways and showed that this could produce differences in  
1141 final SGD estimates by more than an order of magnitude (Michael et al., 2011). Therefore,  
1142 unless there is a comprehensive understanding of the system that allows constraining the  
1143 relative contribution of different pathways, SGD estimates derived from a single Ra isotope  
1144 might not be appropriate at sites with multiple pathways.

1145  
1146 The combination of multiple Ra isotopes can be instrumental in those systems where  
1147 several pathways are hypothesized to significantly contribute to Ra budgets (see also  
1148 section 7.5). Both total SGD and the relative contribution of different SGD pathways can be  
1149 accurately obtained from the concurrent application of multiple Ra isotopes. The number of  
1150 Ra isotopes to be used in the model will depend on the number of SGD pathways to be  
1151 determined, as well as the amount of other potential unknowns (e.g., residence time, river  
1152 contribution). This approach can be applied through concurrent mass balances (see chapter  
1153 6.1; e.g., Rodellas et al., 2017; Tamborski et al., 2017a) or mixing models (e.g., Charette,  
1154 2007), provided that the Ra isotopes used have distinct relative enrichments (i.e., distinct Ra  
1155 isotopic ratios) in the different pathways. Ra isotopes can also be combined with other  
1156 tracers (e.g., silica, radon, salinity, stable isotopes, etc.) (e.g., Burnett et al., 2006; Garcia-  
1157 Solsona et al., 2010; Ogler et al., 2019; Schubert et al., 2015) or approaches (e.g., seepage  
1158 meters, Darcy estimates, heat tracing, tidal prism, hydrogeological models) (e.g., Garcia-  
1159 Orellana et al., 2010; Povinec et al., 2012; Prieto and Destouni, 2005; Rosenberry et al.,  
1160 2020), which can decisively contribute towards the quantification of the different pathways  
1161 and the appropriate characterization of SGD.

#### 1163 [7.4] The Ra isotope(s) used need to be carefully selected

1164  
1165 The selection of the tracer used should ideally be based on the process to be studied and  
1166 the characteristics of the study site, rather than on the methods available (e.g., salinity or  
1167 radon are much better SGD tracers than radium in certain systems). Likewise, the best  
1168 suited Ra isotope for any specific study also needs to be chosen based on the target SGD  
1169 pathway of interest, the area studied and according to the sensitivity of the final estimates  
1170 of Ra inputs and outputs, which is specific for each coastal water system (Tamborski et al.,  
1171 2020). In principle, the time scale of the half life of the chosen Ra isotope should scale with

1172 the size and time scales of the system, such that the short-lived Ra isotopes are most  
1173 effective at nearshore and embayment scales (e.g., Boehm et al., 2004; Knee et al., 2010;  
1174 Rapaglia et al., 2012), while long-lived Ra isotopes are most effective at regional and global-  
1175 scales (residence times > 100 days; e.g., Charette et al., 2015; Kwon et al., 2014; Liu et al.,  
1176 2018; Moore et al., 2008; Rodellas et al., 2015a). In either scenario, radioactive decay can be  
1177 easily estimated from the Ra inventory in the water column and this facilitates  
1178 characterizing total output fluxes in systems where radioactive decay is the primary Ra sink.  
1179 On the contrary, mixing losses of Ra isotopes can be highly uncertain, including both water  
1180 exchange at the boundaries of the system and the Ra endmember concentration (Tamborski  
1181 et al., 2020). Given that long-lived Ra isotopes are highly sensitive to mixing in coastal areas  
1182 (i.e., estuaries, coastal lagoons), they may not be adequate tracers of SGD in coastal  
1183 environments when mixing is uncertain (Ku and Luo, 2008; Rutgers van der Loeff et al.,  
1184 2018). Short-lived Ra isotopes are ideal for coastal areas where timescales are on the order  
1185 of days; however, sediment fluxes must be adequately characterized because they often  
1186 represent a major source of short-lived Ra isotopes (Burt et al., 2014; Rodellas et al., 2015b).  
1187 Water column inventories of short-lived Ra isotopes integrate over time-scales similar to the  
1188 Ra isotope half-life, and therefore multiple samplings are necessary if seasonal or annual  
1189 variations in SGD want to be captured.

1190

#### 1191 [7.5] Ra isotopes can contribute identifying the pathways of SGD

1192

1193 A proper evaluation of SGD requires the understanding of the dominant SGD pathways.  
1194 There are several hydrogeological, geophysical and geochemical characterization techniques  
1195 (e.g., Folch et al., 2020; Gonnee et al., 2018; Swarzenski et al., 2007b, 2006; Zarroca et al.,  
1196 2014), as well as numerical modelling approaches (e.g., Amir et al., 2013; Anwar et al., 2014;  
1197 Danielescu et al., 2009), that provide fundamental information about the origin and spatio-  
1198 temporal scales of the different SGD pathways through the subterranean estuary (Figure 6).  
1199 The characterization of Ra isotopes and especially their activity ratios (e.g.,  $^{228}\text{Ra}/^{226}\text{Ra}$  and  
1200  $^{224}\text{Ra}/^{228}\text{Ra}$ ) in the subterranean estuary can also provide very useful information to  
1201 constrain the presence of different SGD pathways in the study site. For instance, since  $^{228}\text{Ra}$   
1202 and  $^{226}\text{Ra}$  belong to different decay chains (U and Th), the activity ratio of  $^{228}\text{Ra}/^{226}\text{Ra}$  may  
1203 provide information about the Th/U ratio in the host material and thus be used to identify  
1204 and distinguish groundwater inflowing from different geological systems (e.g., Charette and  
1205 Buesseler, 2004; Moore, 2006; Swarzenski et al., 2007). Additionally, the  $^{224}\text{Ra} - ^{228}\text{Ra}$   
1206 parent-daughter relationship enables the use of the  $^{224}\text{Ra}/^{228}\text{Ra}$  activity ratio for  
1207 characterizing different SGD pathways. Whilst short-time-scale SGD pathways are likely to  
1208 be more enriched in short-lived Ra isotopes relative to long-lived ones (Figure 6) presenting  
1209 thus high  $^{224}\text{Ra}/^{228}\text{Ra}$  activity ratios (> 1), long-scale pathways are likely to present similar  
1210  $^{224}\text{Ra}$  and  $^{228}\text{Ra}$  activities (i.e.,  $^{224}\text{Ra}/^{228}\text{Ra} \sim 1$ ) (Diego-Feliu et al., 2021).

1211

1212 Moreover, the activity ratios of Ra isotopes in coastal seawater can also be used to evaluate  
1213 the predominant discharge pathways of SGD, provided that Ra is mainly supplied to the  
1214 coastal ocean by SGD (i.e., absence of any significant source such as diffusion from  
1215 sediments, seawater or rivers). In this case and if radioactive decay is accounted for, the  
1216 activity ratios of coastal seawater must reflect the combined contribution of the different  
1217 SGD pathways, being biased towards the more relevant ones (Boehm et al., 2006; Moore,  
1218 2006b; Rodellas et al., 2014). For instance, at a site dominated by short-scale pathways (e.g.,

1219 porewater exchange), the  $^{224}\text{Ra}/^{228}\text{Ra}$  activity ratio of coastal sea water is expected to be  
1220 comparable to that of porewater (i.e.,  $^{224}\text{Ra}/^{228}\text{Ra} > 1$ ).

1221

## 1222 [7.6] Estimates of SGD-driven solute fluxes need to account for the variable 1223 composition of different pathways

1224

1225 The most commonly applied method to estimate fluxes of dissolved chemicals (e.g.  
1226 nutrients, metals, contaminants) driven by SGD is by multiplying either the (Ra-derived) SGD  
1227 water flow by the average concentration of the chemical solutes in the SGD endmember or  
1228 the SGD-driven Ra flux by the average solute/Ra ratio in the SGD endmember (Charette et  
1229 al., 2016; Hwang et al., 2016; Santos et al., 2011; Tovar-Sánchez et al., 2014). This straight-  
1230 forward approach might be appropriate for systems with one dominant SGD pathway  
1231 (provided that the endmember concentration is appropriately determined), but it should  
1232 not be directly applied in systems with multiple SGD pathways or sources. This is mainly  
1233 because the biogeochemical composition of discharging fluids from different SGD pathways  
1234 may be considerably different depending on the origin of solutes, their transformations  
1235 within the subterranean estuary and the temporal and spatial scales of the different  
1236 pathways (e.g., Rodellas et al., 2018; Santos et al., 2012; Tamborski et al., 2017a; Weinstein  
1237 et al., 2011). Therefore, as discussed for Ra isotopes, the solute concentration obtained  
1238 from averaging groundwater samples (and thus the flux estimates) is likely to be biased  
1239 towards the most sampled pathway, and is not representative of the relative SGD flux from  
1240 that pathway. For instance, terrestrial groundwater discharge (Pathway 1) often contains  
1241 high concentrations of nutrients and other compounds released from anthropogenic  
1242 activities, whereas other SGD pathways may not be influenced by anthropogenic sources.  
1243 Using only solute concentrations from wells and boreholes located within the low-salinity  
1244 part of the subterranean estuary may result in average solute concentrations having a  
1245 strong anthropogenic signal (e.g., high nutrient concentrations) that might not be  
1246 representative of SGD in sites influenced by pathways other than terrestrial groundwater  
1247 discharge (see section 6.2). An appropriate understanding of the magnitude of solute fluxes  
1248 driven by SGD, requires thus a previous identification of the dominant SGD pathways, which  
1249 needs to be based on a detailed knowledge of the studied system. Sampling efforts should  
1250 then be taken to target all the relevant SGD pathways for the particular system, particularly  
1251 over the full-salinity gradient of the subterranean estuary. By doing so, the conservative  
1252 and/or non-conservative behavior of the solute of interest can be determined, since some  
1253 solutes can be chemically modified in the subterranean estuary by varying the ratio of  
1254 solute to Ra along the SGD flow path. This is an essential step towards a correct  
1255 quantification of SGD-driven solute fluxes in sites with multiple pathways and thus, towards  
1256 a comprehensive understanding of the role of SGD for coastal biogeochemical cycles.

1257

## 1258 [8] Additional applications of Ra isotopes in groundwater and marine 1259 studies

1260

1261 Aside from the application of Ra isotopes to quantify SGD, Ra isotopes can also provide  
1262 instrumental information that can help to constrain the different terms needed for SGD  
1263 evaluations (e.g., flushing time of coastal waters), as well as key information for

1264 characterizing hydrological and oceanic systems. In this section, we briefly summarize  
 1265 parallel applications of Ra isotopes in groundwater and marine studies, which include: i)  
 1266 assessing transit times in coastal aquifers; ii) estimating solute fluxes across the sediment–  
 1267 water interface; iii) estimating ages of coastal surface waters; and iv) quantifying shelf-scale  
 1268 solute fluxes.

### 1270 [8.1] Assessment of groundwater transit times in coastal aquifers

1271

1272 Constraining groundwater transit times in a coastal aquifer or in the subterranean estuary is  
 1273 a key question in characterizing coastal hydrogeology. Applications include deriving  
 1274 characteristic distances to the upgradient recharge points, evaluating the connectivity of the  
 1275 coastal aquifer with the sea, determining ages and velocities of groundwater, differentiating  
 1276 variable spatio-temporal scale processes and evaluating the potential transformation of  
 1277 solutes in the subterranean estuary (Gonneea and Charette, 2014; Lerner and Harris, 2009;  
 1278 Werner et al., 2013). Since observational techniques are limited in the subsurface,  
 1279 hydrogeological tracers (e.g. H and O stable isotopes,  $^3\text{He}$ ,  $^{36}\text{Cl}$ , CFCs) are commonly used to  
 1280 obtain key information on groundwater flow (Leiburgut and Seibert, 2011). In recent  
 1281 years, the activities of Ra isotopes have been used to evaluate groundwater dynamics in the  
 1282 subterranean estuary (Bokuniewicz et al., 2015; Kiro et al., 2013; Tamborski et al., 2019,  
 1283 2017b), which can be a complementary method to the other approaches based on  
 1284 atmospheric-introduced tracers, which mainly decay while traveling through an aquifer  
 1285 (Cook and Herczeg, 2012). To evaluate the distribution of Ra in aquifers, each of the inputs  
 1286 and outputs of Ra to groundwater needs to be constrained. These input and output terms,  
 1287 which are summarized in Section 5, include production, decay, desorption, adsorption,  
 1288 weathering and precipitation, as well as dispersion. The most common analysis of Ra  
 1289 distribution in groundwater often utilizes a one-dimensional transport model (Equation 10),  
 1290

$$1291 \quad \frac{\partial A_{Ra}}{\partial t} = L(A_{Ra}) - \lambda R_{Ra} A_{Ra} + \lambda P - \lambda B + \lambda \Gamma \quad (10)$$

1292

1293 where  $A_{Ra}$  [ $\text{Bq m}^{-3}$ ] is the activity of Ra in groundwater,  $t$  [s] is time,  $\lambda$  [ $\text{s}^{-1}$ ] is the decay  
 1294 constant, and  $R_{Ra}$  [-] is the linear retardation factor of Ra. Retardation is defined as the  
 1295 retention of a solute due to interaction with solid phases relative to bulk solution in a  
 1296 dynamic system (McKinley and Russell Alexander, 1993). The first term on the right hand-  
 1297 side of the equation (10) is the linear operator for transport ( $L(A_{Ra}) = -\nabla q A_{Ra} +$   
 1298  $\nabla D \nabla A_{Ra}$ , with  $q$  [ $\text{m s}^{-1}$ ] and  $D$  [ $\text{m}^2 \text{s}^{-1}$ ] as the Darcy flux vector and the dispersion tensor,  
 1299 respectively) that includes the advective and dispersive terms. The second and third terms  
 1300 are the radioactive decay of the exchangeable activity of Ra (i.e., adsorbed and dissolved)  
 1301 and production from Th in solution, solid surfaces, and in the effective alpha recoil zone ( $P$   
 1302 [ $\text{Bq m}^{-3}$ ]). The last two terms refer to the rate of co-precipitation ( $B$  [ $\text{Bq m}^{-3}$ ]) and  
 1303 weathering (i.e., dissolution) ( $\Gamma$  [ $\text{Bq m}^{-3}$ ]) of Ra, respectively.

1304

1305 This equation is often simplified by assuming steady-state conditions ( $\partial A_{Ra}/\partial t = 0$ ),  
 1306 negligible Ra co-precipitation ( $B = 0$ ) and dissolution ( $\Gamma = 0$ ), negligible dispersion relative  
 1307 to advection ( $L(A_{Ra}) = -\nabla q A_{Ra}$ ), and defining a travel time along a streamline (here after  
 1308 transit time,  $\tau$  [s]) (Equation 11; Kiro et al., 2013; Krest and Harvey, 2003; Schmidt et al.,  
 1309 2011; Tamborski et al., 2017b).

1310

1311

$$A_{Ra}(\tau) = \frac{P}{R_{Ra}} + \left( A_{Ra,0} - \frac{P}{R_{Ra}} \right) e^{-\lambda R_{Ra} \tau} \quad (11)$$

1312

1313 where  $A_{Ra,0}$  is the activity of groundwater entering a streamline.

1314

1315 This simple solution implicitly assumes that production rates are constant and thus it  
 1316 neglects the effect of spatial and/or temporal variations in the parent isotope activities (e.g.,  
 1317 geological heterogeneity). Moreover, the determination of groundwater ages, velocities or  
 1318 transit times using this equation strongly relies on an accurate determination of the  
 1319 retardation factor of Ra ( $R_{Ra}$ ), which may also be spatially and temporally variable. The  
 1320 retardation factor of Ra is commonly determined by using the distribution coefficient of Ra  
 1321 (Equation 12; Michael et al., 2011).

1322

1323

$$R_{Ra} = 1 + K_D \frac{\rho_s}{\phi} \quad (12)$$

1324

1325 where  $K_D$  [ $\text{m}^3 \text{kg}^{-1}$ ] is the distribution coefficient,  $\rho_s$  [ $\text{kg m}^{-3}$ ] is the dry bulk mass density, and  
 1326  $\phi$  is the porosity.

1327

1328 If the production rate ( $P$ ), the retardation factor of Ra ( $R_{Ra}$ ) and the inflow boundary  
 1329 activities of Ra ( $A_{Ra,0}$ ) are known, groundwater transit times can be easily derived from  
 1330 equation 11 using a single Ra isotope. However, determinations of  $P$ ,  $R_{Ra}$  and  $A_{Ra,0}$  are  
 1331 usually difficult and induce large uncertainties that must be propagated in the calculation of  
 1332 groundwater transit times. In practice, this may be difficult due to spatial and temporal  
 1333 variability that affects the four Ra isotopes differently. Although the processes are  
 1334 integrated along a single flowpath, short-lived isotopes have a much shorter ‘memory’ than  
 1335 long-lived isotopes, so short-lived Ra activities are more sensitive to production rates and  
 1336 retardation factors more proximal to the sampling point. Alternatively, when the model  
 1337 parameters are unknown, groundwater transit times may be determined by using multiple  
 1338 Ra isotopes or activity ratios (e.g.,  $^{224}\text{Ra}/^{228}\text{Ra}$ ) (Tamborski et al. 2019). When the Ra  
 1339 production rate changes with depth, a depth-dependent 1D reactive transport model can be  
 1340 applied (Liu et al., 2019). Non-steady state conditions like variable hydrological forcing,  
 1341 wave set-up as well as tidal fluctuations may cause non-steady state conditions which may  
 1342 obscure groundwater transit times. Since this model assumes that there is no mixing  
 1343 between two different types of groundwater (with different ages and Ra content), it can  
 1344 cause problems in the interpretation of the transit times when mixing does occur, largely  
 1345 because mixing is a linear process whereas radioactive decay and ingrowth are exponential  
 1346 (Bethke and Johnson, 2002). Since the determination of groundwater transit times requires  
 1347 some assumptions in solving the transport equation (equation 11) and involved terms,  
 1348 independent verifications of Ra-derived transit times are strongly recommended.

1349

## 1350 [8.2] Solute flux across the sediment–water interface derived from Ra isotopes

1351

1352 The transfer of solutes across the sediment-water interface, through both diffusion and  
 1353 advection, can have a major effect on the chemical composition of the overlying waters and  
 1354 shallow sediments. Traditional approaches to quantify water exchange and solute fluxes  
 1355 using Ra isotopes rely upon one-dimensional reactive-transport models to reproduce

1356 porewater activities as a function of sediment production, bioturbation, molecular diffusion,  
 1357 dispersion and advection (Cochran and Krishnaswami, 1980; Krest and Harvey, 2003; Sun  
 1358 and Torgersen, 2001). Recent analytical developments have allowed the measurement of  
 1359 surface-exchangeable  $^{224}\text{Ra}$  and particle-bound  $^{228}\text{Th}$  from sediment cores (Cai et al., 2012).  
 1360 Radioactive disequilibrium between the soluble  $^{224}\text{Ra}$  daughter and its particle-bound  
 1361 parent  $^{228}\text{Th}$  ( $T_{1/2} = 1.9$  y) may be produced in sediments and their interstitial pore fluids  
 1362 from the transport of  $^{224}\text{Ra}$  as a result of molecular diffusion, bioturbation and irrigation  
 1363 and/or SGD. Assuming that the *in-situ* decay of  $^{228}\text{Th}$  is the sole source of sediment  $^{224}\text{Ra}$ , a  
 1364 steady-state mass balance can be written (Cai et al., 2014, 2012) as Equation 13.

$$1366 \quad F_{Ra} = \int_0^{\infty} \lambda_{Ra} (A_{Th} - A_{Ra}) dz \quad (13)$$

1367  
 1368 where  $F_{Ra}$  is the flux of  $^{224}\text{Ra}$  across the sediment-water interface ( $\text{Bq m}^{-2} \text{d}^{-1}$ ),  $z$  is the depth  
 1369 in the sediment where disequilibrium occurs (m),  $\lambda_{Ra}$  is the  $^{224}\text{Ra}$  decay constant ( $0.189 \text{d}^{-1}$ )  
 1370 and  $A_{Th}$  and  $A_{Ra}$  are respectively the activities of bulk  $^{228}\text{Th}$  and  $^{224}\text{Ra}$  ( $\text{Bq cm}^{-3}$ ) of wet  
 1371 sediment, which is obtained from a mass unit considering sediment dry bulk density ( $r_s =$   
 1372  $2.65 \text{g cm}^{-3}$ ) and porosity ( $\phi$ ). A key advantage of the  $^{224}\text{Ra}/^{228}\text{Th}$  disequilibrium method over  
 1373 traditional reactive-transport models (Boudreau, 1997a; Meysman et al., 2005) is that  $^{224}\text{Ra}$   
 1374 production is directly measured (via  $^{228}\text{Th}$ ) for each sediment section, and thus this  
 1375 approach accounts for depth-varying production rates.

1376  
 1377 Derivation of a benthic  $^{224}\text{Ra}$  flux from fine-grained (muddy) sediments can in turn be used  
 1378 to quantify the transfer rate ( $F_i$ ) of a dissolved species across the sediment-water interface  
 1379 (Cai et al., 2014) using Equation 14.

$$1381 \quad F_i = F_{Ra} \left( \frac{D_s^i}{D_s^{Ra}} \right) \left( \frac{\partial A^i / \partial z}{\partial A^{Ra} / \partial z} \right) \quad (14)$$

1382  
 1383 where  $D_s^i$  and  $D_s^{Ra}$  are the *in-situ* molecular diffusion coefficients for dissolved species  $i$  and  
 1384  $^{224}\text{Ra}$ , respectively, corrected for tortuosity and *in-situ* temperature (Boudreau, 1997b). The  
 1385 concentration gradients of dissolved species  $i$  ( $\partial A^i / \partial z$ ) and  $^{224}\text{Ra}$  ( $\partial A^{Ra} / \partial z$ ) are taken as the  
 1386 concentration difference between overlying surface waters and shallow porewaters,  
 1387 typically measured at 1 cm depth, and are thus net solute fluxes (Cai et al., 2014, 2012).  
 1388 Note that the flux obtained in the Equation 14 is translated from an adjusted Fick's First Law  
 1389 (Equation 15).

$$1391 \quad F = -\xi \cdot \Phi \cdot D_s \frac{\partial c}{\partial z} \quad (15)$$

1392  
 1393 where  $\xi$  is an area enhancement factor representing the extended subsurface interface and  
 1394 advective influences on the diffusive flux, and  $\Phi$  is porosity. Although Equation 14 only  
 1395 includes molecular diffusive coefficients of dissolved species  $i$  and  $^{224}\text{Ra}$ , it represents the  
 1396 sum of all processes that affect solute transfer across the sediment-water interface. The  
 1397 inherent assumption is that molecular diffusion is the rate-limiting step for solute transport.  
 1398 This approach is suitable to quantify fluxes across the sediment-water interface from  
 1399 shallow ( $< 20$  cm) sediment cores in benthic and coastal (i.e., salt marsh) mud environments  
 1400 for oxygen (Cai et al., 2014; Dias et al., 2016), dissolved inorganic carbon and nutrients (Cai

1401 et al., 2015), rare earth and trace elements (Hong et al., 2018; Shi et al., 2018, 2019b). Note  
 1402 that solute fluxes derived from Equation 14 integrate over a time-scale of ~10 days and may  
 1403 greatly exceed fluxes determined from porewater gradients (Cai et al., 2015, 2014) and  
 1404 traditional sediment incubations, which alter the physical conditions of the sediments, and  
 1405 therefore may not capture small-scale (mm to cm) advective processes (Hong et al., 2018;  
 1406 Shi et al., 2019b). More complicated diagenetic models of  $^{224}\text{Ra}$  have been developed for  
 1407 systems subject to significant bioturbation and particle reworking, and may thus require  
 1408 parallel sediment measurements of excess  $^{234}\text{Th}$  to accurately constrain  $^{224}\text{Ra}$  fluxes (Cai et  
 1409 al., 2015, 2014).

1410  
 1411 Concurrent sediment and water column  $^{224}\text{Ra}$  mass balances may be used to separate short-  
 1412 scale advective-diffusive processes (i.e., PEX) from other SGD pathways (Hong et al., 2017).  
 1413 In deeper sediment systems, where seepage occurs laterally at depth (i.e., as SGD in coarse-  
 1414 grained sediments), Equation 13 can be used for the horizontal (1-D) export flux of  $^{224}\text{Ra}$ ,  
 1415 and thus horizontal water exchange rates ( $Q$ ;  $\text{L m}^{-2} \text{d}^{-1}$ ) can be estimated (Shi et al., 2019a)  
 1416 using Equation 16,

$$1417 \quad Q = \frac{F_{Ra}}{A_{PW} - A_{sea}} \quad (16)$$

1419  
 1420 where  $A_{PW}$  and  $A_{sea}$  represents the dissolved  $^{224}\text{Ra}$  activity in porewater from the seepage  
 1421 layer and seawater, respectively. In turn, solute fluxes may be estimated by considering the  
 1422 concentration difference between porewater and seawater of a given solute (Shi et al.,  
 1423 2019a). Similarly, a two-dimensional advective cycling model can be used to estimate water  
 1424 exchange and solute fluxes in sandy seabeds subject to wave and tidal pumping (Cai et al.,  
 1425 2020). In conclusion, application of the  $^{224}\text{Ra}/^{228}\text{Th}$  disequilibrium method has been  
 1426 significantly expanded upon since its first introduction (Cai et al., 2012), and likely will  
 1427 continue to be expanded upon as more researchers apply this technique to different coastal  
 1428 environments.

1429  
 1430 Whereas the approaches outlined above describe fluxes across the sediment-water  
 1431 interface, diapycnal mixing (i.e., the mixing away from deep-sea sediments into the interior  
 1432 of the water column) is one further process which can be quantified using Ra isotopes. As  
 1433 bottom sediments are the source of Ra, the concentration gradient above the bottom  
 1434 sediments can be used to calculate vertical eddy diffusivity (see Eq. 8). So far very few  
 1435 studies applied this method (Huh and Ku, 1998; Koch-Larrouy et al., 2015). Nevertheless it  
 1436 may be an important approach to investigate the fate of benthic sourced solutes in the  
 1437 water column.

### 1438 1439 [8.3] Estimation of timescales in coastal surface waters

1440  
 1441 The functioning and vulnerability of a coastal ecosystem (e.g., accumulation of  
 1442 contaminants, risk of eutrophication or harmful algal blooms) are often closely related to  
 1443 the retention of solutes (e.g., nutrients, contaminants, suspended biomass) and thus the  
 1444 transport mechanisms of solutes in the system studied. Therefore, understanding the  
 1445 temporal scales of water and solute fluxes is crucial for coastal oceanography. Obtaining a  
 1446 flushing time of Ra in a coastal study is also a key parameter needed to estimate SGD

1447 through the Ra mass balance or the mixing model approach (see section 6.1). Ra isotopes  
 1448 can provide instrumental information in this regard because the different decay constants  
 1449 of different isotopes can help infer mixing timescales in coastal systems. There are two basic  
 1450 approaches to estimate water ages using Ra isotopes (Moore, 2015): the “mummy” model,  
 1451 appropriate for systems with Ra inputs occurring near the shoreline (Moore, 2000a) and the  
 1452 “continuous input” model, recommended for systems where Ra is added over the entire  
 1453 study area, such as a shallow estuary (Moore et al., 2006). Both approaches are based on  
 1454 using activity ratios of a pair of Ra isotopes to determine water apparent ages, which is the  
 1455 time elapsed since the water sample became enriched in Ra and isolated from the source  
 1456 (Moore, 2000a). Notice that these approaches are used to estimate “apparent ages”,  
 1457 defined as the time spent since a water parcel became isolated from the Ra source.  
 1458 “Apparent ages” are thus not equivalent with “flushing times”, although they are often used  
 1459 indistinctly in SGD literature (Monsen et al., 2002; Moore et al., 2006). However, evaluations  
 1460 of water apparent ages and flushing times might yield similar time estimates if the system is  
 1461 under steady-state and the comparison of flushing times and apparent ages is made across  
 1462 an entire study area (Tomasky-Holmes et al., 2013).

1463  
 1464 Average water apparent ages for a system ( $\tau$ ) can be estimated as follows, depending on  
 1465 whether the Ra inputs occur at the shoreline (Mummy model; Equation 17) or continuously  
 1466 (Continuous input model; Equation 18):

$$1467 \tau = \frac{\ln(AR_{in}) - \ln(AR_{sys})}{\lambda_s - \lambda_l} \quad (17)$$

$$1469 \tau = \frac{AR_{in} - AR_{sys}}{AR_{sys}\lambda_s - AR_{in}\lambda_l} \quad (18)$$

1471  
 1472 where  $AR_{in}$  and  $AR_{sys}$  are the activity ratios of the shorter-lived Ra isotope to the longer-lived  
 1473 one in the source (considering all the potential sources) and in the system, respectively, and  
 1474  $\lambda_s$  and  $\lambda_l$  are the decay constants of the shorter-lived and longer-lived Ra isotope,  
 1475 respectively. The term  $\lambda_l$  can be neglected when a long-lived Ra isotope is used ( $^{226}\text{Ra}$  and/or  
 1476  $^{228}\text{Ra}$ ). Both models assume that i) Ra activities and ARs are highest in the source ( $AR_{in} >$   
 1477  $AR_{sys}$ ), ii) the  $AR_{in}$  is constant, iii) the only Ra losses are due to mixing and radioactive decay,  
 1478 and iv) the open ocean contains negligible activities of the Ra isotopes used (Charette et al.,  
 1479 2001; Knee et al., 2011; Moore, 2006b, 2000a). The activity ratio of any pair of Ra isotopes  
 1480 can be used to estimate water apparent ages, provided that the half-life of the shorter-lived  
 1481 Ra isotope is appropriate for the water mixing time-scales expected in the study area  
 1482 (Moore, 2015). Typical water apparent ages estimated using  $^{223}\text{Ra}$  and  $^{224}\text{Ra}$  as the shorter-  
 1483 lived isotope range from  $\sim 1$  to  $\sim 50$  days (e.g., Dulaiova et al., 2009; Hancock et al., 2006;  
 1484 Krall et al., 2017; Moore et al., 2006; Rengarajan and Sarma, 2015; Sanial et al., 2015). The  
 1485 accuracy of these AR-based apparent water ages will depend on the analytical uncertainties  
 1486 associated with the isotopes used (e.g., uncertainties of 50 – 100% when water apparent  
 1487 ages are shorter than 3 – 5 days (Knee et al., 2011). It should be noted that if water masses  
 1488 with different Ra content mix, the relative fractions of each water should be known for  
 1489 reliable apparent age estimates, otherwise the apparent age will tentatively be biased  
 1490 towards the younger water mass (Delhez et al., 2003; Hougham and Moran, 2007).  
 1491

## 1492 [8.4] Ra-228 as tracer of offshore solute fluxes

1493

1494 Solute fluxes from the coastal ocean derived from SGD, shelves and other continental  
 1495 sources have the potential to contribute to biogeochemical cycles of the open ocean via  
 1496 shelf-ocean exchange processes. However, while solute inputs to the coastal zone are  
 1497 relatively straightforward to obtain (e.g., Homoky et al., 2016), calculating their net input to  
 1498 the ocean has been a greater challenge owing to solute removal or addition processes that  
 1499 take place in estuaries or over the shelf. To address this shortcoming, Charette and co-  
 1500 workers (2016) proposed the use of  $^{228}\text{Ra}$  as a shelf solute flux gauge, which takes  
 1501 advantage of the global shelf  $^{228}\text{Ra}$  flux model developed by Kwon et al. (2014). The method  
 1502 is most easily applied where shelf-ocean exchange is primarily driven by eddy diffusion,  
 1503 whereby the net cross-shelf solute (S) flux can be linearly scaled with the net cross-shelf  
 1504  $^{228}\text{Ra}$  flux as follows (see also 6.1.):

1505

$$1506 \quad S_{flux} = {}^{228}\text{Ra}_{flux} \times \left( \frac{S_{shelf} - S_{ocean}}{{}^{228}\text{Ra}_{shelf} - {}^{228}\text{Ra}_{ocean}} \right) \quad (19)$$

1507

1508 where  $S_{shelf}$  and  ${}^{228}\text{Ra}_{shelf}$  are the average concentration of the solute (e.g. trace metals,  
 1509 nutrients, dissolved organic carbon) of interest and  ${}^{228}\text{Ra}$  over the shelf water column (<200  
 1510 m). Because the shelf water is exchanging with the open ocean via mixing, the shelf solute  
 1511 and  ${}^{228}\text{Ra}$  concentrations must be corrected for their concentrations in the open ocean  
 1512 ( $S_{ocean}$  and  ${}^{228}\text{Ra}_{ocean}$ ).

1513

1514 This technique only requires paired measurements of  ${}^{228}\text{Ra}$  and the solute of interest along  
 1515 a shelf-ocean transect. Given that lateral inputs of solutes to the ocean have been shown to  
 1516 be important on a global basis, for example as is the case with dissolved iron (Tagliabue et  
 1517 al., 2014), this method is particularly valuable for oceanographic field studies where solute  
 1518 mass balance budgets are required. However, the application of this method requires  
 1519 validating the assumptions of negligible advection and steady-state conditions on the scale  
 1520 of the tracer used, which are not valid for all the systems.

1521

## 1522 [9] Conclusions and the Future stage (>2020)

1523

### 1524 [9.1] Guidelines to conduct a SGD study

1525

1526 This article reviews the application of Ra isotopes as tracers of SGD-derived inputs of water  
 1527 and solutes to the coastal ocean. In this final chapter, we provide a step-by-step protocol  
 1528 that should serve as simplified guidelines to perform a SGD study using Ra isotopes. This  
 1529 protocol is based on the 7 steps illustrated in Figure 12.

1530

1531 **Step 1 – Definition of the objective of the study:** SGD studies often focus on determining  
 1532 the significance of SGD in the water cycle or on its implications for coastal biogeochemical  
 1533 cycles. This objective determines the spatial scale of the study (e.g., nearshore vs shelf scale;  
 1534 evaluate spatial variability vs produce integrated estimates; spatial resolution), as well as  
 1535 the temporal scale (e.g., snap-shot observations vs continuous observations; base  
 1536 conditions vs episodic events; temporal resolution). The method(s) used to quantify SGD

1537 (e.g., water budgets, groundwater flow models, seepage meter or natural tracers such as  
1538 radium, radon, salinity or heat) should be selected according to the specific objective of the  
1539 study and the characteristics of the system. In case of using Ra isotopes, a clear definition of  
1540 the objective will facilitate progressing towards the following steps.

1541

1542 **Step 2 – Characterization of the study site:** Identifying the hydrological (e.g., magnitude of  
1543 surface water inputs, groundwater table elevation, system geology) and oceanographic  
1544 characteristics (e.g., circulation drivers, system timescales, water depths and stratification)  
1545 characteristics, the potential Ra sources and sinks, as well as the potential SGD pathways  
1546 discharging to the study site (see Figure 3). This characterization usually involves a  
1547 combination of literature review, potentially preliminary samplings and the use of  
1548 complementary techniques (e.g., salinity profiles, electrical resistivity tomography (ERT),  
1549 thermal infrared (TIR) images, Rn surveys, water level measurements) from different  
1550 disciplines (e.g., hydrogeology, geophysics, oceanography).

1551

1552 **Step 3 – Construction of a conceptual model:** A conceptual model should consider the main  
1553 SGD pathways, the predominant sources and sinks of Ra isotopes and the characteristics of  
1554 the study site (e.g., water residence time). The conceptual model is fundamental to  
1555 selecting the appropriate Ra isotope(s) to be used, and to determining the quantification  
1556 approach, assumptions made and overall sampling approach. It is important that  
1557 researchers clearly identify the assumptions of the approach they are applying and validate  
1558 them. This step is crucial to characterize the limitations of the method used, to constrain the  
1559 uncertainties of the final estimates and, thus, to produce reliable and justifiable SGD  
1560 estimates (see section 7.1).

1561

1562 **Step 4 – Selection of the Ra isotopes:** Ra isotopes applied in the study should be chosen  
1563 according to the target process or pathway, the enrichment in Ra of discharging  
1564 groundwaters, the potential sources and sinks in the study site and the residence time of  
1565 the isotope in the study area (see Sections 7.3 and 7.4).

1566

1567 **Step 5 – Sampling Ra in all the compartments:** Samples for Ra isotopes should be collected  
1568 both in seawater and in all the potential endmembers (SGD from different pathways, open  
1569 ocean, surface water, surface discharges, etc.). The collection of sediment samples or cores  
1570 might also be required to evaluate inputs of Ra from sediments. Aside from Ra isotopes,  
1571 concurrent samples for other parameters (e.g., salinity, water composition, stable isotopes  
1572 ( $\delta^2\text{H}$ ,  $\delta^{18}\text{O}$ ) of water, concentrations of nutrients, metals, contaminants) might also be  
1573 collected depending on the objectives of the study.

1574

1575 **Step 6 – Quantification of SGD using Ra:** The quantification approach (mass balance,  
1576 endmember mixing model or export offshore) must be chosen according to the  
1577 characteristics of the study site and considering the validity of model assumptions (see  
1578 section 6.1). The quantification of SGD requires constraining the sources and sinks of Ra  
1579 isotopes in the study area (step 6.1) and characterizing the appropriate Ra concentration in  
1580 the SGD endmembers (step 6.2). In complex settings, the contribution from the different  
1581 SGD pathways needs to be accurately accounted for to provide reliable SGD estimates. We  
1582 note that this may not be possible in some study sites, and so the use of other tracers  
1583 should be considered. Ideally, the estimates derived from Ra isotopes should be compared

1584 with other methods (e.g. seepage meters, other tracers, hydrogeological models) to validate  
 1585 and better constrain the results obtained.

1586

1587 **Step 6.1 – Constraining Ra sources and sinks:** The accuracy of SGD estimates strongly rely  
 1588 on the appropriate quantification of the relevant sources and sinks of Ra at the study site.  
 1589 The significance of sources and sinks (and thus the accuracy with which these parameters  
 1590 need to be determined) depend on the characteristics of the study site (Figure 8 and 9) and  
 1591 the Ra isotope used (see 7.3).

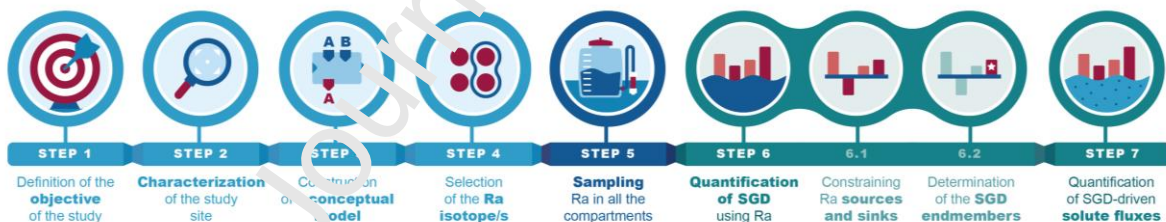
1592

1593 **Step 6.2 – Determination of the SGD endmember(s):** The determination of the Ra  
 1594 concentration in the SGD endmember(s) is often the major source of uncertainty of SGD  
 1595 estimates. In coastal system with a dominant SGD pathway, the Ra endmember  
 1596 concentration should be representative of this pathway. However, in more complex  
 1597 settings, the respective Ra endmembers for each of the pathways, as well as its proportion  
 1598 of SGD contribution should be determined when possible (see Sections 6.2 and 7.5). Ra-  
 1599 based SGD assessments should focus their effort on accurately determining these  
 1600 endmembers.

1601

1602 **Step 7 – Quantification of SGD-driven solute fluxes:** A representative concentration of  
 1603 solutes or solute/Ra ratios in the SGD endmember/s needs to be determined to estimate  
 1604 SGD-driven solute fluxes. Importantly, the solute composition of different SGD pathways  
 1605 may be considerably different and specific endmembers should be determined for the  
 1606 different components. This is especially important for studies that aim to quantify SGD-  
 1607 driven solute fluxes (nutrients, metals, contaminants, etc) or to evaluate the significance of  
 1608 SGD in coastal biogeochemical cycles (see Section 7.6).

1609



1610 **Figure 12.** Recommended step-by-step protocol to conduct SGD studies by using Ra  
 1611 isotopes based on the current state of the art.

1610

1611

## 1612 [9.2] Knowledge gaps and research needs

1613

1614 Despite the advances in the use of Ra isotopes as SGD tracer over the last decades reviewed  
 1615 in this article, several major research gaps remain open. We believe that the following  
 1616 issues should be addressed in future studies to improve the use of Ra isotopes as a tracer in  
 1617 SGD studies.

1618

1619 **Discriminating SGD pathways.** As highlighted in this review, identifying the SGD pathways  
1620 or mechanisms that are most significant in contributing Ra isotopes at a specific study site is  
1621 crucial to obtaining realistic SGD estimates. There is thus a need to obtain a conceptual  
1622 understanding of the systems prior to the application of Ra isotopes to trace SGD. The  
1623 combination of different Ra isotopes can be instrumental to quantify not only the total  
1624 magnitude of SGD, but also the respective water flows supplied by different pathways. Their  
1625 discrimination will allow obtaining accurate estimations of the solute fluxes supplied by  
1626 SGD, which will decisively contribute towards a better understanding of the role SGD plays  
1627 in coastal biogeochemical cycles.

1628  
1629 **Multi-method studies.** Comparisons of Ra-based SGD estimates with independent methods  
1630 (e.g., other tracers, seepage meters, hydrological modelling) are a key step towards the  
1631 validation and refinement of Ra-derived estimates. However, estimates derived from  
1632 different methods are not always directly comparable because different approaches often  
1633 capture different components of SGD or integrate over unique spatio-temporal scales. Using  
1634 Ra isotopes to discriminate SGD pathways will thus facilitate multi-method comparisons  
1635 and, at the same time, multi-method studies can contribute to distinguishing different SGD  
1636 components.

1637  
1638 **Spatial and temporal Ra variability within the subterranean estuary.** There are still few  
1639 studies constraining the spatial and temporal variability of Ra isotopes in the subsurface and  
1640 Ra behaviour in the subterranean estuary is not properly understood. Field measurements  
1641 should also be combined with reactive transport models to understand the spatio-temporal  
1642 variability of Ra isotopes within the subterranean estuary and the role of physical  
1643 mechanisms driving groundwater.

1644  
1645 **Development of new analytical techniques for the measurement of Ra isotopes.** Most of  
1646 the methods applied to measure Ra isotopes require pre-concentration of Ra from large  
1647 sample volumes (usually 10 – 100 L) and measurements via radiometric techniques such as  
1648 the RaDeCC system, gamma spectrometry, ICP-MS and TIMS systems. However, there is still  
1649 the need for an accurate and easy methodology to measure the four Ra isotopes in small  
1650 volumes of water (<1 L), allowing for the routine analysis of a large number of samples, and  
1651 for determining Ra concentrations in compartments where only small volumes can be  
1652 sampled (e.g., porewaters, deep ocean). These developments would facilitate the  
1653 improvement of the spatial and temporal resolution of Ra samples collected both in the  
1654 subterranean estuary and the ocean and would allow, for instance, to assess Ra  
1655 concentration changes over time, obtaining detailed Ra profiles in the water column or high-  
1656 resolution Ra distributions in the subterranean estuary. These methodological  
1657 improvements are thus crucial to move towards a better understanding of the different SGD  
1658 pathways and their spatio-temporal scales.

1659  
1660 **Uncertainties of Ra-derived SGD estimates.** SGD fluxes obtained from Ra isotopes have  
1661 large uncertainties that are frequently overlooked. Propagated uncertainties associated  
1662 with estimates should always and clearly be reported in SGD studies to facilitate  
1663 understanding of the precision of tracer approaches. Importantly, an accurate assessment  
1664 of uncertainties should not only consider the uncertainties linked to individual parameters  
1665 (e.g., analytical errors of Ra measurements, the standard deviation of Ra averages), but also

1666 those errors linked to the conceptualization of the system (e.g., assumption of steady state,  
1667 selection of the endmember, assumptions linked to mixing loss assessments).

1668  
1669 **Towards more robust Ra-derived SGD estimates.** All studies using Ra isotopes to quantify  
1670 SGD processes are based on numerous assumptions that should be validated in order to  
1671 produce accurate SGD estimates. In other words, most of the investigations using Ra  
1672 isotopes produce SGD estimates, but the estimated fluxes are only meaningful and reliable  
1673 if the assumptions and uncertainties of the model are properly understood, acknowledged,  
1674 quantified, and accounted for. Authors working on SGD-related investigations should always  
1675 be aware of the limitations of the tracers and approaches used. In some cases, traditional  
1676 approaches (or the tracer itself) might not be appropriate for the system studied or the  
1677 objective of the investigation, requiring the development of more complex models or the  
1678 use of alternative/complementary methods.

1679

1680

## 1681 **Acknowledgements**

1682

1683 The authors would like to thank T. Horscroft for the invitation to write this review and W.S.  
1684 Moore, S. Lamontagne and three anonymous reviewers for their constructive comments on  
1685 the manuscript. J.Garcia-Orellana acknowledge the financial support of the Spanish Ministry  
1686 of Science, Innovation and Universities, through the “Maria de Maeztu” programme for  
1687 Units of Excellence (CEX2019-000940-M), the Generalitat de Catalunya (MERS; 2017 SGR –  
1688 1588) and the project OPAL (PID2019-110111RB-C21). V. Rodellas acknowledges financial  
1689 support from the Beatriu de Pinós postdoctoral program of the Generalitat de Catalunya  
1690 (2017-BP-00334 and 2019-BP-00241), M. Charette received support from the U.S. National  
1691 Science Foundation (OCE-1736277). J. Scholten acknowledges the support through the  
1692 SEAMOUNT BONUS project (art. 135), which is funded jointly by the EU and the Federal  
1693 Ministry of Education and Research of Germany (BMBF, grant no. 03F0771B). P. van Beek  
1694 and T. Stieglitz acknowledge support from the French ANR (project MED-SGD (ANR-15-CE01-  
1695 0004) and chair @RAction MED-LOC (ANR-14-ACHN-0007-01)). A. Alorda-Kleinglass  
1696 acknowledges financial support from ICTA “Unit of Excellence” (MinECo, MDM2015-0552-  
1697 17-1) and PhD fellowship, BES-2017-080740. H. Michael acknowledges support from the  
1698 U.S. National Science Foundation (EAR-1759879). M. Diego-Feliu acknowledges the financial  
1699 support from the FI-2017 fellowships of the Generalitat de Catalunya autonomous  
1700 government (2017FI\_B\_00365). Figures 3, 4, 7 and 12 were designed by Gemma Solà  
1701 (www.gemmasola.com).

1702

## 1703 **References**

1704

- 1705 Adolf, J.E., Burns, J., Walker, J.K., Gamiao, S., 2019. Near shore distributions of  
1706 phytoplankton and bacteria in relation to submarine groundwater discharge-fed  
1707 fishponds, Kona coast, Hawai‘i, USA. *Estuar. Coast. Shelf Sci.* 219, 341–353.  
1708 <https://doi.org/10.1016/j.ecss.2019.01.021>
- 1709 Alorda-Kleinglass, A., Garcia-Orellana, J., Rodellas, V., Cerdà-Domènech, M., Tovar-Sánchez,  
1710 A., Diego-Feliu, M., Trezzi, G., Sánchez-Quilez, D., Sanchez-Vidal, A., Canals, M., 2019.  
1711 Remobilization of dissolved metals from a coastal mine tailing deposit driven by  
1712 groundwater discharge and porewater exchange. *Sci. Total Environ.* 688, 1359–1372.

- 1713 <https://doi.org/10.1016/j.scitotenv.2019.06.224>
- 1714 Amir, N., Kafri, U., Herut, B., Shalev, E., 2013. Numerical Simulation of Submarine  
1715 Groundwater Flow in the Coastal Aquifer at the Palmahim Area, the Mediterranean  
1716 Coast of Israel. *Water Resour. Manag.* 27, 4005–4020. [https://doi.org/10.1007/s11269-](https://doi.org/10.1007/s11269-013-0392-2)  
1717 [013-0392-2](https://doi.org/10.1007/s11269-013-0392-2)
- 1718 Andrisoa, A., Lartaud, F., Rodellas, V., Neveu, I., 2019. Enhanced Growth Rates of the  
1719 Mediterranean Mussel in a Coastal Lagoon Driven by Groundwater Inflow. *Front. Mar.*  
1720 *Sci.* 6, 1–14. <https://doi.org/10.3389/fmars.2019.00753>
- 1721 Annett, A.L., Henley, S.F., Van Beek, P., Souhaut, M., Ganeshram, R., Venables, H.J.,  
1722 Meredith, M.P., Geibert, W., Beek, P.V.A.N., Souhaut, M., Ganeshram, R., Venables,  
1723 H.J., Meredith, M.P., Geibert, W., 2013. Use of radium isotopes to estimate mixing  
1724 rates and trace sediment inputs to surface waters in northern Marguerite Bay,  
1725 Antarctic Peninsula. *Antarct. Sci.* 25, 445–456.  
1726 <https://doi.org/10.1017/S0954102012000892>
- 1727 Anwar, N., Robinson, C., Barry, D. a., 2014. Influence of tides and waves on the fate of  
1728 nutrients in a nearshore aquifer: Numerical simulations. *Adv. Water Resour.* 73, 203–  
1729 213. <https://doi.org/10.1016/j.advwatres.2014.08.017>
- 1730 Baudron, P., Cockenpot, S., Lopez-Castejon, F., Radakovitch, O., Gilibert, J., Mayer, A.,  
1731 Garcia-Arostegui, J.L., Martinez-Vicente, D., Le Roy, E., Claude, C., 2015. Combining  
1732 radon, short-lived radium isotopes and hydrodynamic modeling to assess submarine  
1733 groundwater discharge from an anthropized semiarid watershed to a Mediterranean  
1734 lagoon (Mar Menor, SE Spain). *J. Hydrol.* 525, 55–71.  
1735 <https://doi.org/10.1016/j.jhydrol.2015.03.015>
- 1736 Beck, A.J., Charette, M.A., Cochran, J.K., Conneea, M.E., Peucker-Ehrenbrink, B., 2013.  
1737 Dissolved strontium in the subterranean estuary – Implications for the marine  
1738 strontium isotope budget. *Geochim. Cosmochim. Acta* 117, 33–52.
- 1739 Beck, A.J., Cochran, M.A., 2013. Control on solid-solution partitioning of radium in  
1740 saturated marine sands. *Mar. Chem.* 156, 38–48.  
1741 <https://doi.org/http://dx.doi.org/10.1016/j.marchem.2013.01.008>
- 1742 Beck, A.J., Rapaglia, J.P., Cochran, J.K., Bokuniewicz, H.J., 2007. Radium mass-balance in  
1743 Jamaica Bay, NY: Evidence for a substantial flux of submarine groundwater. *Mar. Chem.*  
1744 106, 419–441. <http://doi.org/10.1016/j.marchem.2007.03.008>
- 1745 Beck, A.J., Rapaglia, J.P., Cochran, J.K., Bokuniewicz, H.J., Yang, S., 2008. Submarine  
1746 groundwater discharge to Great South Bay, NY, estimated using Ra isotopes. *Mar.*  
1747 *Chem.* 109, 279–291. <https://doi.org/10.1016/j.marchem.2007.07.011>
- 1748 Bejannin, S., Tamborski, J.J., van Beek, P., Souhaut, M., Stieglitz, T., Radakovitch, O., Claude,  
1749 C., Conan, P., Pujol-Pay, M., Crispi, O., Le Roy, E., Estournel, C., 2020. Nutrient Fluxes  
1750 Associated With Submarine Groundwater Discharge From Karstic Coastal Aquifers  
1751 (Côte Bleue, French Mediterranean Coastline). *Front. Environ. Sci.* 7, 1–20.  
1752 <https://doi.org/10.3389/fenvs.2019.00205>
- 1753 Beneš, P., Borovec, Z., Strejc, P., 1985. Interaction of radium with freshwater sediments and  
1754 their mineral components - II. Kaolinite and montmorillonite. *J. Radioanal. Nucl. Chem.*  
1755 *Artic.* 89, 339–351. <https://doi.org/10.1007/BF02040598>
- 1756 Beneš, P., Strejc, P., Lukavec, Z., 1984. Interaction of radium with freshwater sediments and  
1757 their mineral components. I. - Ferric hydroxide and quartz. *J. Radioanal. Nucl. Chem.*  
1758 *Artic.* 82, 275–285. <https://doi.org/10.1007/BF02037050>
- 1759 Bethke, C.M., Johnson, T.M., 2002. Paradox of groundwater age. *Geology* 30, 107–110.

- 1760 [https://doi.org/doi.org/10.1130/0091-7613\(2002\)030<0107:POGA>2.0.CO;2](https://doi.org/doi.org/10.1130/0091-7613(2002)030<0107:POGA>2.0.CO;2)
- 1761 Blanchard, R.L., Oakes, D., 1965. Relationships between uranium and radium in coastal  
1762 marine shells and their environment. *J. Geophys. Res.* 70, 2911–2921.
- 1763 <https://doi.org/10.1029/jz070i012p02911>
- 1764 Boehm, A.B., Paytan, A., Shellenbarger, G.G., Davis, K.A., 2006. Composition and flux of  
1765 groundwater from a California beach aquifer: Implications for nutrient supply to the  
1766 surf zone. *Cont. Shelf Res.* 26, 269–282. <https://doi.org/10.1016/j.csr.2005.11.008>
- 1767 Boehm, A.B., Shellenbarger, G.G., Paytan, A., 2004. Groundwater Discharge: Potential  
1768 Association with Fecal Indicator Bacteria in the Surf Zone. *Environ. Sci. Technol.* 38,  
1769 3558–3566.
- 1770 Bokuniewicz, H., Cochran, J.K., Garcia-orellana, J., Rodellas, V., Daniel, J.W., Heilbrun, C.,  
1771 2015. Intertidal percolation through beach sands as a source of  $^{224}\text{Ra}$  to Long  
1772 Island Sound, New York, and Connecticut, United States. *J. Mar. Res.* 73, 123–140.
- 1773 Bokuniewicz, H.J., 1992. Analytical Descriptions of Subaqueous Groundwater Seepage.  
1774 *Estuaries* 15, 458. <https://doi.org/10.2307/1352390>
- 1775 Bokuniewicz, H.J., 1980. Groundwater seepage into Great South Bay, New York. *Estuar.*  
1776 *Coast. Shelf Sci.* 10, 437–444. [https://doi.org/10.1016/00302-3524\(80\)80122-8](https://doi.org/10.1016/00302-3524(80)80122-8)
- 1777 Bollinger, M.S., Moore, W.S., 1993. Evaluation of salt marsh hydrology using radium as a  
1778 tracer. *Geochim. Cosmochim. Acta* 57, 2203–2212.
- 1779 Bollinger, M.S., Moore, W.S.W.S., 1984. Radium fluxes from a salt marsh. *Nature* 309, 444.
- 1780 Boudreau, B.P., 1997a. *Diagenetic Models and Their Implementation*. Springer Verlag, Berlin,  
1781 Heidelberg.
- 1782 Boudreau, B.P., 1997b. *Diagenetic Models and Their Implementation: Modelling Transport*  
1783 *and Reactions in Aquatic Sediments*. Springer, Verlag, Berlin, Heidelberg, NY.
- 1784 Broecker, W.S., Li, Y.-H., John, C., 1967. Radium-226 and Radon-222 : Concentration in  
1785 Atlantic and Pacific Oceans. *Science (30-. )*. 158, 1307–1311.  
1786 <https://doi.org/10.1126/science.158.3806.1307>
- 1787 Burnett, B., Chanton, J., Christoff, J., Kontar, E., Krupa, S., Lambert, M., Moore, W.,  
1788 O'Rourke, D., Paulsen, R., Smith, C., Smith, L., Taniguchi, M., 2002. Assessing  
1789 methodologies for measuring groundwater discharge to the Ocean. *Eos (Washington*  
1790 *DC)*. 83, 1–5. <https://doi.org/10.1029/2002EO000069>
- 1791 Burnett, W., Taniguchi, M., Oberdorfer, J., 2001. Measurement and significance of the direct  
1792 discharge of groundwater into the coastal zone. *J. Sea Res.* 46, 109–116.
- 1793 Burnett, W.C., Aggarwal, P.K., Aureli, A., Bokuniewicz, H., Cable, J.E., Charette, M.A., Kontar,  
1794 E., Krupa, S., Kulkarni, K.M., Loveless, A., Moore, W.S., Oberdorfer, J.A., Oliveira, J.,  
1795 Ozyurt, N., Povinec, P., Privitera, A.M.G., Rajar, R., Ramassur, R.T., Scholten, J., Stieglitz,  
1796 T., Taniguchi, M., Turner, J. V, 2006. Quantifying submarine groundwater discharge in  
1797 the coastal zone via multiple methods. *Sci. Total Environ.* 367, 498–543.  
1798 <https://doi.org/10.1016/j.scitotenv.2006.05.009>
- 1799 Burnett, W.C., Bokuniewicz, H., Huettel, M., Moore, W., Taniguchi, M., 2003. Groundwater  
1800 and pore water inputs to the coastal zone. *Biogeochemistry* 66, 3–33.
- 1801 Burnett, W.C., Cowart, J.B., Deetae, S., 1990. Radium in the Suwannee River and Estuary  
1802 Spring and river input to the Gulf of Mexico. *Biogeochemistry* 10, 237–255.
- 1803 Burt, W.J., Thomas, H., Auclair, J.P., 2013a. Short-lived radium isotopes on the Scotian Shelf:  
1804 Unique distribution and tracers of cross-shelf  $\text{CO}_2$  and nutrient transport. *Mar. Chem.*  
1805 156, 120–129. <https://doi.org/http://dx.doi.org/10.1016/j.marchem.2013.05.007>
- 1806 Burt, W.J., Thomas, H., Fennel, K., Horne, E., 2013b. Sediment-water column fluxes of

- 1807 carbon, oxygen and nutrients in Bedford Basin, Nova Scotia, inferred from  $^{224}\text{Ra}$   
1808 measurements. *Biogeosciences* 10, 53–66. <https://doi.org/10.5194/bg-10-53-2013>
- 1809 Burt, W.J., Thomas, H., Pätsch, J., Omar, A.M., Schrum, C., Daewel, U., Brenner, H., Baar,  
1810 H.J.W., 2014. Radium isotopes as a tracer of sediment-water column exchange in the  
1811 North Sea. *Global Biogeochem. Cycles* 786–804.  
1812 <https://doi.org/10.1002/2014GB004825>. Received
- 1813 Cai, P., Shi, X., Hong, Q., Li, Q., Liu, L., Guo, X., Dai, M., 2015. Using  $^{224}\text{Ra}/^{228}\text{Th}$   
1814 disequilibrium to quantify benthic fluxes of dissolved inorganic carbon and nutrients  
1815 into the Pearl River Estuary. *Geochim. Cosmochim. Acta* 170, 188–203.  
1816 <https://doi.org/10.1016/j.gca.2015.08.015>
- 1817 Cai, P., Shi, X., Moore, W.S., Dai, M., 2012. Measurement of Ra-224:Th-228 disequilibrium in  
1818 coastal sediments using a delayed coincidence counter. *Mar. Chem.* 138, 1–6.  
1819 <https://doi.org/10.1016/j.marchem.2012.05.004>
- 1820 Cai, P., Shi, X., Moore, W.S., Peng, S., Wang, G., Dai, M., 2014.  $^{224}\text{Ra}:^{228}\text{Th}$  disequilibrium in  
1821 coastal sediments: Implications for solute transfer across the sediment-water interface.  
1822 *Geochim. Cosmochim. Acta* 125, 68–84. <https://doi.org/10.1016/j.gca.2013.09.029>
- 1823 Cai, P., Wei, L., Geibert, W., Koehler, D., Ye, Y., Liu, W., Shi, X., 2020. Carbon and nutrient  
1824 export from intertidal sand systems elucidated by  $^{224}\text{Ra}/^{228}\text{Th}$  disequilibria. *Geochim.*  
1825 *Cosmochim. Acta* 274, 302–316. <https://doi.org/10.1016/j.gca.2020.02.007>
- 1826 Capone, D.G., Bautista, M.F., 1985. A groundwater source of nitrate in nearshore marine  
1827 sediments. *Nature* 318, 806–809. <https://doi.org/10.1038/316507a0>
- 1828 Cerdà-Domènech, M., Rodellas, V., Folch, A., Garcia-Orellana, J., 2017. Constraining the  
1829 temporal variations of Ra isotopes and  $\text{Ra}$  in the groundwater end-member:  
1830 Implications for derived SGD estimates. *Sci. Total Environ.* 595, 849–857.  
1831 <https://doi.org/10.1016/j.scitotenv.2017.03.005>
- 1832 Chabaux, F., Riotte, J., Dequincey, O., 2003. U-Th-Ra fractionation during weathering and  
1833 river transport. *Uranium-series Geochemistry* 52, 533–576.  
1834 <https://doi.org/10.2113/0520533>
- 1835 Chan, L.H., Drummond, D., Edmond, J.M., Grant, B., 1977. On the barium data from the  
1836 Atlantic GEOSECS expedition. *Deep. Res.* 24, 613–649. [https://doi.org/10.1016/0146-6291\(77\)90505-7](https://doi.org/10.1016/0146-6291(77)90505-7)
- 1837
- 1838 Charette, M. a., Buesseler, K.O., 2004. Submarine groundwater discharge of nutrients and  
1839 copper to an urban estuary of Chesapeake Bay (Elizabeth River). *Limnol. Oceanogr.*  
1840 49, 376–385. <https://doi.org/10.4319/lo.2004.49.2.0376>
- 1841 Charette, M. a., Morris, P.J., Henderson, P.B., Moore, W.S., 2015. Radium isotope  
1842 distributions during the US GEOTRACES North Atlantic cruises. *Mar. Chem.* 177, 1–12.  
1843 <https://doi.org/10.1016/j.marchem.2015.01.001>
- 1844 Charette, M.A., 2007. Hydrologic forcing of submarine groundwater discharge: Insight from  
1845 a seasonal study of radium isotopes in a groundwater-dominated salt marsh estuary.  
1846 *Limnol. Oceanogr.* 52, 230–239.
- 1847 Charette, M.A., Buesseler, K.O., Andrews, J.R.E., 2001. Utility of radium isotopes for  
1848 evaluating the input and transport of groundwater-derived nitrogen to a Cape Cod  
1849 estuary. *Limnol. Oceanogr.* 46, 465–470.
- 1850 Charette, M.A., Gonner, M.E., Morris, P.J., Statham, P., Fones, G., Planquette, H., Salter, I.,  
1851 Garabato, A.N., 2007. Radium isotopes as tracers of iron sources fueling a Southern  
1852 Ocean phytoplankton bloom. *Deep Sea Res. Part II Top. Stud. Oceanogr.* 54, 1989–  
1853 1998. <https://doi.org/10.1016/j.dsr2.2007.06.003>

- 1854 Charette, M.A., Henderson, P.B., Breier, C.F., Liu, Q., 2013. Submarine groundwater  
1855 discharge in a river-dominated Florida estuary. *Mar. Chem.* 156, 3–17.  
1856 <https://doi.org/http://dx.doi.org/10.1016/j.marchem.2013.04.001>
- 1857 Charette, M.A., Lam, P.J., Lohan, M.C., Kwon, E.Y., Hatje, V., Jeandel, C., Shiller, A.M., Cutter,  
1858 G., Thomas, A.L., Boyd, P.W., Homoky, W.B., Milne, A., Thomas, H., Andersson, P.S.,  
1859 Porcelli, D., Tanaka, T., Geibert, W., Dehairs, F., Garcia-Orellana, J., 2016. Coastal ocean  
1860 and shelf-sea biogeochemical cycling of trace elements and isotopes: lessons learned  
1861 from GEOTRACES. *Trans. R. Soc.* 374.  
1862 <https://doi.org/http://doi.org/10.1098/rsta.2016.0076>
- 1863 Charette, M.A., Moore, W.S., Burnett, W.C., 2008. Uranium-and Thorium- Series Nuclides as  
1864 Tracers of Submarine Groundwater Discharge CHAPTER-5 Uranium-and Thorium-Series  
1865 Nuclides as Tracers of Submarine Groundwater Discharge. *Radioact. Environ.* 13, 234–  
1866 289. [https://doi.org/10.1016/S1569-4860\(07\)00005-8](https://doi.org/10.1016/S1569-4860(07)00005-8)
- 1867 Charette, M.A., Sholkovitz, E.R., 2006. Trace element cycling in a subterranean estuary: Part  
1868 2. Geochemistry of the pore water. *Geochim. Cosmochim. Acta* 70, 811–826.  
1869 <https://doi.org/10.1016/j.gca.2005.10.019>
- 1870 Charette, M.A., Splivallo, R., Herbold, C., Bollinger, M.S., Moore, W.S., 2003. Salt marsh  
1871 submarine groundwater discharge as traced by radium isotopes. *Mar. Chem.* 84, 113–  
1872 121. <https://doi.org/10.1016/j.marchem.2003.07.001>
- 1873 Chen, C., Liu, H., Beardsley, R.C., 2003. An unstructured grid, finite-volume, three-  
1874 dimensional, primitive equations ocean model: Application to coastal ocean and  
1875 estuaries. *J. Atmos. Ocean. Technol.* 20, 159–186. [https://doi.org/10.1175/1520-0426\(2003\)020<0159:AUGFVT>2.0.CO;2](https://doi.org/10.1175/1520-0426(2003)020<0159:AUGFVT>2.0.CO;2)
- 1877 Cho, H.-M., Kim, G., 2016. Determining groundwater Ra endmember values for the  
1878 estimation of the magnitude of submarine groundwater discharge using Ra isotope  
1879 tracers. *Geophys. Res. Lett.* 1–7. <https://doi.org/10.1002/2016GL068805>
- 1880 Cho, H.-M., Kim, G., Kwon, E.Y., Mousdrof, N., Garcia-Orellana, J., Santos, I.R., 2018. Radium  
1881 tracing nutrient inputs through submarine groundwater discharge in the global ocean.  
1882 *Sci. Rep.* 8, 2439. <https://doi.org/10.1038/s41598-018-20806-2>
- 1883 Church, T.M., 1996. An underground route for the water cycle. *Nature* 380, 579.
- 1884 Cochran, J.K., Krishnaswami, S., 1980. Radium, thorium, uranium, and Pb210 in deep-sea  
1885 sediments and sediment pore waters from the North Equatorial Pacific. *Am. J. Sci.*  
1886 <https://doi.org/10.2475/ajs.280.9.849>
- 1887 Colbert, S.L., Hammond, D.E., 2007. Temporal and spatial variability of radium in the coastal  
1888 ocean and its impact on computation of nearshore cross-shelf mixing rates. *Cont. Shelf*  
1889 *Res.* 27, 1477–1500. <https://doi.org/https://doi.org/10.1016/j.csr.2007.01.003>
- 1890 Colbert, S.L.S.L., Hammond, D.E.D.E., 2008. Shoreline and seafloor fluxes of water and short-  
1891 lived Ra isotopes to surface water of San Pedro Bay, CA. *Mar. Chem.* 108, 1–17.  
1892 <https://doi.org/10.1016/j.marchem.2007.09.004>
- 1893 Cook, P.G., Herczeg, A.L., 2012. *Environmental Tracers in Subsurface Hydrology*. Springer  
1894 Science, New York.
- 1895 Cook, P.G., Rodellas, V., Stieglitz, T.C., 2018. Quantifying Surface Water, Porewater and  
1896 Groundwater Interactions Using Tracers: Tracer Fluxes, Water Fluxes and Endmember  
1897 Concentrations. *Water Resour. Res.* 1–14. <https://doi.org/10.1002/2017WR021780>
- 1898 Cooper, H.H., 1959. A hypothesis concerning the dynamic balance of fresh water and salt  
1899 water in a coastal aquifer. *J. Geophys. Res.* 64, 461–467.  
1900 <https://doi.org/10.1029/JZ064i004p00461>

- 1901 Copenhagen, S.A., Krishnaswami, S., Turekian, K.K., Epler, N., Cochran, J.K., 1993.  
 1902 Retardation of  $^{238}\text{U}$  and  $^{232}\text{Th}$  decay chain radionuclides in Long Island and  
 1903 Connecticut aquifers. *Geochim. Cosmochim. Acta* 57, 597–603.  
 1904 [https://doi.org/10.1016/0016-7037\(93\)90370-C](https://doi.org/10.1016/0016-7037(93)90370-C)
- 1905 Copenhagen, S.A., Krishnaswami, S., Turekian, K.K., Shaw, H., 1992.  $^{238}\text{U}$  and  $^{232}\text{Th}$  series  
 1906 nuclides in groundwater from the J-13 well at the Nevada Test Site: Implications for ion  
 1907 retardation. *Geophys. Res. Lett.* 19, 1383–1386. <https://doi.org/10.1029/92GL01437>
- 1908 Danielescu, S., MacQuarrie, K.T.B., Faux, R.N., 2009. The integration of thermal infrared  
 1909 imaging, discharge measurements and numerical simulation to quantify the relative  
 1910 contributions of freshwater inflows to small estuaries in Atlantic Canada. *Hydrol.*  
 1911 *Process.* 23, 2847–2859. <https://doi.org/10.1002/hyp.7383>
- 1912 Delhez, É.J.M., Deleersnijder, É., Mouchet, A., Beckers, J.M., 2003. A note on the age of  
 1913 radioactive tracers. *J. Mar. Syst.* 38, 277–286. [https://doi.org/10.1016/S0924-7963\(02\)00245-2](https://doi.org/10.1016/S0924-7963(02)00245-2)
- 1915 Dias, T.H., de Oliveira, J., Sanders, C.J., Carvalho, F., Sanders, J.M., Machado, E.C., Sá, F.,  
 1916 2016. Radium isotope ( $^{223}\text{Ra}$ ,  $^{224}\text{Ra}$ ,  $^{226}\text{Ra}$  and  $^{228}\text{Ra}$ ) distribution near Brazil's largest port,  
 1917 Paranaguá Bay, Brazil. *Mar. Pollut. Bull.* 111, 443–448.  
 1918 <https://doi.org/10.1016/j.marpolbul.2016.07.004>
- 1919 Diego-Feliu, M., Rodellas, V., Alorda-Kleinglass, A., Tamborski, J., van Beek, P., Heins, L.,  
 1920 Bruach-Menchén, J.M., Arnold, R., Garcia-Orellana, J., 2020. Guidelines and limits for  
 1921 the quantification of Ra isotopes and related radionuclides with the Radium Delayed  
 1922 Coincidence Counter (RaDeCC). *J. Geophys. Res. C Ocean.* 125.  
 1923 <https://doi.org/10.1029/2019JC015544>
- 1924 Diego-Feliu, M., Rodellas, V., Saaltink, M.W., Alorda-Kleinglass, A., Goyetche, T., Martínez-  
 1925 Pérez, L., Folch, A., Garcia-Orellana, J., 2021. New perspectives on the use of  
 1926  $^{224}\text{Ra}/^{228}\text{Ra}$  and  $^{222}\text{Rn}/^{226}\text{Ra}$  activity ratios in groundwater studies. *J. Hydrol.* 596,  
 1927 126043. <https://doi.org/10.1016/j.jhydrol.2021.126043>
- 1928 Dulaiova, H., Ardelan, M. V., Henderson, P.B., Charette, M.A., 2009. Shelf-derived iron inputs  
 1929 drive biological productivity in the southern Drake Passage. *Global Biogeochem. Cycles*  
 1930 23, 1–14. <https://doi.org/10.1029/2008GB003406>
- 1931 Dulaiova, H., Burnett, W.C., Charlton, J.P., Moore, W.S., Bokuniewicz, H.J., Charette, M.A.,  
 1932 Sholkovitz, E., 2006. Assessment of groundwater discharges into West Neck Bay, New  
 1933 York, via natural tracers. *Cont. Shelf Res.* 26, 1971–1983.  
 1934 <https://doi.org/10.1016/j.csr.2006.07.011>
- 1935 Dulaiova, H., Burnett, W.C., Wattayakorn, G., Sojisuporn, P., 2006. Are groundwater inputs  
 1936 into river-dominated areas important? The Chao Phraya River - Gulf of Thailand.  
 1937 *Limnol. Oceanogr.* 51, 2232–2247. <https://doi.org/10.4319/lo.2006.51.5.2232>
- 1938 Duque, C., Knee, K.L., Russoniello, C.J., Sherif, M., Abu Risha, U.A., Sturchio, N.C., Michael,  
 1939 H.A., 2019. Hydrogeological processes and near shore spatial variability of radium and  
 1940 radon isotopes for the characterization of submarine groundwater discharge. *J. Hydrol.*  
 1941 579, 124192. <https://doi.org/10.1016/j.jhydrol.2019.124192>
- 1942 Duque, C., Michael, H.A., Wilson, A.M., 2020. The subterranean estuary: Technical term,  
 1943 simple analogy, or source of confusion? *Water Resour. Res.* 1–7.  
 1944 <https://doi.org/10.1029/2019wr026554>
- 1945 Dyer, K., 1973. *Estuaries: a Physical Introduction*. John Wiley, London.
- 1946 Elsinger, R.J., Moore, W.S., 1983.  $^{224}\text{Ra}$ ,  $^{228}\text{Ra}$ , and  $^{226}\text{Ra}$  in Winyah Bay and Delaware Bay.  
 1947 *Earth Planet. Sci. Lett.* 64, 430–436. [https://doi.org/10.1016/0012-821X\(83\)90103-6](https://doi.org/10.1016/0012-821X(83)90103-6)

- 1948 Elsinger, Robert J., Moore, W.S., 1983. 224Ra, 228Ra, and 226Ra in Winyah Bay and  
 1949 Delaware Bay. *Earth Planet. Sci. Lett.* 64, 430–436.
- 1950 Elsinger, R.J., Moore, W.S., 1980. 226Ra behavior in the Pee Dee River-Winyah Bay estuary.  
 1951 *Earth Planet. Sci. Lett.* 48, 239–249. [https://doi.org/10.1016/0012-821X\(80\)90187-9](https://doi.org/10.1016/0012-821X(80)90187-9)
- 1952 Eriksen, D., Sidhu, R., Ramsøy, T., Strålberg, E., Iden, K.I., Rye, H., Hylland, K., Ruus, A.,  
 1953 Berntssen, M.H.G., 2009. Radioactivity in produced water from Norwegian oil and gas  
 1954 installations - Concentrations, bioavailability, and doses to marine biota.  
 1955 *Radioprotection* 44, 869–874. <https://doi.org/10.1051/radiopro/20095155>
- 1956 Evans, R.D., Kip, A.F., E.G., M., 1938. The radium and radon content of Pacific Ocean water,  
 1957 life, and sediments. *Am. J. Sci.* 214, 241–259.
- 1958 Evans, T.B., Wilson, A.M., 2017. Submarine groundwater discharge and solute transport  
 1959 under a transgressive barrier island. *J. Hydrol.* 547, 97–110.  
 1960 <https://doi.org/10.1016/j.jhydrol.2017.01.028>
- 1961 Ferrarin, C., Rapaglia, J., Zaggia, L., Umgiesser, G., Zuppi, G.M., 2008. Coincident application  
 1962 of a mass balance of radium and a hydrodynamic model for the seasonal quantification  
 1963 of groundwater flux into the Venice Lagoon, Italy. *Mar. Chem.* 112, 179–188.  
 1964 <https://doi.org/10.1016/j.marchem.2008.08.008>
- 1965 Folch, A., Val, L., Luquot, L., Martínez-pérez, L., Bellmont, T., Lay, H. Le, 2020. Combining fi  
 1966 ber optic DTS, cross-hole ERT and time-lapse induction logging to characterize and  
 1967 monitor a coastal aquifer. *J. Hydrol.* 588, 125050.  
 1968 <https://doi.org/10.1016/j.jhydrol.2020.125050>
- 1969 Freeze, R.A., Cherry, J.A., 1979. *Groundwater*. Prentice Hall, Englewood Cliff's, New Jersey.
- 1970 Garces, E., Basterretxea, G., Tovar-Sanchez, A., 2011. Changes in microbial communities in  
 1971 response to submarine groundwater input. *Mar. Ecol. Prog. Ser.* 438, 47–58.  
 1972 <https://doi.org/10.3354/meps09311>
- 1973 Garcia-Orellana, J., Cochran, J.K., Bokuniewicz, H., Yang, S., Beck, A.J., 2010. Time-series  
 1974 sampling of 223Ra and 224Ra at the inlet to Great South Bay (New York): A strategy for  
 1975 characterizing the dominant terms in the Ra budget of the bay.  
 1976 <https://doi.org/10.1016/j.jenvrad.2009.12.005>
- 1977 Garcia-Orellana, J., Cochran, J.K., Bokuniewicz, H., Daniel, J.W.R.W.R., Rodellas, V.,  
 1978 Heilbrun, C., 2014. Evaluation of 224Ra as a tracer for submarine groundwater  
 1979 discharge in Long Island Sound (NY). *Geochim. Cosmochim. Acta* 141, 314–330.  
 1980 <https://doi.org/10.1016/j.gca.2014.05.009>
- 1981 Garcia-Orellana, J., López-Castillo, E., Casacuberta, N., Rodellas, V., Masqué, P., Carmona-  
 1982 Catot, G., Vilarrasa, M., García-Berthou, E., 2016. Influence of submarine groundwater  
 1983 discharge on 210Po and 210Pb bioaccumulation in fish tissues. *J. Environ. Radioact.*  
 1984 155–156, 46–54. <https://doi.org/10.1016/j.jenvrad.2016.02.005>
- 1985 Garcia-Solsona, E., Garcia-Orellana, J., Masque, P., Garces, E., Radakovitch, O., Mayer, A.,  
 1986 Estrade, S., Basterretxea, G., 2010. An assessment of karstic submarine groundwater  
 1987 and associated nutrient discharge to a Mediterranean coastal area (Balearic Islands,  
 1988 Spain) using radium isotopes. *Biogeochemistry* 97, 211–229.  
 1989 <https://doi.org/10.1007/s10533-009-9368-y>
- 1990 Garcia-Solsona, E., Garcia-Orellana, J., Masque, P., Rodellas, V., Mejias, M., Ballesteros, B.,  
 1991 Dominguez, J.A., 2010. Groundwater and nutrient discharge through karstic coastal  
 1992 springs (Castello, Spain). *Biogeosciences* 7, 2625–2638. <https://doi.org/10.5194/bg-7-2625-2010>
- 1993
- 1994 Garcia-Solsona, Ester, Garcia-Orellana, J., Masqué, P., Rodellas, V., Mejías, M., Ballesteros,

- 1995 B., Domínguez, J.A., 2010. Groundwater and nutrient discharge through karstic coastal  
 1996 springs (Castelló, Spain). <https://doi.org/10.5194/bg-7-2625-2010>
- 1997 Garcia-Solsona, E., Masqué, P., Garcia-Orellana, J., Rapaglia, J., Beck, A.J., Cochran, J.K.,  
 1998 Bokuniewicz, H.J., Zaggia, L., Collavini, F., 2008. Estimating submarine groundwater  
 1999 discharge around Isola La Cura, northern Venice Lagoon (Italy), by using the radium  
 2000 quartet. <https://doi.org/10.1016/j.marchem.2008.02.007>
- 2001 Gattacceca, J.C., Mayer, A., Cucco, A., Claude, C., Radakovitch, O., Vallet-Coulomb, C.,  
 2002 Hamelin, B., 2011. Submarine groundwater discharge in a subsiding coastal lowland: A  
 2003 Ra-226 and Rn-222 investigation in the Southern Venice lagoon. *Appl. Geochemistry*  
 2004 26, 907–920. <https://doi.org/10.1016/j.apgeochem.2011.03.001>
- 2005 Geibert, W., Rodellas, V., Annett, A., van Beek, P., Garcia-Orellana, J., Hsieh, Y.-T., Masque,  
 2006 P., 2013. 226Ra determination via the rate of 222Rn ingrowth with the Radium Delayed  
 2007 Coincidence Counter (RaDeCC). *Limnol. Oceanogr. Methods* 11, 594–603.  
 2008 <https://doi.org/10.4319/lom.2013.11.594>
- 2009 George, C., Moore, W.S., White, S.M., Smoak, E., Joye, S.B., Leier, A., Wilson, A.M., 2020. A  
 2010 New Mechanism for Submarine Groundwater Discharge From Continental Shelves.  
 2011 *Water Resour. Res.* 56, 1–17. <https://doi.org/10.1029/2019WR026866>
- 2012 Giffin, C., Kaufman, A., Broecker, W.S., 1963. Delayed Coincidence Counter for the assay of  
 2013 actinon and thoron. *J. Geophys. Res.* 68, 1749–1757.
- 2014 Gilfedder, B.S., Frei, S., Hofmann, H., Cartwright, I., 2015. Groundwater discharge to  
 2015 wetlands driven by storm and flood events: Quantification using continuous Radon-222  
 2016 and electrical conductivity measurements and dynamic mass-balance modelling.  
 2017 *Geochim. Cosmochim. Acta* 165, 161–177.  
 2018 <https://doi.org/10.1016/j.gca.2015.05.037>
- 2019 Glover, R.E., 1959. The pattern of fresh-water flow in a coastal aquifer. *J. Geophys. Res.* 64,  
 2020 457–459. <https://doi.org/10.1029/JZ064i004p00457>
- 2021 Gonnee, M.E., Charette, M.A., 2014. Hydrologic controls on nutrient cycling in an  
 2022 unconfined coastal aquifer. *Environ. Sci. Technol.* 48, 14178–14185.  
 2023 <https://doi.org/10.1021/es503313t>
- 2024 Gonnee, M.E., Morris, P.J., Delaliova, H., Charette, M.A., 2008. New perspectives on radium  
 2025 behavior within a subterranean estuary. *Mar. Chem.* 109, 250–267.  
 2026 <https://doi.org/10.1016/j.marchem.2007.12.002>
- 2027 Gonnee, M.E., Mulligan, A.E., Charette, M.A., 2013. Seasonal cycles in radium and barium  
 2028 within a subterranean estuary: Implications for groundwater derived chemical fluxes to  
 2029 surface waters. *Geochim. Cosmochim. Acta* 119, 164–177.  
 2030 <https://doi.org/10.1016/j.gca.2013.05.034>
- 2031 Gu, H., Moore, W.S., Zhang, L., Du, J., Zhang, J., 2012. Using radium isotopes to estimate the  
 2032 residence time and the contribution of submarine groundwater discharge (SGD) in the  
 2033 Changjiang effluent plume, East China Sea. *Cont. Shelf Res.* 35, 95–107.  
 2034 <https://doi.org/10.1016/j.csr.2012.01.002>
- 2035 Hancock, G., Webster, I., Ford, P., Moore, W., 2000. Using Ra isotopes to examine  
 2036 transport processes controlling benthic fluxes into a shallow estuarine lagoon.  
 2037 *Geochim. Cosmochim. Acta* 64, 3685–3699. [https://doi.org/10.1016/S0016-](https://doi.org/10.1016/S0016-7037(00)00469-5)  
 2038 [7037\(00\)00469-5](https://doi.org/10.1016/S0016-7037(00)00469-5)
- 2039 Hancock, G.J., Webster, I.T., Stieglitz, T.C., 2006. Horizontal mixing of great Barrier Reef  
 2040 waters: Offshore diffusivity determined from radium isotope distribution. *J. Geophys.*  
 2041 *Res. Ocean.* 111, 1–14. <https://doi.org/10.1029/2006JC003608>

- 2042 Homoky, W.B., Weber, T., Berelson, W.M., Conway, T.M., Henderson, G.M., Van Hulten, M.,  
2043 Jeandel, C., Severmann, S., Tagliabue, A., 2016. Quantifying trace element and isotope  
2044 fluxes at the ocean-sediment boundary: A review, *Philosophical Transactions of the*  
2045 *Royal Society A: Mathematical, Physical and Engineering Sciences*.  
2046 <https://doi.org/10.1098/rsta.2016.0246>
- 2047 Hong, Q., Cai, P., Geibert, W., Cao, Z., Stimac, I., Liu, L., Li, Q., 2018. Benthic fluxes of metals  
2048 into the Pearl River Estuary based on  $^{224}\text{Ra}/^{228}\text{Th}$  disequilibrium: From alkaline earth  
2049 (Ba) to redox sensitive elements (U, Mn, Fe). *Geochim. Cosmochim. Acta* 237, 223–239.  
2050 <https://doi.org/10.1016/j.gca.2018.06.036>
- 2051 Hong, Q., Cai, P., Shi, X., Li, Q., Wang, G., 2017. Solute transport into the Jiulong River  
2052 estuary via pore water exchange and submarine groundwater discharge: New insights  
2053 from  $^{224}\text{Ra}/^{228}\text{Th}$  disequilibrium. *Geochim. Cosmochim. Acta* 198, 338–359.  
2054 <https://doi.org/10.1016/j.gca.2016.11.002>
- 2055 Hougham, A.L., Moran, S.B., 2007. Water mass ages of coastal waters estimated using  $^{223}\text{Ra}$   
2056 and  $^{224}\text{Ra}$  as tracers. *Mar. Chem.* 105, 194–207.  
2057 <https://doi.org/10.1016/j.marchem.2007.01.013>
- 2058 Hsieh, Y. Te, Henderson, G.M., 2011. Precise measurement of  $^{228}\text{Ra}/^{226}\text{Ra}$  ratios and Ra  
2059 concentrations in seawater samples by multi-collector ICP mass spectrometry. *J. Anal.*  
2060 *At. Spectrom.* 26, 1338–1346. <https://doi.org/10.1039/c1ja10013k>
- 2061 Huh, C.A., Ku, T.L., 1998. A 2-D section of  $^{228}\text{Ra}$  and  $^{226}\text{Ra}$  in the Northeast Pacific.  
2062 *Oceanol. Acta* 21, 533–542. [https://doi.org/10.1016/S0399-1784\(98\)80036-4](https://doi.org/10.1016/S0399-1784(98)80036-4)
- 2063 Hussain, N., 1995. Supply rates of natural U-Th series radionuclides from aquifer solids into  
2064 groundwater. *Geophys. Res. Lett.* 22, 1521–1524.  
2065 <https://doi.org/10.1029/95GL01006>
- 2066 Hwang, D.-W., Lee, I.-S., Choi, M., Kim, T.-H., 2016. Estimating the input of submarine  
2067 groundwater discharge (SGD) and SGD-derived nutrients in Geoje Bay, Korea using  
2068  $^{222}\text{Rn}$ -Si mass balance model. *Mar. Pollut. Bull.* 110, 119–126.  
2069 <https://doi.org/10.1016/j.marpolbul.2016.06.073>
- 2070 Hwang, D.W., Lee, Y.W., Kim, C., 2005. Large submarine groundwater discharge and benthic  
2071 eutrophication in Bangda Bay on volcanic Jeju Island, Korea. *Limnol. Oceanogr.* 50,  
2072 1393–1403.
- 2073 Ivanovich, M., Harmon, R.S., 1992. Uranium-series Disequilibrium: Applications to Earth,  
2074 Marine, and Environmental Sciences. Clarendon Press.
- 2075 Iyengar, M. a. R., Rao, K.M., 1990. Uptake of radium by marine animals, in: *The*  
2076 *Environmental Behaviour of Radium Vol. 1 (Technical Reports Series No. 310)*. IAEA,  
2077 Vienna, p. 600.
- 2078 Jeandel, C., 2016. Overview of the mechanisms that could explain the “Boundary Exchange”  
2079 at the land-ocean contact. *Philos. Trans. R. Soc. A Math. Phys. Eng. Sci.* 374.  
2080 <https://doi.org/10.1098/rsta.2015.0287>
- 2081 Johannes, R., 1980. The Ecological Significance of the Submarine Discharge of Groundwater.  
2082 *Mar. Ecol. Prog. Ser.* 3, 365–373. <https://doi.org/10.3354/meps003365>
- 2083 Joly, J., 1908. On the radium-content of deep-sea sediments. London, Edinburgh, Dublin  
2084 *Philos. Mag. J. Sci.* 16, 190–197. <https://doi.org/10.1080/14786440708636499>
- 2085 Kadko, D.C., Moore, W.S., 1988. Radiochemical constraints on the crustal residence time of  
2086 submarine hydrothermal fluids: Endeavour Ridge. *Geochim. Cosmochim. Acta* 52, 659–  
2087 668. [https://doi.org/10.1016/0016-7037\(88\)90328-6](https://doi.org/10.1016/0016-7037(88)90328-6)
- 2088 Kaufman, A., Trier, R.M., Broecker, W.S., Feely, H.W., 1973. Distribution of  $^{228}\text{Ra}$  in the

- 2089 world ocean. *J. Geophys. Res.* 78, 8827–8848.  
 2090 <https://doi.org/10.1029/jc078i036p08827>
- 2091 Kelly, R.P., Moran, S.B., 2002. Seasonal changes in groundwater input to a well-mixed  
 2092 estuary estimated using radium isotopes and implications for coastal nutrient budgets.  
 2093 *Limnol. Oceanogr.* 47, 1796–1807. <https://doi.org/10.4319/lo.2002.47.6.1796>
- 2094 Key, R.M., Stallard, R.F., Moore, W., Sarmiento, J.L., 1985. Distribution and flux of Ra-226  
 2095 and Ra-228 in the Amazon River Estuary. *J. Geophys. Res.* 90, 6995–7004.
- 2096 Kigoshi, K., 1971. Alpha-recoil thorium-234: dissolution into water and the uranium-  
 2097 234/uranium-238 disequilibrium in nature. *Science (80-. )*. 173, 47–48.  
 2098 <https://doi.org/10.1126/science.173.3991.47>
- 2099 Kim, G., Ryu, J.-W., Hwang, D.-W., 2008. Radium tracing of submarine groundwater  
 2100 discharge (SGD) and associated nutrient fluxes in a highly-permeable bed coastal zone,  
 2101 Korea. *Mar. Chem.* 109, 307–317. <https://doi.org/10.1016/j.marchem.2007.07.002>
- 2102 Kim, G., Ryu, J.W., Yang, H.S., Yun, S.T., 2005. Submarine groundwater discharge (SGD) into  
 2103 the Yellow Sea revealed by Ra-228 and Ra-226 isotopes. Implications for global silicate  
 2104 fluxes. *Earth Planet. Sci. Lett.* 237, 156–166. <https://doi.org/10.1016/j.epsl.2005.06.011>
- 2105 King, J.N., 2012. Synthesis of benthic flux components in the Patos Lagoon coastal zone, Rio  
 2106 Grande do Sul, Brazil. *Water Resour. Res.* 48, 1–10.  
 2107 <https://doi.org/10.1029/2011WR011477>
- 2108 Kiro, Y., Weinstein, Y., Starinsky, A., Yechieli, Y., 2010. Groundwater ages and reaction rates  
 2109 during seawater circulation in the Dead Sea aquifer. *Geochim. Cosmochim. Acta* 74, 17–35. <https://doi.org/10.1016/j.gca.2010.03.005>
- 2110 Kiro, Y., Yechieli, Y., Voss, C.I., Starinsky, A., Weinstein, Y., 2012. Modeling radium  
 2111 distribution in coastal aquifers during sea level changes: The Dead Sea case. *Geochim.*  
 2112 *Cosmochim. Acta* 88, 237–254. <https://doi.org/10.1016/j.gca.2012.03.022>
- 2113 Knauss, K.G., Ku, T.-L., Moore, W.S., 1978. Radium and thorium isotopes in the surface  
 2114 waters of the East Pacific and coastal Southern California. *Earth Planet. Sci. Lett.* 39,  
 2115 235–249. [https://doi.org/https://doi.org/10.1016/0012-821X\(78\)90199-1](https://doi.org/10.1016/0012-821X(78)90199-1)
- 2116 Knee, K.L., Garcia-Solsona, E., Garcia-Orellana, J., Boehm, A.B., Paytan, A., 2011. Using  
 2117 radium isotopes to characterize water ages and coastal mixing rates: A sensitivity  
 2118 analysis. *Limnol. Oceanogr.* 56, 380–395. <https://doi.org/10.4319/lom.2011.9.380>
- 2119 Knee, K.L., Paytan, A., 2011. Submarine Groundwater Discharge: A Source of Nutrients,  
 2120 Metals, and Pollutants to the Coastal Ocean. *Treatise Estuar. Coast. Sci.* 4.
- 2121 Knee, K.L., Street, J.H., Grossman, E.E., Boehm, A.B., Paytan, A., 2010. Nutrient inputs to the  
 2122 coastal ocean from submarine groundwater discharge in a groundwater-dominated  
 2123 system: Relation to land use (Kona coast, Hawaii, USA). *Limnol. Oceanogr.* 55, 1105–  
 2124 1122. <https://doi.org/10.4319/lo.2010.55.3.1105>
- 2125 Koch-Larrouy, A., Atmadipoera, A., van Beek, P., Madec, G., Aucan, J., Lyard, F., Grelet, J.,  
 2126 Souhaut, M., 2015. Estimates of tidal mixing in the Indonesian archipelago from  
 2127 multidisciplinary INDOMIX in-situ data. *Deep. Res. Part I Oceanogr. Res. Pap.* 106, 136–  
 2128 153. <https://doi.org/10.1016/j.dsr.2015.09.007>
- 2129 Koczy, F.F., 1963. Natural radio nuclides in the ocean: radioactive tracers in oceanography,  
 2130 in: *International Union of Geodesy and Geophysics Monograph No. 20. Tenth Pacific*  
 2131 *Science Congress. Honolulu, Hawaii*, pp. 1–9.
- 2132 Koczy, F.F., 1958. Natural radium as a tracer in the ocean, in: *2nd U.N. Int. Conf. Peaceful*  
 2133 *Uses of Atomic Energy*, 18. Geneva, pp. 351–357.
- 2134 Kohout, F.A., 1966. Submarine springs: A neglected phenomenon of coastal hydrology.

- 2136 Hydrology 26, 391–413.
- 2137 Kraemer, T.F., 2005. Radium isotopes in Cayuga Lake, New York: Indicators of inflow and  
2138 mixing processes. *Limnol. Oceanogr.* 50, 158–168.  
2139 <https://doi.org/10.4319/lo.2005.50.1.0158>
- 2140 Krall, L., Trezzi, G., Garcia-Orellana, J., Rodellas, V., Mörth, C.-M., Andersson, P., 2017.  
2141 Submarine groundwater discharge at Forsmark, Gulf of Bothnia, provided by Ra  
2142 isotopes. *Mar. Chem.* 196, 162–172. <https://doi.org/10.1016/j.marchem.2017.09.003>
- 2143 Krest, J.M., Harvey, J.W., 2003. Using natural distributions of short-lived radium isotopes to  
2144 quantify groundwater discharge and recharge. *Limnol. Oceanogr.* 48, 290–298.  
2145 <https://doi.org/10.4319/lo.2003.48.1.0290>
- 2146 Krest, J.M., Moore, W.S., Gardner, L.R., Morris, J.T., 2000. Marsh nutrient export supplied by  
2147 groundwater discharge: Evidence from radium measurements. *Global Biogeochem.*  
2148 *Cycles* 14, 167–176. <https://doi.org/10.1029/1999GB001197>
- 2149 Krest, J.M., Moore, W.S., Rama, 1999. <sup>226</sup>Ra and <sup>228</sup>Ra in the mixing zones of the  
2150 Mississippi and Atchafalaya rivers: Indicators of groundwater input. *Mar. Chem.* 64,  
2151 129–152. [https://doi.org/10.1016/S0304-4203\(98\)00070-X](https://doi.org/10.1016/S0304-4203(98)00070-X)
- 2152 Krishnaswami, S., Graystein, W.C., Turekian, K.K., Dowd, J.F., 1982. Radium, Thorium and  
2153 Radioactive Lead Isotopes in Groundwaters' Application to the in Situ Determination of  
2154 Adsorption-Desorption. *Water Resour. Res.* 18, 1631–1675.
- 2155 Kronfeld, J., Ilani, S., Strull, A., 1991. Radium precipitation and extreme <sup>238</sup>U-series  
2156 disequilibrium along the Dead Sea coast, Israel. *Appl. Geochemistry* 6, 355–361.  
2157 [https://doi.org/https://doi.org/10.1016/0883-2927\(91\)90011-D](https://doi.org/https://doi.org/10.1016/0883-2927(91)90011-D)
- 2158 Ku, T.-L., Luo, S., 2008. Ocean Circulation, Mixing Studies with Decay-Series Isotopes, in:  
2159 Krishnaswami, S., Cochran, J.K.B.T.-K. (Eds.), *U-Th Series Nuclides in Aquatic*  
2160 *Systems*. Elsevier, pp. 307–344. [https://doi.org/https://doi.org/10.1016/S1569-](https://doi.org/https://doi.org/10.1016/S1569-4860(07)00009-5)  
2161 [4860\(07\)00009-5](https://doi.org/https://doi.org/10.1016/S1569-4860(07)00009-5)
- 2162 Kumar, A., Rout, S., Pulhani, V., Kumar, A.V., 2020. A review on distribution coefficient (K<sub>d</sub>)  
2163 of some selected radionuclides in soil/sediment over the last three decades. *J.*  
2164 *Radioanal. Nucl. Chem.* 373, 12–26. <https://doi.org/10.1007/s10967-019-06930-x>
- 2165 Kwon, E.Y., Kim, G., Primeau, F., Moore, W.S., Cho, H.-M., DeVries, T., Sarmiento, J.L.,  
2166 Charette, M.A., Cho, Y.-Y., 2014. Global estimate of submarine groundwater discharge  
2167 based on an observationally constrained radium isotope model. *Geophys. Res. Lett.* 1–  
2168 7. <https://doi.org/10.1002/2014GL061574>.Received
- 2169 Lamontagne, S., Webster, I.T., 2019a. Theoretical assessment of the effect of vertical  
2170 dispersivity on coastal seawater radium distribution. *Front. Mar. Sci.* 6, 1–10.  
2171 <https://doi.org/10.3389/fmars.2019.00357>
- 2172 Lamontagne, S., Webster, I.T., 2019b. Cross-Shelf Transport of Submarine Groundwater  
2173 Discharge Tracers: A Sensitivity Analysis. *J. Geophys. Res. Ocean.* 124, 453–469.  
2174 <https://doi.org/10.1029/2018JC014473>
- 2175 Lecher, A.L., Fisher, A.T., Paytan, A., 2016. Submarine groundwater discharge in Northern  
2176 Monterey Bay, California: Evaluation by mixing and mass balance models. *Mar. Chem.*  
2177 179, 44–55. <https://doi.org/10.1016/j.marchem.2016.01.001>
- 2178 Lee, C.M., Jiao, J.J., Luo, X., Moore, W.S., 2012. Estimation of submarine groundwater  
2179 discharge and associated nutrient fluxes in Tolo Harbour, Hong Kong. *Sci. Total Environ.*  
2180 433, 427–433. <https://doi.org/10.1016/j.scitotenv.2012.06.073>
- 2181 Leibundgut, C., Seibert, J., 2011. <sup>226</sup>Ra - Tracer Hydrology, in: Wilderer, P.B.T.-T. (Ed.),  
2182 *...*. Elsevier, Oxford, pp. 215–236. <https://doi.org/https://doi.org/10.1016/B978-0-444->

- 2183 53199-5.00036-1
- 2184 Lerner, D.N., Harris, B., 2009. The relationship between land use and groundwater resources  
2185 and quality. *Land use policy* 26, S265–S273.  
2186 <https://doi.org/https://doi.org/10.1016/j.landusepol.2009.09.005>
- 2187 Levy, D.M., Moore, W.S., 1985. Ra in continental shelf waters. *Earth Planet. Sci. Lett.* 73,  
2188 226–230.
- 2189 Li, X., Ke, T., Wang, Y., Zhou, T., Li, D., Tong, F., Wen, J., 2020. Hydraulic Conductivity  
2190 Behaviors of Karst Aquifer With Conduit-Fissure Geomaterials. *Front. Earth Sci.* 8, 1–10.  
2191 <https://doi.org/10.3389/feart.2020.00030>
- 2192 Li, Y.-H., Chan, L.-H., 1979. Desorption of Ba and Ra-226 from river-borne sediments in the  
2193 Hudson Estuary. *Earth Planet. Sci. Lett.* 43, 343–350.
- 2194 Li, Y.-H., Mathieu, G., Biscaye, P., Simpson, H.J., 1977. The flux of Ra-226 from estuarine and  
2195 continental shelf sediments. *Earth Planet. Sci. Lett.* 37, 273–241.
- 2196 Liao, F., Wang, G., Yi, L., Shi, Z., Cheng, G., Kong, Q., Mu, W., Guo, L., Cheng, K., Dong, N., Liu,  
2197 C., 2020. Applying radium isotopes to estimate groundwater discharge into Poyang  
2198 Lake, the largest freshwater lake in China. *J. Hydrol.* 585, 124782.  
2199 <https://doi.org/10.1016/j.jhydrol.2020.124782>
- 2200 Lin, L., Liu, Z., 2019. Partial residence times: determining residence time composition in  
2201 different subregions. *Ocean Dyn.* 69, 1023–1030. <https://doi.org/10.1007/s10236-019-01298-8>
- 2202
- 2203 Liu, J., Su, N., Wang, X., Du, J., 2018. Submarine groundwater discharge and associated  
2204 nutrient fluxes into the Southern Yellow Sea: A case study for semi- enclosed and  
2205 oligotrophic seas-implication for green tide bloom. *J. Geophys. Res. Ocean.* 121, 3372–  
2206 3380. <https://doi.org/10.1002/2015JC011421>.Received
- 2207 Liu, Q., Charette, M.A., Henderson, P.R., McCorkle, D.C., Martin, W., Dai, M., 2014. Effect of  
2208 submarine groundwater discharge on the coastal ocean inorganic carbon cycle. *Limnol.*  
2209 *Oceanogr.* 59, 1529–1554. <https://doi.org/10.4319/lo.2014.59.5.1529>
- 2210 Liu, Y., Jiao, J.J., Mao, R., Luo, X., Liang, W., Robinson, C.E., 2019. Spatial characteristics  
2211 reveal the reactive transport of radium isotopes ( $^{224}\text{Ra}$ ,  $^{223}\text{Ra}$ , &  $^{228}\text{Ra}$ ) in an  
2212 intertidal aquifer. *Water Resour. Res.* 2019WR024849.  
2213 <https://doi.org/10.1029/2019WR024849>
- 2214 Luek, J.L.J.L., Beck, A.J.A.L., 2014. Radium budget of the York River estuary (VA, USA)  
2215 dominated by submarine groundwater discharge with a seasonally variable  
2216 groundwater end-member. *Mar. Chem.* 165, 55–65.  
2217 <https://doi.org/10.1016/j.marchem.2014.08.001>
- 2218 Luijendijk, E., Gleeson, T., Moosdorf, N., 2020. Fresh groundwater discharge insignificant  
2219 for the world's oceans but important for coastal ecosystems. *Nat. Commun.* 11, 1260.  
2220 <https://doi.org/10.1038/s41467-020-15064-8>
- 2221 Luo, X., Jiao, J.J., Moore, W.S., Cherry, J.A., Wang, Y., Liu, K., 2018. Significant chemical fluxes  
2222 from natural terrestrial groundwater rival anthropogenic and fluvial input in a large-  
2223 river deltaic estuary. *Water Res.* 144, 603–615.  
2224 <https://doi.org/10.1016/j.watres.2018.07.004>
- 2225 Ma, Q., Zhang, Y., 2020. Global research trends and hotspots on submarine groundwater  
2226 discharge (SGD): A bibliometric analysis. *Int. J. Environ. Res. Public Health* 17.  
2227 <https://doi.org/10.3390/ijerph17030830>
- 2228 Manheim, F.T., 1967. Evidence for submarine discharge of water on the Atlantic continental  
2229 slope of the southern United States, and suggestions for further search. *Trans. N. Y.*

- 2230 Acad. Sci. 29, 839–853. <https://doi.org/10.1111/j.2164-0947.1967.tb02825.x>
- 2231 Mathieu, G.G., Biscaye, P.E., Lupton, R.A., Hammond, D.E., 1988. System for measurements  
2232 of  $^{222}\text{Rn}$  at low levels in natural waters. *Health Phys.* 55.
- 2233 McAllister, S.M., Barnett, J.M., Heiss, J.W., Findlay, A.J., MacDonald, D.J., Dow, C.L., Luther,  
2234 G.W., Michael, H.A., Chan, C.S., 2015. Dynamic hydrologic and biogeochemical  
2235 processes drive microbially enhanced iron and sulfur cycling within the intertidal mixing  
2236 zone of a beach aquifer. *Limnol. Oceanogr.* 60, 329–345.  
2237 <https://doi.org/10.1111/lno.10029>
- 2238 McKinley, I.G., Russell Alexander, W., 1993. Assessment of radionuclide retardation: uses  
2239 and abuses of natural analogue studies. *J. Contam. Hydrol.* 13, 249–259.  
2240 [https://doi.org/10.1016/0169-7722\(93\)90060-6](https://doi.org/10.1016/0169-7722(93)90060-6)
- 2241 Meier, H., Zimmerhackl, E., Zeitler, G., Menge, P., 2015. Parameter Studies of Radionuclide  
2242 Sorption in Site-Specific Sediment/Groundwater Systems. *Radiochim. Acta* 66–67.  
2243 <https://doi.org/10.1524/ract.1994.6667.special-issue.277>
- 2244 Meysman, F.J.R., Boudreau, B.P., Middelburg, J.J., 2005. Modeling reactive transport in  
2245 sediments subject to bioturbation and compaction. *Geochim. Cosmochim. Acta* 69,  
2246 3601–3617. <https://doi.org/https://doi.org/10.1016/j.gca.2005.01.004>
- 2247 Michael, H.A., Charette, M.A., Harvey, C.F., 2011. Patterns and variability of groundwater  
2248 flow and radium activity at the coast: A case study from Waquoit Bay, Massachusetts.  
2249 *Mar. Chem.* 127, 100–114. <https://doi.org/10.1016/j.marchem.2011.08.001>
- 2250 Michael, H.A., Mulligan, A.E., Harvey, C.F., 2005. Seasonal oscillations in water exchange  
2251 between aquifers and the coastal ocean. *Nature* 436, 1145–1148.  
2252 <https://doi.org/10.1038/nature03975>
- 2253 Molina-Porras, A., Condomines, M., Legea, P.L., Bailly-Comte, V., Seidel, J.L., 2020. Radium  
2254 Isotopes as a Tracer of Water Sources and Mixing in the Vidourle Stream (South of  
2255 France). *Aquat. Geochemistry* 20, 110–136. <https://doi.org/10.1007/s10498-020-09371-1>
- 2256
- 2257 Monsen, N.E., Cloern, J.E., Lucas, L.V., Monismith, S.G., 2002. A comment on the use of  
2258 flushing time, residence time, and age as transport time scales. *Limnol. Oceanogr.* 47,  
2259 1545–1553. <https://doi.org/10.4319/lo.2002.47.5.1545>
- 2260 Montiel, D., Dimova, N., Anuger, B., Prieto, J., García-Orellana, J., Rodellas, V., 2018.  
2261 Assessing submarine groundwater discharge (SGD) and nitrate fluxes in highly  
2262 heterogeneous coastal karst aquifers: Challenges and solutions. *J. Hydrol.* 557, 222–  
2263 242. <https://doi.org/10.1016/j.jhydrol.2017.12.036>
- 2264 Moore, W.S., 2015. Inappropriate attempts to use distributions of  $^{228}\text{Ra}$  and  $^{226}\text{Ra}$  in  
2265 coastal waters to model mixing and advection rates. *Cont. Shelf Res.* 105, 95–100.  
2266 <https://doi.org/10.1016/j.csr.2015.05.014>
- 2267 Moore, W.S., 2010. The Effect of Submarine Groundwater Discharge on the Ocean, in:  
2268 *Annual Review of Marine Science*. pp. 59–88. <https://doi.org/10.1146/annurev-marine-120308-081019>
- 2269
- 2270 Moore, W.S., 2008. Fifteen years experience in measuring  $^{224}\text{Ra}$  and  $^{223}\text{Ra}$  by delayed-  
2271 coincidence counting. *Mar. Chem.* 109, 188–197.  
2272 <https://doi.org/10.1016/j.marchem.2007.06.015>
- 2273 Moore, W.S., 2007. Seasonal distribution and flux of radium isotopes on the southeastern  
2274 US continental shelf. *J. Geophys. Res.* 112, 1–16.  
2275 <https://doi.org/10.1029/2007jc004199>
- 2276 Moore, W.S., 2006a. The role of submarine groundwater discharge in coastal

- 2277 biogeochemistry. *J. Geochemical Explor.* 88, 389–393.
- 2278 <https://doi.org/10.1016/j.gexplo.2005.08.082>
- 2279 Moore, W.S., 2006b. Radium isotopes as tracers of submarine groundwater discharge in  
2280 Sicily. *Cont. Shelf Res.* 26, 852–861. <https://doi.org/10.1016/j.csr.2005.12.004>
- 2281 Moore, W.S., 2003. Sources and fluxes of submarine groundwater discharge delineated by  
2282 radium isotopes. *Biogeochemistry* 66, 75–93.
- 2283 <https://doi.org/10.1023/B:BIOG.0000006065.77764.a0>
- 2284 Moore, W.S., 2000a. Ages of continental shelf waters determined from  $^{223}\text{Ra}$  and  $^{224}\text{Ra}$ . *J.*  
2285 *Geophys. Res.* 22117–22122.
- 2286 Moore, W.S., 2000b. Determining coastal mixing rates using radium isotopes. *Cont. Shelf*  
2287 *Res.* 20, 1993–2007. [https://doi.org/10.1016/S0278-4343\(00\)00054-6](https://doi.org/10.1016/S0278-4343(00)00054-6)
- 2288 Moore, W.S., 1999. The subterranean estuary: a reaction zone of groundwater and  
2289 seawater. *Mar. Chem.* 65, 111–125.
- 2290 Moore, W.S., 1997. High fluxes of radium and barium from the mouth of the Ganges-  
2291 Brahmaputra River during low river discharge suggest a large groundwater source.  
2292 *Earth Planet. Sci. Lett.* 150, 141–150. [https://doi.org/10.1016/S0012-821X\(97\)00083-6](https://doi.org/10.1016/S0012-821X(97)00083-6)
- 2293 Moore, W.S., 1996. Large groundwater inputs to coastal waters revealed by  $^{226}\text{Ra}$   
2294 enrichments. *Nature* 380, 612–614.
- 2295 Moore, W.S., 1987. Radium  $^{228}$  in the South Atlantic Bight. *J. Geophys. Res. Ocean.* 92,  
2296 5177–5190. <https://doi.org/10.1029/JC092iC05p05177>
- 2297 Moore, W.S., 1981. Radium isotopes in the Chesapeake Bay. *Estuar. Coast. Shelf Sci.* 12,  
2298 713–723. [https://doi.org/10.1016/S0303-3524\(81\)80067-9](https://doi.org/10.1016/S0303-3524(81)80067-9)
- 2299 Moore, W.S., 1976. Sampling  $^{228}\text{Ra}$  in the deep ocean. *Deep. Res.* 23, 647–651.
- 2300 Moore, W.S., 1972. Radium-228: Application to thermocline mixing studies. *Earth Planet.*  
2301 *Sci. Lett.* 16, 421–422.
- 2302 Moore, Willard S., 1969. Oceanic concentrations of  $^{228}\text{Radium}$ . *Earth Planet. Sci. Lett.* 6,  
2303 437–446. [https://doi.org/10.1016/0012-821x\(69\)90113-7](https://doi.org/10.1016/0012-821x(69)90113-7)
- 2304 Moore, Willard S., 1969. Measurement of  $^{228}\text{Ra}$  and  $^{228}\text{Th}$  in Sea Water. *J. Geophys. Res.*  
2305 74, 694–704.
- 2306 Moore, W.S., Arnold, R., 1996. Measurement of  $^{223}\text{Ra}$  and  $^{224}\text{Ra}$  in coastal waters using a  
2307 delayed coincidence counter. *J. Geophys. Res.* 101, 1321–1329.
- 2308 Moore, W.S., Astwood, H., Lindstrom, C., 1995. Radium isotopes in coastal waters on the  
2309 Amazon shelf. *Geochim. Cosmochim. Acta* 59, 4285–4298.
- 2310 [https://doi.org/10.1016/0016-7037\(95\)00242-R](https://doi.org/10.1016/0016-7037(95)00242-R)
- 2311 Moore, W.S., Blanton, J.O., Joye, S.B., 2006. Estimates of flushing times, submarine  
2312 groundwater discharge, and nutrient fluxes to Okatee Estuary, South Carolina. *J.*  
2313 *Geophys. Res.* 111, 1–14. <https://doi.org/10.1029/2005jc003041>
- 2314 Moore, W.S., Dymond, J., 1991. Fluxes of  $^{226}\text{Ra}$  and barium in the Pacific Ocean: The  
2315 importance of boundary processes. *Earth Planet. Sci. Lett.* 107, 55–68.
- 2316 [https://doi.org/10.1016/0012-821X\(91\)90043-H](https://doi.org/10.1016/0012-821X(91)90043-H)
- 2317 Moore, W.S., Humphries, M.S., Benitez-Nelson, C.R., Pillay, L., Higgs, C., 2019. Transport of  
2318 Radium and Nutrients Through Eastern South African Beaches. *J. Geophys. Res. Ocean.*  
2319 124, 2010–2027. <https://doi.org/10.1029/2018JC014772>
- 2320 Moore, W.S., Kjerfve, B., Todd, J.F., 1998. Identification of rain-freshened plumes in the  
2321 coastal ocean using Ra isotopes and Si. *J. Geophys. Res. Ocean.* 103, 7709–7717.
- 2322 <https://doi.org/10.1029/98jc00246>
- 2323 Moore, W.S., Reid, D.F., 1973. Extraction of Radium from Natural Waters Using Manganese-

- 2324 Impregnated Acrylic Fibers. *J. Geophys. Res.* 78, 8880–8886.  
2325 <https://doi.org/10.1029/JC078i036p08880>
- 2326 Moore, W.S., Sarmiento, J.L., Key, R.M., 2008. Submarine groundwater discharge revealed  
2327 by Ra-228 distribution in the upper Atlantic Ocean. *Nat. Geosci.* 1, 309–311.  
2328 <https://doi.org/10.1038/ngeo183>
- 2329 Moore, W.S., Shaw, T.J., 2008. Fluxes and behavior of radium isotopes, barium, and uranium  
2330 in seven Southeastern US rivers and estuaries. *Mar. Chem.* 108, 236–254.  
2331 <https://doi.org/10.1016/j.marchem.2007.03.004>
- 2332 Nathwani, J.S., Phillips, C.R., 1979. Adsorption of <sup>226</sup>Ra by soils (I). *Chemosphere* 8, 285–  
2333 291. [https://doi.org/10.1016/0045-6535\(79\)90111-5](https://doi.org/10.1016/0045-6535(79)90111-5)
- 2334 Neff, J.M., 2002. Bioaccumulation in marine organisms: effect of contaminants from oil well  
2335 produced water. Elsevier.
- 2336 Neff, J.M., Sauer, T.C., 1995. Barium in produced water: Fate and effects in the marine  
2337 environment. Washington, D.C.
- 2338 Neuholz, R., Schnetger, B., Kleint, C., Koschinsky, A., Lettmann, K., Sander, S., Türke, A.,  
2339 Walter, M., Zitoun, R., Brumsack, H.J., 2020. Near-field hydrothermal plume dynamics  
2340 at Brothers Volcano (Kermadec Arc): A short-lived radium isotope study. *Chem. Geol.*  
2341 533, 119379. <https://doi.org/10.1016/j.chemgeo.2019.119379>
- 2342 Oehler, T., Tamborski, J., Rahman, S., Moosdorf, N., Ahrens, J., Mori, C., Neuholz, R.,  
2343 Schnetger, B., Beck, M., 2019. DSI as a Tracer for Submarine Groundwater Discharge.  
2344 *Front. Mar. Sci.* 6, 1–13. <https://doi.org/10.3389/fmars.2019.00563>
- 2345 Okubo, A., 1976. Remarks on the use of 'diffusion diagrams' in modeling scale-dependent  
2346 diffusion. *Deep Sea Res. Oceanogr. (Abs. Ser. 2)*, 1213–1214.  
2347 [https://doi.org/https://doi.org/10.1016/0011-7471\(76\)90897-4](https://doi.org/https://doi.org/10.1016/0011-7471(76)90897-4)
- 2348 Ollivier, P., Claude, C., Radakovitch, C., Hamelin, B., 2008. TIMS measurements of Ra-226  
2349 and Ra-228 in the Gulf of Lion, an attempt to quantify submarine groundwater  
2350 discharge. *Mar. Chem.* 109, 337–354. <https://doi.org/10.1016/j.marchem.2007.08.006>
- 2351 Paytan, A., Boehm, A.B., Shellenbarger, G.G., 2004. Bacterial Contamination and Submarine  
2352 Groundwater Discharge: A Possible Link. *Environ. Chem.* 1, 29–30.
- 2353 Paytan, A., Shellenbarger, G.G., Street, J.H., Gonneea, M.E., Davis, K., Young, M.B., Moore,  
2354 W.S., 2006. Submarine groundwater discharge: An important source of new inorganic  
2355 nitrogen to coral reef ecosystems. *Limnol. Oceanogr.* 51, 343–348.
- 2356 Petermann, E., Knöller, K., Koča, C., Scholten, J., Stollberg, R., Weiß, H., Schubert, M., 2018.  
2357 Coupling End-Member Mixing Analysis and Isotope Mass Balancing (<sup>222</sup>Rn) for  
2358 Differentiation of Fresh and Recirculated Submarine Groundwater Discharge Into  
2359 Knysna Estuary, South Africa. *J. Geophys. Res. Ocean.* 123, 952–970.  
2360 <https://doi.org/10.1002/2017JC013008>
- 2361 Peterson, R.N., Burnett, W.C., Dimova, N., Santos, I.R., 2009. Comparison of measurement  
2362 methods for radium-226 on manganese-fiber. *Limnol. Oceanogr. Methods* 7, 196–205.  
2363 <https://doi.org/10.4319/lom.2009.7.196>
- 2364 Porcelli, D., Kim, C.-K., Martin, P., Moore, W.S., Phaneuf, M., 2014. The environmental  
2365 behaviour of radium: revised edition TRS No. 476, in: *Behaviour of Radium : Revised*  
2366 *Edition*. IAEA, International Atomic Energy Agency, Vienna, pp. 6–32.
- 2367 Porcelli, D., Swarzenski, P.W., 2003. The behavior of U- and Th-series nuclides in  
2368 groundwater, in: Bourdon, B., Henderson, G.M., Lundstorm, C.C., Turner, S.P. (Ed.),  
2369 *Uranium- Series Geochemistry*. The Mineralogical Society of America, Washington, D.C.,  
2370 pp. 317–361.

- 2371 Povinec, P.P., Burnett, W.C., Beck, A., Bokuniewicz, H., Charette, M., Gonnee, M.E.,  
2372 Groening, M., Ishitobi, T., Kontar, E., Kwong, L.L.W., Marie, D.E.P., Moore, W.S.,  
2373 Oberdorfer, J.A., Peterson, R., Ramessur, R., Rapaglia, J., Stieglitz, T., Top, Z., 2012.  
2374 Isotopic, geophysical and biogeochemical investigation of submarine groundwater  
2375 discharge: IAEA-UNESCO intercomparison exercise at Mauritius Island. *J. Environ.*  
2376 *Radioact.* 104, 24–45. <https://doi.org/10.1016/j.jenvrad.2011.09.009>  
2377 Prieto, C., Destouni, G., 2005. Quantifying hydrological and tidal influences on groundwater  
2378 discharges into coastal waters. *Water Resour. Res.* 41.  
2379 <https://doi.org/W1242710.1029/2004wr003920>  
2380 Puigdomenech, I., Bergstrom, U., 1995. Calculation of distribution coefficients for  
2381 radionuclides in soils and sediments. *Nucl. Saf.* 36, 142–154.  
2382 Rahman, S., Tamborski, J.J., Charette, M.A., Cochran, J.K., 2019. Dissolved silica in the  
2383 subterranean estuary and the impact of submarine groundwater discharge on the  
2384 global marine silica budget. *Mar. Chem.* 208, 29–42.  
2385 <https://doi.org/10.1016/j.marchem.2018.11.006>  
2386 Rajaomahefasoa, R.E., Voltaggio, M., Rakotomandrindra, F.F., Ratsimbazafy, J.B., Spadoni,  
2387 M., Rakoto, H.A., 2019. Radium isotopes for groundwater age and sustainability in the  
2388 highland of Antananarivo, Madagascar. *J. African Earth Sci.* 156, 94–107.  
2389 <https://doi.org/10.1016/j.jafrearsci.2019.05.011>  
2390 Rama, Moore, W.S., 1996. Using the radium quartet for evaluating groundwater input and  
2391 water exchange in salt marshes. *Geochim. Cosmochim. Acta* 60, 4645–4652.  
2392 [https://doi.org/10.1016/S0016-7037\(96\)00269-X](https://doi.org/10.1016/S0016-7037(96)00269-X)  
2393 Rama, Moore, W.S., 1984. Mechanism of transport of U-Th series radioisotopes from solids  
2394 into ground water. *Geochim. Cosmochim. Acta* 48, 395–399.  
2395 [https://doi.org/https://doi.org/10.1016/0016-7037\(84\)90261-8](https://doi.org/https://doi.org/10.1016/0016-7037(84)90261-8)  
2396 Rapaglia, J., Ferrarin, C., Zaggia, L., Moore, W.S., Umgiesser, G., Garcia-Solsona, E., Garcia-  
2397 Orellana, J., Masque, P., 2010. Investigation of residence time and groundwater flux in  
2398 Venice Lagoon: comparing radium isotope and hydrodynamical models. *J. Environ.*  
2399 *Radioact.* 101, 571–581. <https://doi.org/10.1016/j.jenvrad.2009.08.010>  
2400 Rapaglia, J., Koukoulas, S., Zaggia, L., Lichter, M., Manfe, G., Vafeidis, A.T., Manfé, G.,  
2401 Vafeidis, A.T., 2012. Quantification of submarine groundwater discharge and optimal  
2402 radium sampling distribution in the Lesina Lagoon, Italy. *J. Mar. Syst.* 91, 11–19.  
2403 <https://doi.org/10.1016/j.jmarsys.2011.09.003>  
2404 Regan, H.M., Colyvan, M., Burgman, M.A., 2002. A TAXONOMY AND TREATMENT OF  
2405 UNCERTAINTY FOR ECOLOGY AND CONSERVATION BIOLOGY. *Ecol. Appl.* 12, 618–628.  
2406 [https://doi.org/10.1890/1051-0761\(2002\)012\[0618:ATATOU\]2.0.CO;2](https://doi.org/10.1890/1051-0761(2002)012[0618:ATATOU]2.0.CO;2)  
2407 Relyea, J.F., 1982. Theoretical and experimental considerations for the use of the column  
2408 method for determining retardation factors. *Radioact Waste Manag. Nucl Fuel Cycle* 3,  
2409 151–166.  
2410 Rengarajan, R., Sarma, V.V.S.S., 2015. Submarine groundwater discharge and nutrient  
2411 addition to the coastal zone of the Godavari estuary. *Mar. Chem.* 172, 57–69.  
2412 <https://doi.org/10.1016/j.marchem.2015.03.008>  
2413 Robinson, C.E., Xin, P., Santos, I.R., Charette, M.A., Li, L., Barry, D.A., 2018. Groundwater  
2414 dynamics in subterranean estuaries of coastal unconfined aquifers: Controls on  
2415 submarine groundwater discharge and chemical inputs to the ocean. *Adv. Water*  
2416 *Resour.* 115, 315–331. <https://doi.org/10.1016/j.advwatres.2017.10.041>  
2417 Rocha, C., Robinson, C.E., Santos, I.R., Waska, H., Michael, H.A., Bokuniewicz, H.J., 2021. A

- 2418 place for subterranean estuaries in the coastal zone. *Estuar. Coast. Shelf Sci.* 250,  
 2419 107167. <https://doi.org/10.1016/j.ecss.2021.107167>
- 2420 Rodellas, R., Garcia-Orellana, J., Garcia-Solsona, E., Masqué, P., Domínguez, J.A., Ballesteros,  
 2421 B., Mejías, M., 2012. Quantifying groundwater discharge from different sources into a  
 2422 Mediterranean wetland by using  $^{222}\text{Rn}$  and  $\text{Ra}$  isotopes. *J. Hydrol.* 466–467.
- 2423 Rodellas, V., Cook, P.G., Mccallum, J., Andrisoa, A., Stieglitz, T.C., 2020. Temporal variations  
 2424 in porewater fluxes to a coastal lagoon driven by wind waves and changes in lagoon  
 2425 water depths. *J. Hydrol.* 124363. <https://doi.org/10.1016/j.jhydrol.2019.124363>
- 2426 Rodellas, V., Garcia-Orellana, J., Masqué, P., Feldman, M., Weinstein, Y., 2015a. Submarine  
 2427 groundwater discharge as a major source of nutrients to the Mediterranean Sea. *Proc.*  
 2428 *Natl. Acad. Sci.* 112, 3926–3930. <https://doi.org/10.1073/pnas.1419049112>
- 2429 Rodellas, V., Garcia-Orellana, J., Masqué, P., Font-Muñoz, J.S., 2015b. The influence of  
 2430 sediment sources on radium-derived estimates of Submarine Groundwater Discharge.  
 2431 *Mar. Chem.* 171, 107–117. <https://doi.org/10.1016/j.marchem.2015.02.010>
- 2432 Rodellas, V., Garcia-Orellana, J., Tovar-Sánchez, A., Basterretxea, G., López-García, J.M.,  
 2433 Sánchez-Quilez, D., Garcia-Solsona, E., Masqué, P., 2014. Submarine groundwater  
 2434 discharge as a source of nutrients and trace metals in a Mediterranean bay (Palma  
 2435 Beach, Balearic Islands). *Mar. Chem.* 160, 56–66.
- 2436 Rodellas, V., Garcia-Orellana, J., Trezzi, G., Masqué, P., Stieglitz, T.C., Bokuniewicz, H., Kirk  
 2437 Cochran, J., Berdalet, E., 2017. Using the radium quartet to quantify submarine  
 2438 groundwater discharge and porewater exchange. *Geochim. Cosmochim. Acta* 196, 58–  
 2439 73. <https://doi.org/10.1016/j.gca.2016.09.015>
- 2440 Rodellas, V., Stieglitz, T.C., Andrisoa, A., Cook, P.G., Raimbault, P., Tamborski, J.J., van Beek,  
 2441 P., Radakovitch, O., 2018. Groundwater-driven nutrient inputs to coastal lagoons: The  
 2442 relevance of lagoon water recirculation as a conveyor of dissolved nutrients. *Sci. Total*  
 2443 *Environ.* 642, 764–780. <https://doi.org/10.1016/j.scitotenv.2018.06.095>
- 2444 Rodellas, V., Stieglitz, T.C., Tamborski, J.J., van Beek, P., Andrisoa, A., Cook, P.G., 2021.  
 2445 Conceptual uncertainties in groundwater and porewater fluxes estimated by radon and  
 2446 radium mass balances. *Limnol. Oceanogr.* 1–19. <https://doi.org/10.1002/lno.11678>
- 2447 Rosenberry, D.O., Duque, C., Lee, D.R., 2020. History and evolution of seepage meters for  
 2448 quantifying flow between groundwater and surface water: Part 1 – Freshwater  
 2449 settings. *Earth-Science Rev.* 204, 103167.  
 2450 <https://doi.org/10.1016/j.earscirev.2020.103167>
- 2451 Ruiz-González, C., Rodellas, V., Garcia-Orellana, J., 2021. The microbial dimension of  
 2452 submarine groundwater discharge: current challenges and future directions. *FEMS*  
 2453 *Microbiol. Rev.* 1–25. <https://doi.org/10.1093/femsre/fuab010>
- 2454 Rutgers van der Loeff, M., Kipp, L., Charette, M.A., Moore, W.S., Black, E., Stimac, I., Charkin,  
 2455 A., Bauch, D., Valk, O., Karcher, M., Krumpfen, T., Casacuberta, N., Smethie, W.,  
 2456 Rember, R., 2018. Radium Isotopes Across the Arctic Ocean Show Time Scales of Water  
 2457 Mass Ventilation and Increasing Shelf Inputs. *J. Geophys. Res. Ocean.* 123, 4853–4873.  
 2458 <https://doi.org/10.1029/2018JC013888>
- 2459 Sanial, V., van Beek, P., Lansard, B., Souhaut, M., Kestenare, E., D’Ovidio, F., Zhou, M., Blain,  
 2460 S., 2015. Use of  $\text{Ra}$  isotopes to deduce rapid transfer of sediment-derived inputs off  
 2461 Kerguelen. *Biogeosciences Discuss.* 12, 1415–1430. <https://doi.org/10.5194/bg-12-1415-2015>
- 2463 Santos, I.R., Chen, X., Lecher, A.L., Sawyer, A.H., Moosdorf, N., 2021. Submarine  
 2464 groundwater discharge impacts on coastal nutrient biogeochemistry. *Nat. Rev. Earth*

- 2465 Environ. 0123456789. <https://doi.org/10.1038/s43017-021-00152-0>
- 2466 Santos, I.R., Eyre, B.D., Huettel, M., 2012. The driving forces of porewater and groundwater  
2467 flow in permeable coastal sediments: A review. *Estuar. Coast. Shelf Sci.* 98, 1–15.  
2468 <https://doi.org/10.1016/j.ecss.2011.10.024>
- 2469 Santos, I.R., Lechuga-Deveze, C., Peterson, R.N., Burnett, W.C., 2011. Tracing submarine  
2470 hydrothermal inputs into a coastal bay in Baja California using radon. *Chem. Geol.* 282,  
2471 1–10. <https://doi.org/10.1016/j.chemgeo.2010.12.024>
- 2472 Sawyer, A.H., Shi, F., Kirby, J.T., Michael, H.A., 2013. Dynamic response of surface water-  
2473 groundwater exchange to currents, tides, and waves in a shallow estuary. *J. Geophys.*  
2474 *Res. Ocean.* 118, 1749–1758. <https://doi.org/10.1002/jgrc.20154>
- 2475 Schmidt, C., Hanfland, C., Regnier, P., Van Cappellen, P., Schlueter, M., Knauthe, U., Stimac,  
2476 I., Geibert, W., 2011. Ra-228, Ra-226, Ra-224 and Ra-223 in potential sources and sinks  
2477 of land-derived material in the German Bight of the North Sea: implications for the use  
2478 of radium as a tracer. *Geo-Marine Lett.* 31, 259–269. <https://doi.org/10.1007/s00367-011-0231-5>
- 2480 Schubert, M., Knoeller, K., Rocha, C., Einsiedl, F., 2015. Evaluation and source attribution of  
2481 freshwater contributions to Kinvarra Bay, Ireland, using  $^{222}\text{Rn}$ , EC and stable isotopes  
2482 as natural indicators. *Environ. Monit. Assess.* 187, 1–15.  
2483 <https://doi.org/10.1007/s10661-015-4274-3>
- 2484 Selzer, S., Annett, A.L., Homoky, W.B., 2021. RaDeCC Reader: Fast, accurate and automated  
2485 data processing for Radium Delayed Coincidence Counting systems. *Comput. Geosci.*  
2486 149. <https://doi.org/10.1016/j.cageo.2021.104699>
- 2487 Semkow, T.M., 1990. Recoil-emanation theory applied to radon release from mineral grains.  
2488 *Geochim. Cosmochim. Acta* 54, 425–440.  
2489 [https://doi.org/10.1016/0016-7037\(90\)90331-E](https://doi.org/10.1016/0016-7037(90)90331-E)
- 2490 Sheldon, J.E., Alber, M., 2008. The Calculation of Estuarine Turnover Times Using Freshwater  
2491 Fraction and Tidal Prism Models: A Critical Evaluation. *Estu* 29, 133–146.
- 2492 Shellenbarger, G.G.G.G., Monismith, S.G.S.G., Genin, A., Paytan, A., 2006. The importance of  
2493 submarine groundwater discharge to the nearshore nutrient supply in the Gulf of  
2494 Aqaba (Israel). *Limnol. Oceanogr.* 51, 1876–1886.  
2495 <https://doi.org/10.4319/lno.2006.51.4.1876>
- 2496 Shi, X., Benitez-Nelson, C.R., Cai, P., He, L., Moore, W.S., 2019a. Development of a two-layer  
2497 transport model in layered muddy-permeable marsh sediments using  $^{224}\text{Ra}$ – $^{228}\text{Th}$   
2498 disequilibria. *Limnol. Oceanogr.* 64, 1672–1687. <https://doi.org/10.1002/lno.11143>
- 2499 Shi, X., Mason, R.P., Charette, M.A., Mazrui, N.M., Cai, P., 2018. Mercury flux from salt  
2500 marsh sediments: Insights from a comparison between  $^{224}\text{Ra}/^{228}\text{Th}$  disequilibrium  
2501 and core incubation methods. *Geochim. Cosmochim. Acta* 222, 569–583.  
2502 <https://doi.org/10.1016/j.gca.2017.10.033>
- 2503 Shi, Xiangming, Wei, L., Hong, Q., Liu, L., Wang, Y., Shi, Xueying, Ye, Y., Cai, P., 2019b. Large  
2504 benthic fluxes of dissolved iron in China coastal seas revealed by  $^{224}\text{Ra}/^{228}\text{Th}$   
2505 disequilibria. *Geochim. Cosmochim. Acta* 260, 49–61.  
2506 <https://doi.org/10.1016/j.gca.2019.06.026>
- 2507 Simpson, G.C., Wright, C.S., Schuster, A., 1911. Atmospheric electricity over the ocean. *Proc.*  
2508 *R. Soc. London. Ser. A, Contain. Pap. a Math. Phys. Character* 85, 175–199.  
2509 <https://doi.org/10.1098/rspa.1911.0031>
- 2510 Snavely, E.S., 1989. Radionuclides in Produced Water. Washington, D.C.
- 2511 Stieglitz, T.C., Clark, J.F., Hancock, G.J., 2013. The mangrove pump: The tidal flushing of

- 2512 animal burrows in a tropical mangrove forest determined from radionuclide budgets.  
 2513 *Geochim. Cosmochim. Acta* 102, 12–22. <https://doi.org/10.1016/j.gca.2012.10.033>
- 2514 Sugimoto, R., Kitagawa, K., Nishi, S., Honda, H., Yamada, M., Kobayashi, S., Shoji, J., Ohsawa,  
 2515 S., Taniguchi, M., Tominaga, O., 2017. Phytoplankton primary productivity around  
 2516 submarine groundwater discharge in nearshore coasts. *Mar. Ecol. Prog. Ser.* 563.  
 2517 <https://doi.org/10.3354/meps11980>
- 2518 Sun, H., Semkow, T.M., 1998. Mobilization of thorium, radium and radon radionuclides in  
 2519 ground water by successive alpha-recoils. *J. Hydrol.* 205, 126–136.  
 2520 [https://doi.org/https://doi.org/10.1016/S0022-1694\(97\)00154-6](https://doi.org/https://doi.org/10.1016/S0022-1694(97)00154-6)
- 2521 Sun, Y., Torgersen, T., 2001. Adsorption-desorption reactions and bioturbation transport of  
 2522 <sup>224</sup>Ra in marine sediments: A one-dimensional model with applications. *Mar. Chem.*  
 2523 74, 227–243. [https://doi.org/10.1016/S0304-4203\(01\)00017-2](https://doi.org/10.1016/S0304-4203(01)00017-2)
- 2524 Swarzenski, P.W., 2007. U/Th series radionuclides as coastal groundwater tracers. *Chem.*  
 2525 *Rev.* 107, 663–674. <https://doi.org/10.1021/cr0503761>
- 2526 Swarzenski, P.W., Burnett, W.C., Greenwood, W.J., Herut, B., Peterson, R., Dimova, N.,  
 2527 Shalem, Y., Yechieli, Y., Weinstein, Y., 2006. Combined time-series resistivity and  
 2528 geochemical tracer techniques to examine submarine groundwater discharge at Dor  
 2529 Beach, Israel. *Geophys. Res. Lett.* 33. <https://doi.org/10.1029/2006gl028282>
- 2530 Swarzenski, P.W., Reich, C., Kroeger, K.D., Baskaran, M., 2007a. Ra and Rn isotopes as  
 2531 natural tracers of submarine groundwater discharge in Tampa Bay, Florida. *Mar. Chem.*  
 2532 104, 69–84. <https://doi.org/10.1016/j.marchem.2006.08.001>
- 2533 Swarzenski, P.W., Simonds, F.W., Paulson, A.J., Kruse, S., Reich, C., 2007b. Geochemical and  
 2534 geophysical examination of submarine groundwater discharge and associated nutrient  
 2535 loading estimates into Lynch Cove, Hood Canal, WA. *Environ. Sci. Technol.* 41, 7022–  
 2536 7029. <https://doi.org/10.1021/es070881a>
- 2537 Szabo, B.J., 1967. Radium content in plankton and sea water in the Bahamas. *Geochim.*  
 2538 *Cosmochim. Acta* 31, 1321–1331. [https://doi.org/10.1016/S0016-7037\(67\)80018-8](https://doi.org/10.1016/S0016-7037(67)80018-8)
- 2539 Tachi, Y., Shibutani, T., Sato, H., Nui, M., 2001. Experimental and modeling studies on  
 2540 sorption and diffusion of radium in bentonite. *J. Contam. Hydrol.* 47, 171–186.  
 2541 [https://doi.org/10.1016/S0169-7722\(00\)00147-9](https://doi.org/10.1016/S0169-7722(00)00147-9)
- 2542 Tagliabue, A., Aumont, O., Berner, L., 2014. of Iron on the Global Carbon Cycle. *Geophys. Res.*  
 2543 *Lett.* 318, 920–926. <https://doi.org/10.1002/2013GL059059>.Received
- 2544 Tamborski, J., Beek, P., van, Conan, P., Pujol-pay, M., Odobel, C., Ghiglione, J., Seidel, J., Ar,  
 2545 B., Diego-Feliu, M., Garcia-Orellana, J., Szafran, A., Souhaut, M., 2020. Submarine  
 2546 karstic springs as a source of nutrients and bioactive trace metals for the oligotrophic  
 2547 Northwest Mediterranean Sea. *Sci. Total Environ.* 732, 1–14.  
 2548 <https://doi.org/10.1016/j.scitotenv.2020.139106>
- 2549 Tamborski, J., van Beek, P., Rodellas, V., Monnin, C., Bergsma, E., Stieglitz, T., Heilbrun, C.,  
 2550 Cochran, J.K., Charbonnier, C., Anschutz, P., Bejannin, S., Beck, A., 2019. Temporal  
 2551 variability of lagoon–sea water exchange and seawater circulation through a  
 2552 Mediterranean barrier beach. *Limnol. Oceanogr.* 64, 2059–2080.  
 2553 <https://doi.org/10.1002/lno.11169>
- 2554 Tamborski, J.J., Bejannin, S., Garcia-Orellana, J., Souhaut, M., Charbonnier, C., Anschutz, P.,  
 2555 Pujol-Pay, M., Conan, P., Crispi, O., Monnin, C., Stieglitz, T., Rodellas, V., Andrisoa, A.,  
 2556 Claude, C., van Beek, P., 2018. A comparison between water recirculation and  
 2557 terrestrially-driven dissolved silica fluxes to the Mediterranean Sea traced using radium  
 2558 isotopes. *Geochim. Cosmochim. Acta* 238, 496–515.

- 2559 <https://doi.org/10.1016/j.gca.2018.07.022>
- 2560 Tamborski, J.J., Cochran, J.K., Bokuniewicz, H., Heilbrun, C., Garcia-Orellana, J., Rodellas, V.,  
2561 Wilson, R., 2020. Radium mass balance sensitivity analysis for submarine groundwater  
2562 discharge estimation in semi-enclosed basins: The case study of Long Island Sound.  
2563 *Front. Environ. Sci.* 8, 108. <https://doi.org/10.3389/FENVS.2020.00108>
- 2564 Tamborski, J.J., Cochran, J.K., Bokuniewicz, H.J., 2017a. Submarine groundwater discharge  
2565 driven nitrogen fluxes to Long Island Sound, NY: Terrestrial vs. marine sources.  
2566 *Geochim. Cosmochim. Acta* 218, 40–57. <https://doi.org/10.1016/j.gca.2017.09.003>
- 2567 Tamborski, J.J., Cochran, J.K., Bokuniewicz, H.J., 2017b. Application of  $^{224}\text{Ra}$  and  $^{222}\text{Rn}$  for  
2568 evaluating seawater residence times in a tidal subterranean estuary. *Mar. Chem.* 189,  
2569 32–45. <https://doi.org/10.1016/j.marchem.2016.12.006>
- 2570 Tamborski, J.J., Cochran, J.K., Heilbrun, C., Rafferty, P., Fitzgerald, P., Zhu, Q., Salazar, C.,  
2571 2017c. Investigation of pore water residence times and drainage velocities in salt  
2572 marshes using short-lived radium isotopes. *Mar. Chem.* 196, 107–115.  
2573 <https://doi.org/10.1016/j.marchem.2017.08.007>
- 2574 Tamborski, J.J., Eagle, M., Kurylyk, B.L., Kroeger, K.D., Wang, Z.A., Henderson, P., Charette,  
2575 M.A., 2021. Pore water exchange-driven inorganic carbon export from intertidal salt  
2576 marshes. *Limnol. Oceanogr.* 1–19. <https://doi.org/10.1002/lno.11721>
- 2577 Tamborski, J.J., Rogers, A.D., Bokuniewicz, H.J., Cochran, J.K., Young, C.R., 2015.  
2578 Identification and quantification of diffuse fresh submarine groundwater discharge via  
2579 airborne thermal infrared remote sensing. *Remote Sens. Environ.* 171.  
2580 <https://doi.org/10.1016/j.rse.2015.10.010>
- 2581 Taniguchi, M., Burnett, W.C., Cable, J.E., Turner, J. V., 2002. Investigation of submarine  
2582 groundwater discharge. *Hydrol. Processes.* 16, 2115–2129.  
2583 <https://doi.org/10.1002/hyp.1145>
- 2584 Taniguchi, M., Dulai, H., Burnett, K.M., Santos, I.R., Sugimoto, R., Stieglitz, T., Kim, G.,  
2585 Moosdorf, N., Burnett, W.C., 2019. Submarine Groundwater Discharge: Updates on Its  
2586 Measurement Techniques, Geophysical Drivers, Magnitudes, and Effects. *Front.*  
2587 *Environ. Sci.* 7, 1–26. <https://doi.org/10.3389/fenvs.2019.00141>
- 2588 Tomasky-Holmes, G., Valiela, I., Charette, M.A., 2013. Determination of water mass ages  
2589 using radium isotopes as tracers: Implications for phytoplankton dynamics in estuaries.  
2590 *Mar. Chem.* 156, 18–26  
2591 <https://doi.org/https://dx.doi.org/10.1016/j.marchem.2013.02.002>
- 2592 Toth, J., 1963. A Theoretical Analysis of Groundwater Flow in Small Drainage Basins 1 of phe  
2593 - low order stream and having similar the outlet of lowest impounded body of a  
2594 relatively. *J. Geophys. Res.* 68, 4795–4812. <https://doi.org/10.1029/JZ068i016p04795>
- 2595 Tovar-Sánchez, A., Basterretxea, G., Rodellas, V., Sánchez-Quiles, D., García-Orellana, J.,  
2596 Masqué, P., Jordi, A., López, J.M., Garcia-Solsona, E., 2014. Contribution of  
2597 groundwater discharge to the coastal dissolved nutrients and trace metal  
2598 concentrations in Majorca Island: karstic vs detrital systems. *Environ. Sci. Technol.* 48,  
2599 11819–11827. <https://doi.org/10.1021/es502958t>
- 2600 Trezzi, G., Garcia-Orellana, J., Santos-Echeandia, J., Rodellas, V., Garcia-Solsona, E., Garcia-  
2601 Fernandez, G., Masqué, P., 2016. The influence of a metal-enriched mining waste  
2602 deposit on submarine groundwater discharge to the coastal sea. *Mar. Chem.* 178, 35–  
2603 45. <https://doi.org/10.1016/j.marchem.2015.12.004>
- 2604 Tricca, A., Wasserburg, G.J., Porcelli, D., Baskaran, M., 2001. The transport of U- and Th-  
2605 series nuclides in sandy confined aquifers. *Geochim. Cosmochim. Acta* 65, 1187–1210.

- 2606 [https://doi.org/10.1016/S0016-7037\(02\)01341-8](https://doi.org/10.1016/S0016-7037(02)01341-8)
- 2607 Trier, R.M., Broecker, W.S., Feely, H.W., 1972. Radium-228 profile at the second geosecs  
2608 intercalibration station, 1970, in the North Atlantic. *Earth Planet. Sci. Lett.* 16, 141–145.
- 2609 van Beek, P., François, R., Conte, M., Reyss, J.-L., Souhaut, M., Charette, M., 2007.  
2610 228Ra/226Ra and 226Ra/Ba ratios to track barite formation and transport in the water  
2611 column. *Geochim. Cosmochim. Acta* 71, 71–86.  
2612 <https://doi.org/10.1016/j.gca.2006.07.041>
- 2613 Veeh, H.H., Moore, W.S., Smith, S. V., 1995. The behaviour of uranium and radium in an  
2614 inverse estuary. *Cont. Shelf Res.* 15, 1569–1583. [https://doi.org/10.1016/0278-](https://doi.org/10.1016/0278-4343(95)00031-U)  
2615 [4343\(95\)00031-U](https://doi.org/10.1016/0278-4343(95)00031-U)
- 2616 Vengosh, A., Hirschfeld, D., Vinson, D., Dwyer, G., Raanan, H., Rimawi, O., Al-Zoubi, A.,  
2617 Akkawi, E., Marie, A., Haquin, G., Zaarur, S., Ganor, J., 2009. High naturally occurring  
2618 radioactivity in fossil groundwater from the middle east. *Environ. Sci. Technol.* 43,  
2619 1769–1775. <https://doi.org/10.1021/es802969r>
- 2620 Vieira, L.H., Achterberg, E.P., Scholten, J., Beck, A.J., Liebetrau, V., Mills, M.M., Arrigo, K.R.,  
2621 2019. Benthic fluxes of trace metals in the Chukchi Sea and their transport into the  
2622 Arctic Ocean. *Mar. Chem.* 208, 43–55. <https://doi.org/10.1016/j.marchem.2018.11.001>
- 2623 Vieira, L.H., Geibert, W., Stimac, I., Koehler, D., Rutgers van der Loeff, M.M., 2021. The  
2624 analysis of 226Ra in 1-liter seawater by isotope dilution via single-collector sector-field  
2625 ICP-MS. *Limnol. Oceanogr. Methods.* <https://doi.org/10.1002/lom3.10428>
- 2626 Vieira, L.H., Krisch, S., Hopwood, M.J., Beck, A.J., Scholten, J., Liebetrau, V., Achterberg, E.P.,  
2627 2020. Unprecedented Fe delivery from the Congo River margin to the South Atlantic  
2628 Gyre. *Nat. Commun.* 11, 1–8. <https://doi.org/10.1038/s41467-019-14255-2>
- 2629 Wang, X., Du, J., 2016. Submarine groundwater discharge into typical tropical lagoons: A  
2630 case study in eastern Hainan Island, China. *Geochemistry Geophys. Geosystems* 17,  
2631 4366–4382. <https://doi.org/10.1002/2016GC006502>
- 2632 Wang, X., Du, J., Ji, T., Wen, T., Liu, S., Zhang, J., 2014. An estimation of nutrient fluxes via  
2633 submarine groundwater discharge into the Sanggou Bay-A typical multi-species culture  
2634 ecosystem in China. *Mar. Chem.* 167. <https://doi.org/10.1016/j.marchem.2014.07.002>
- 2635 Warner, J.C., Rockwell Geyer, W., Arango, H.G., 2010. Using a composite grid approach in a  
2636 complex coastal domain to estimate estuarine residence time. *Comput. Geosci.* 36,  
2637 921–935. <https://doi.org/10.1016/j.cageo.2009.11.008>
- 2638 Waska, H., Kim, S., Kim, G., Peterson, R.N., Burnett, W.C., 2008. An efficient and simple  
2639 method for measuring Ra-226 using the scintillation cell in a delayed coincidence  
2640 counting system (RaDeCC). *J. Environ. Radioact.* 99, 1859–1862.  
2641 <https://doi.org/10.1016/j.jenvrad.2008.08.008>
- 2642 Webster, I.T., Hancock, G.J., Murray, A.S., 1995. Modelling the effect of salinity on radium  
2643 desorption from sediments. *Geochim. Cosmochim. Acta* 59, 2469–2476.  
2644 [https://doi.org/10.1016/0016-7037\(95\)00141-7](https://doi.org/10.1016/0016-7037(95)00141-7)
- 2645 Weinstein, Y., Burnett, W.C., Swarzenski, P.W., Shalem, Y., Yechieli, Y., Herut, B., 2007. Role  
2646 of aquifer heterogeneity in fresh groundwater discharge and seawater recycling: An  
2647 example from the Carmel coast, Israel. *J. Geophys. Res.* 112.  
2648 <https://doi.org/10.1029/2007jc004112>
- 2649 Weinstein, Y., Yechieli, Y., Shalem, Y., Burnett, W.C., Swarzenski, P.W., Herut, B., 2011. What  
2650 Is the Role of Fresh Groundwater and Recirculated Seawater in Conveying Nutrients to  
2651 the Coastal Ocean? *Environ. Sci. Technol.* 45, 5195–5200.  
2652 <https://doi.org/10.1021/es104394r>

- 2653 Werner, A.D., Bakker, M., Post, V.E.A., Vandenbohede, A., Lu, C., Ataie-Ashtiani, B.,  
2654 Simmons, C.T., Barry, D.A., 2013. Seawater intrusion processes, investigation and  
2655 management: Recent advances and future challenges. *Adv. Water Resour.* 51, 3–26.  
2656 <https://doi.org/https://doi.org/10.1016/j.advwatres.2012.03.004>
- 2657 Willett, I.R., Bond, W.J., 1995. Sorption of manganese, uranium, and radium by highly  
2658 weathered soils. *J. Environ. Qual.* 24, 834–845.  
2659 <https://doi.org/10.2134/jeq1995.00472425002400050006x>
- 2660 Young, M.B., Gonnee, M.E., Fong, D.A., Moore, W.S., Herrera-Silveira, J., Paytan, A., 2008.  
2661 Characterizing sources of groundwater to a tropical coastal lagoon in a karstic area  
2662 using radium isotopes and water chemistry. *Mar. Chem.* 109, 377–394.  
2663 <https://doi.org/10.1016/j.marchem.2007.07.010>
- 2664 Zarroca, M., Linares, R., Rodellas, V., Garcia-Orellana, J., Roqué, C., Bach, J., Masqué, P.,  
2665 2014. Delineating coastal groundwater discharge processes in a wetland area by means  
2666 of electrical resistivity imaging, <sup>224</sup>Ra and <sup>222</sup>Rn. <https://doi.org/10.1002/hyp.9793>
- 2667 Zhang, Y., Li, H., Xiao, K., Wang, Xuejing, Lu, X., Zhang, M., An, A., Qu, W., Wan, L., Zheng, C.,  
2668 Wang, Xusheng, Jiang, X., 2017. Improving Estimation of Submarine Groundwater  
2669 Discharge Using Radium and Radon Tracers: Application in Jiaozhou Bay, China. *J.*  
2670 *Geophys. Res. Ocean.* 122, 8263–8277. <https://doi.org/10.1002/2017JC013237>
- 2671 Zhang, Y., Schaap, M.G., 2019. Estimation of saturated hydraulic conductivity with  
2672 pedotransfer functions: A review. *J. Hydrol.* 575, 1011–1030.  
2673 <https://doi.org/10.1016/j.jhydrol.2019.05.053>
- 2674 Zhou, Y.Q., Befus, K.M., Sawyer, A.H., David, C.H., 2018. Opportunities and Challenges in  
2675 Computing Fresh Groundwater Discharge to Continental Coastlines: A Multimodel  
2676 Comparison for the United States Gulf and Atlantic Coasts. *Water Resour. Res.* 54,  
2677 8363–8380. <https://doi.org/10.1029/2018WR023126>
- 2678